



THE PENNSYLVANIA  
STATE UNIVERSITY

# IONOSPHERIC RESEARCH

Scientific Report 424

## ELECTRON COLLECTION THEORY FOR A D-REGION SUBSONIC BLUNT ELECTROSTATIC PROBE

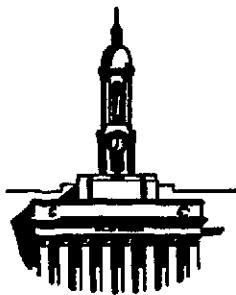
by

Thomas Wai-Kwong Lai

May 20, 1974

*The research reported in this document has been supported by  
The National Aeronautics and Space Administration under Con-  
tract Grant No. NGL 39-009-003 and Contract Grant No. NGR  
39-009-218.*

IONOSPHERE RESEARCH LABORATORY



University Park, Pennsylvania

(NASA-CR-138518) ELECTRON COLLECTION  
THEORY FOR A D-REGION SUBSONIC BLUNT  
ELECTROSTATIC PROBE (Pennsylvania State  
Univ.) 447 p HC \$10.50 CSCI 03B  
148  
N74-26874  
63/13 Unclas  
41134

## DOCUMENT CONTROL DATA - R &amp; D

(Security classification of title, body of abstract and indexing annotation must be entered when the overall report is classified)

1. ORIGINATING ACTIVITY (Corporate author)		2a. REPORT SECURITY CLASSIFICATION	
The Ionosphere Research Laboratory		2b. GROUP	
3. REPORT TITLE			
Electron Collection Theory for a D-Region Subsonic Blunt Electrostatic Probe			
4. DESCRIPTIVE NOTES (Type of report and, inclusive dates)			
Scientific Report			
5. AUTHOR(S) (First name, middle initial, last name)			
Thomas Wai-Kwong Lai			
6. REPORT DATE		7a. TOTAL NO. OF PAGES	7b. NO. OF REFS
May 20, 1974		131	
8a. CONTRACT OR GRANT NO.		9a. ORIGINATOR'S REPORT NUMBER(S)	
NASA NGR 39-009-218		PSU-IRL-SCI-424	
b. PROJECT NO.		9b. OTHER REPORT NO(S) (Any other numbers that may be assigned this report)	
NASA NGL 39-009-003			
10. DISTRIBUTION STATEMENT			
Supporting Agencies			
11. SUPPLEMENTARY NOTES		12. SPONSORING MILITARY ACTIVITY	
		The National Aeronautics and Space Administration	
13. ABSTRACT			
<p>Blunt probe theory for subsonic flow in a weakly ionized and collisional gas is reviewed, and an electron collection theory for the relatively unexplored case, <math>\lambda_D/L \sim 1</math>, which occurs in the lower ionosphere (D-region), is developed. It is found that the dimensionless Debye length (<math>\lambda_D/L</math>) is no longer an electric field screening parameter, and the space charge field effect can be neglected. For ion collection, Hoult-Sonin theory is recognized as a correct description of the thin, ion density-perturbed layer adjacent to the blunt probe surface.</p> <p>The large volume with electron density perturbed by a positively biased probe renders the usual thin boundary layer analysis inapplicable. Theories relating free stream conditions to the electron collection rate for both stationary and moving blunt probes are obtained. A model based on experimental nonlinear electron drift velocity data is proposed. For a subsonically moving probe, it is found that the perturbed region can be divided into four regions with distinct collection mechanisms. Since <math>\lambda_e - n &gt; L/\phi_w</math>, the diffusion layer concept is irrelevant for electron collection, and is replaced by a collisionless layer. The electron current expressions for both stationary and moving probes are found to be approximately identical. The electron density predicted by this analysis is lower in magnitude than the earlier calculations below 60 km, and is found to be higher above this altitude. This continuum theory is valid up to 80 km.</p>			

PSU-IRL-SCI-424  
Classification Number 1.5.1

Scientific Report 424

Electron Collection Theory for a  
D-Region Subsonic Blunt Electrostatic Probe

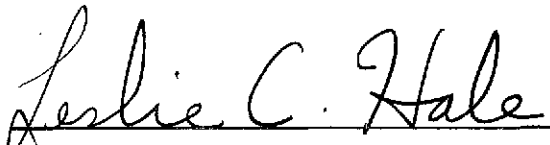
by

Thomas Wai-Kwong Lai

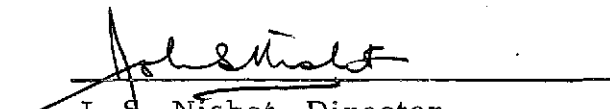
May 20, 1974

The research reported in this document has been supported by The National Aeronautics and Space Administration under Contract Grant No. NGL 39-009-003 and Contract Grant No. NGR 39-009-218.

Submitted by:

  
L. C. Hale, Professor of  
Electrical Engineering  
Project Supervisor

Approved by:

  
J. S. Nisbet, Director  
Ionosphere Research Laboratory

Ionosphere Research Laboratory  
The Pennsylvania State University  
University Park, Pennsylvania 16802

ia

#### ACKNOWLEDGEMENTS

The author wishes to express deep gratitude and appreciation to Dr. Thomas M. York for his patience in providing advice and continual guidance throughout the course of this work.

This work was partially supported by National Aeronautics and Space Administration under Grant NGL 39-009-003 and NGR 39-009-218.

## TABLE OF CONTENTS

	Page
ACKNOWLEDGEMENTS. . . . .	ii
LIST OF TABLES. . . . .	vi
LIST OF FIGURES . . . . .	vii
NOTATION. . . . .	x
CHAPTER I	
INTRODUCTION . . . . .	1
1.1 Preface . . . . .	1
1.2 The Subsonic Blunt Probe. . . . .	3
CHAPTER II	
REVIEW OF RELATED PROBE WORK . . . . .	5
2.1 Fundamental Concepts. . . . .	5
2.2 Theories Including Space Charge Effect. . . . .	8
2.2.1 Stationary Probe . . . . .	8
2.2.2 Moving Probe . . . . .	11
2.3 Theories with No Space Charge Effect. . . . .	16
2.4 Discussion. . . . .	17
CHAPTER III	
BASIC PARAMETERS AND EQUATIONS FOR A D-REGION BLUNT PROBE. . . . .	20
3.1 The Composition of the D-Region . . . . .	20
3.2 Physical Quantities of the Medium . . . . .	21
3.3 Magnetic Field Effect on Probe. . . . .	23
3.4 Interaction of a Biased Probe with the D-Region Plasma. . . . .	24
3.5 Similarity Parameters . . . . .	28
3.6 Zero Space Charge Theory. . . . .	30

CHAPTER IV	Page
SUBSONIC CONTINUUM BLUNT PROBE THEORY. . . . .	37
4.1 Introduction. . . . .	37
4.2 Ion Collection Theory . . . . .	38
4.2.1 Attracted Ions . . . . .	38
4.2.2 Repelled Ions. . . . .	46
4.2.3 Justification of Hoult's Ionic Theory in the D-Region . . . . .	47
4.3 Electron Collection Theory. . . . .	48
4.3.1 Stationary Blunt Probe Theory. . . . .	48
4.3.2 Identification of Characteristic Layers for a Moving Blunt Probe . . . . .	61
4.3.3 A Simple Model Based on Particle Convection. .	68
4.3.4 Collisionless Surface Layer. . . . .	82
4.3.5 Validity of the Electron Collection Theory in the D-Region . . . . .	87
4.3.6 Electron Current to a Negatively Biased Probe.	89
CHAPTER V	
COLLISIONLESS BLUNT PROBE THEORY . . . . .	93
5.1 Theory, 82 km to 300 km . . . . .	93
5.1.1 Applicability of Thin Sheath Concept . . . . .	93
5.1.2 Thin Sheath Theory . . . . .	99
5.2 Discussion: 70 km to 82 km . . . . .	99
CHAPTER VI	
THE D-REGION ELECTRON DATA REDUCTION . . . . .	101
6.1 Data Reduction by Continuum Theory. . . . .	101

	Page
6.2 Data Reduction by Collisionless Theory. . . . .	113
CHAPTER VII	
CLOSURE. . . . .	115
7.1 Summary . . . . .	115
7.2 Suggestions for Further Research. . . . .	118
REFERENCES. . . . .	120
APPENDIX A	
Solution of the Electric Boundary Layer Equation . . . . .	126

# LIST OF TABLES

Table		Page
1	The Mean Free Path of Charged Particles in the D-Region. . . . .	22
2	Dimensionless Parameters and Various Length Scales in the D-Region. . . . .	31
3	Evaluation of the Strong Field Parameter for Data from "D-16" . . . . .	49
4	Evaluation of the Strong Field Parameter for Data from "Cert" . . . . .	50
5	Variation of the Parameter, $E_w/p$ , the Electron Collecting Surface Area, $A_o$ , to the Collector Disc, and the Perturbed Length Scale, $\gamma_o$ , and the Free Stream Velocity, $\bar{U}$ , for the Launch on December 5, 1972. . . . .	59
6	Comparison of Various Length Scales for the Mo- bility Layer. . . . .	74



## LIST OF FIGURES

Figure		Page
1	Typical Ionospheric Concentration for both Minima and Maxima of the Solar Cycle. . . . .	2
2	Typical Electrostatic Probe Current-Voltage Characteristics. . . . .	6
3	Electric Field of a Charged Circular Disc. . . . .	39
4	Axisymmetric Stagnation Flow Over the Blunt Probe. . .	42
5	Boundary Surfaces of the Perturbed Plasma: (A) Open Boundary Surface, (B) Closed Boundary Surface. . . . .	52
6	Boundary Configurations of the Blunt Probe: (A) A Two-Sided Disc, (B) A One-Sided Disc . . . . .	53
7	Experimental Data Obtained by Park, Voshall and Phelps on the Drift Velocity of Electrons in Nitrogen . . . . .	56
8	The Approximate Electron Drift Velocity versus $E/p$ Plot for Stationary Blunt Probe Theory . . . . .	57
9	Schematic Representation of Loss and Gain of Electron in the Diffusion Layer . . . . .	65
10a	Diffusion Layer on the Probe . . . . .	71
10b	Mobility Layer on the Probe. . . . .	71
11	Perturbed Regions Surrounding a Positively Biased Probe. . . . .	77
12	The Influence of the Altitude on the Mobility Layer Radius with Varying Probe's Potential. . . . .	80

Figure		Page
13	The Influence of the Altitude on the Ratio of Electron Number Density at the Outer Diffusion Layer Edge to the Ambient Electron Density with Varying Probe Potential. . . . .	81
14	Perturbed Regions around a Positively Biased Probe when: (A) the Electron-Neutral Mean Free Path is Small Compared with Probe Diameter, (B) the Electron- Neutral Mean Free Path is Small Compared with Probe Diameter . . . . .	84
15	Various Length Scales in the D-Region for December 5, 1972 . . . . .	90
16	Variation of Measured Neutral and Electron Temperature with Altitude for (A) Puerto Rico in January 1967, (B) Millstone in December 1966 . . . . .	94
17	Variation of the Electric Field of the Probe with Altitude at which Measurements were made . . . . .	97
18	Electron Diffusion Layer Thickness with Varying Altitude . . . . .	103
19	Electron Density Profile for December 5, 1972. . . . .	104
20	Electron Density Profile for January 31, 1972. . . . .	105
21	Electron Density Profile for January 16, 1973. . . . .	106
22	Electron Density Profile for January 6, 1972 . . . . .	107
23	Electron Density Profile for February 2, 1973. . . . .	108
24	The Descending Velocity of the Probe at Various Altitude for December 5, 1972. . . . .	109
25	Typical Pressure Profile in the D-Region . . . . .	111

Figure		Page
26	Electron and Positive Ion Density Profile for January 31, 1972, Wallops Island, Virginia . . . . .	112
27	Comparison of Electron Density Profiles Reduced by Continuum Theory and Collisionless Theory. . . . .	114

## NOTATION

### English Letter Symbols

$a$	radius of probe
$A$	area
$A_{col}$	area of collector disc
$A_s$	area of sheath
$B$	magnetic induction
$c$	local sonic speed
$\bar{c}$	thermal velocity
$d$	radial distance
$d_{para}$	diameter of parachute
$D$	diffusion coefficient
$e$	electron charge
$\bar{e}_r, \bar{e}_\theta$	unit vectors (Figure 11)
$E$	electric field
$f$	dimensionless stream function
$g$	stagnation point inviscid flow velocity gradient
$I$	current to the probe's collector disc
$j$	current density
$j_r$	random current density
$k$	Boltzmann's constant
$l_p$	characteristic length
$L$	diameter of probe
$L_{mob}$	characteristic length of mobility
$L_p$	length parameter of the probe
$L_r$	length parameter of the return electrode

# English Letter Symbols (cont'd)

m	particle mass
M	Mach number
n	number density
N	neutral gas density
p	neutral gas pressure
q	flow velocity vector
r	radial distance
R	radius of probe
R <sub>cal</sub>	resistance of the calibration resistor
Rd	diffusion Reynolds number
Re	Reynolds number
Res	$= \frac{ga^2}{v}$
R <sub>i</sub>	$= \frac{U\lambda_D}{D_1}$
s	transformation independent variable
S	sheath thickness
Sc	Schmidt number
T	temperature
u	flow velocity in x direction (Figure 4)
u <sub>b</sub>	viscous boundary layer edge velocity in x direction
$\bar{U}$	free stream velocity
v	flow velocity in y direction (Figure 4)
v <sub>d</sub>	drift velocity
v <sub>⊥</sub>	particle velocity in the plane perpendicular to B
V	electrical potential
V <sub>s</sub>	plasma potential

### English Letter Symbols (cont'd)

$V_f$	floating potential
$w$	diffusive flow velocity
$x, y$	coordinates (Figure 4)
$z$	number of electron charge
$(\Delta f / \Delta t)_{cal}$	slope of the preflight calibration ramp
$(\Delta f / \Delta t)_{data}$	slope of the in-flight data waveform

### Greek Letter Symbols

$\alpha$	$= \frac{\lambda_D}{L}$
$\beta$	$= \frac{D_i}{D_e}$
$\delta$	boundary layer thickness
$\Delta$	dimensionless sheath thickness
$\epsilon$	$= \frac{T_i}{T_e}$
$\eta$	viscous boundary layer coordinate
$\gamma$	radial distance
$\gamma_r$	Larmor radius
$\theta$	angle (Figure 11)
$\lambda$	$= \frac{n_o}{n_{eo}}$
$\lambda_D$	Debye length
$\lambda_{s-n}$	mean free path for neutral-species s collisions
$\mu$	mobility
$\nu$	kinematic viscosity

## Greek Letter Symbols

$\nu_e$	electron-neutral collision frequency
$\rho$	neutral gas density
$\sigma$	conductivity
$U$	$= \frac{V}{V_w}$
$U_{app}$	dimensionless electrical potential due to applied field
$U_{sp}$	dimensionless electric potential due to space charges
$\bar{\psi}$	dimensionless stream function
$\phi$	dimensionless electric potential

## Subscripts

A	evaluated at the outer edge of the convection-mobility dominant region
B	evaluated at the inner edge of the convection-mobility dominant region
C	evaluated at the inner edge of the mobility layer
col	refers to electron
e	refers to electron
i	refers to ion
n	refers to neutral
s	refers to species s
w	evaluated at the probe surface
$\lambda$	evaluated at the outer edge of the collisionless surface layer

### Subscripts

- +**            refers to positive ion
- refers to negative ion
- o**            evaluated at the free stream state



## ABSTRACT

Blunt probe theory for subsonic flow in a weakly ionized and collisional gas is reviewed, and an electron collection theory for the relatively unexplored case,  $\lambda_D/L \sim 1$ , which occurs in the lower ionosphere (D-region), is developed.

It is found that the dimensionless Debye length ( $\lambda_D/L$ ) is no longer an electric field screening parameter, and the space charge field effect can be neglected. For ion collection, Hoult-Sonin theory is recognized as a correct description of the thin, ion density-perturbed layer adjacent to the blunt probe surface.

The large volume with electron density perturbed by a positively biased probe renders the usual thin boundary layer analysis inapplicable. Theories relating free stream conditions to the electron collection rate for both stationary and moving blunt probes are obtained. A model based on experimental nonlinear electron drift velocity data is proposed. For a subsonically moving probe, it is found that the perturbed region can be divided into four regions with distinct collection mechanisms. Since  $\lambda_{e-n} > L/\phi_w$ , the diffusion layer concept is irrelevant for electron collection, and is replaced by a collisionless layer. The electron current expressions for both stationary and moving probes are found to be approximately identical. The electron density predicted by this analysis is lower in magnitude than the earlier calculations below 60 km, and is found to be higher above this altitude. This continuum theory is valid up to 80 km.

## CHAPTER I

## INTRODUCTION

## 1.1 Preface

The ionosphere is the region above the earth's standard atmosphere where ions and electrons are dense enough to affect the propagation of radio waves. The symbols D, E, F1 and F2, as shown in Figure 1, are used to distinguish its various parts. The present work is concerned with probing the composition of D-region, the lowest part of the ionosphere.

The D-region, characterized by its relatively high ambient neutral gas density and the presence of the negative ions, extends nominally from 50 km to 80 km in altitude. In the pursuit of a better understanding of the chemical composition of the ionosphere, the D-region has been energetically explored by various aeronomy groups. Typical recent investigations have considered the pronounced diurnal variation of the D-region ionization in Winter (1), sunrise effect on the D-region photochemistry (2), and the relationship of the D-region absorption to stratosphere warming (3).

Both ground-based and rocket-borne propagation experiments have been used for the experimental study of the D-region. However, such investigations give only a measurement averaged over a large volume of the medium being studied (4). As an example of the alternative local measurement by flying a Gerdien Condenser probe subsonically and supersonically (5) has been attempted. The electron density can be obtained from conductivity ( $\sigma$ ) measurements in standard fashion:  $\sigma = n_{eo} e^2 (2 m_e \nu)^{-1}$ , where  $n_{eo}$  is the ambient electron density,  $e$  is the electron charge,  $m_e$

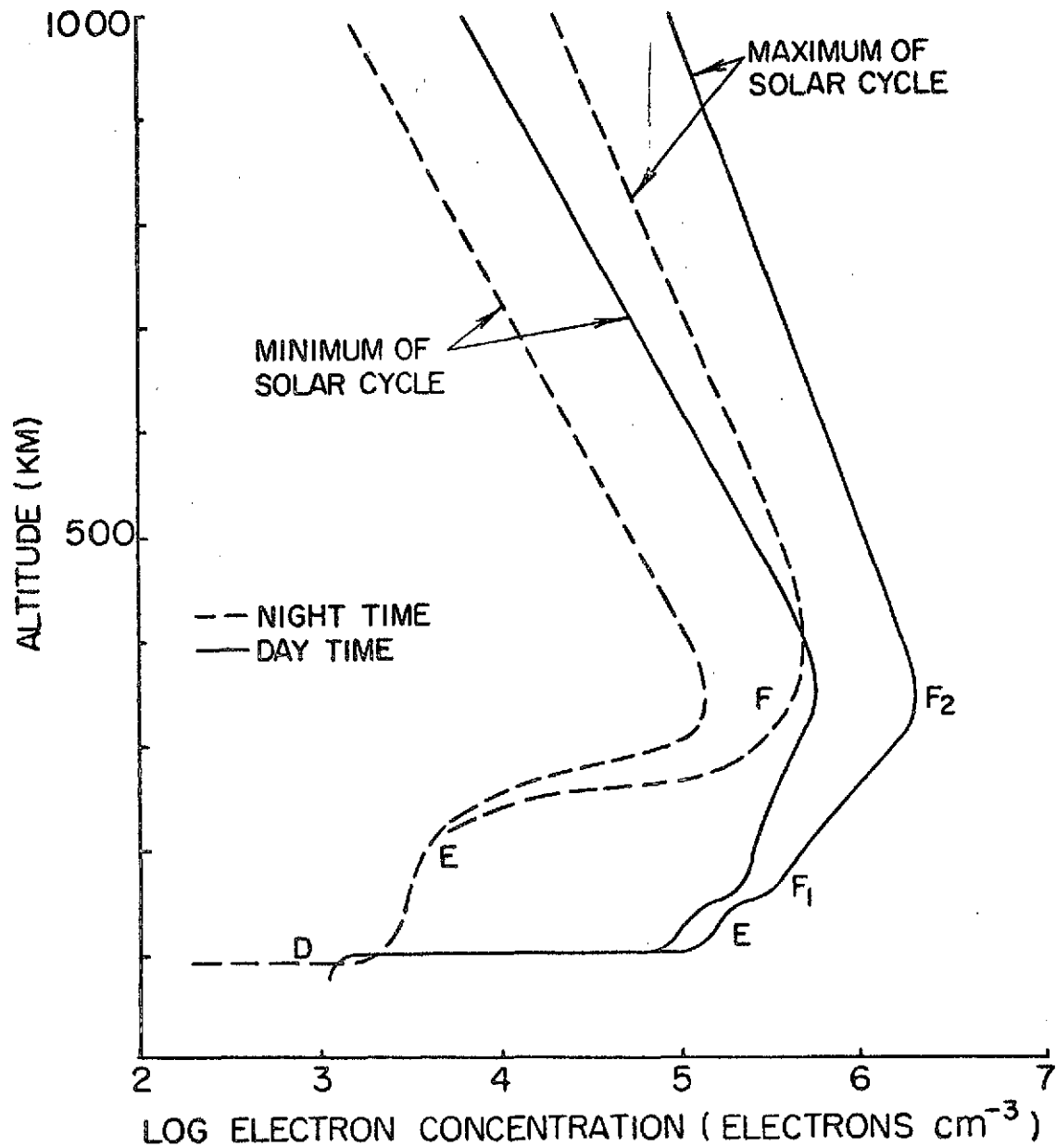


Figure 1. Typical Ionospheric Concentration for both Minima and Maxima of the Solar Cycle (Figures 4 and 5 of Ref. 4)

is the mass of electron, and  $\nu_e$  is the electron collision frequency. Conductivity is measured by applying a small voltage across a suitable electrode system (e.g., the Gerdien capacitor arrangement), and measuring the resulting currents. Beginning for a zero voltage reference, the voltage-current characteristic shows a slope proportional to the charged particle mobility. At high electric fields, where all the particles entering are collected, a saturation would be expected; however, in some cases, no saturation region was found (6) for reasons which are not clear. Also, this type of device is aspect sensitive and the effect of shock waves produced needs further investigation.

The local charge density can also be found by measuring the current to an electrostatic probe. Basically, an electrostatic probe is merely a small metallic electrode (a wire or a surface) inserted into a plasma (ionosphere). By biasing the probe potential positive and negative relative to the plasma, and measuring current collected, one can obtain information about the conditions in the plasma. However, the presence of the probe in the plasma perturbs the local composition and to relate the current collected and ambient condition is a fairly difficult undertaking. This task is the goal of the present work.

## 1.2 Subsonic Blunt Probe

The standard D-region ion and electron collection subsonic electrostatic probe theory and instrumentation were presented by Hale and Hoult in 1965 (7). The actual experiment employed a parachute-borne blunt electrostatic probe which was flown by a meteorological rocket, ejected, and descended from 90 km to 45 km with an average terminal speed of 100 m/sec. The voltage-current characteristics relates the

current collected to the ambient charged particle density. This simple device has the advantage that its planar configuration is easy to construct, and the probe being facing earthward and covered by the parachute above is shielded from solar radiation. The subsonic blunt probe system is better than a supersonic probe, because the latter can drastically affect the composition of the medium through shock waves which are yaw-dependent.

In addition to earlier blunt probe data, another eleven rockets have recently been fired by the Ionospheric Research Laboratory in The Pennsylvania State University over the period of October 1971 to February 1972. With such a body of experience, it is reasonable to conclude that the experimental technique has been thoroughly examined and well understood. The interpretation of electron collection data, however, requires further investigation (8), and will be the primary consideration here.

The intent of the present work is to critically review past D-region subsonic blunt probe theory for ion collection (negatively based probe), and to find a new analytic electron collection theory (positively biased probe). This new theory will then be used to interpret the available blunt probe data.

## CHAPTER II

## REVIEW OF RELATED PROBE WORK

## 2.1 Fundamental Concepts

It is appropriate to begin with a discussion of the general response of a plasma in the presence of a stationary biased probe. A typical current-voltage plot is given in Figure 2. The general shape of the curve, but not absolute values, is relatively the same for various probe geometries at different plasma pressures. The probe is at the same potential as the plasma at the point  $V_g$ . There is no potential difference between the probe and plasma at this point, and the charged particles migrate to the probe at thermal velocity. Electrons, being faster, are the dominant contributor of the current collected by the probe.

When the probe is made positive relative to the plasma, electrons are attracted while ions are repelled. Therefore, near the probe surface that is an excess of negative charge, which builds up until the total charge is equal to the virtual positive charge on the probe. (Notice that this phenomenon will happen only when the density of the charged particles in the plasma is dense enough.) This layer of charge imbalance will shield the rest of the plasma from the influence of the probe. This region, where most of the potential drop occurs, is called the sheath. The electron current is that which enters the sheath through random thermal motion; and since the area of the sheath changes little with the probe potential, the probe characteristic here (portion A) is more or less flat. This is called the region of saturation electron current.

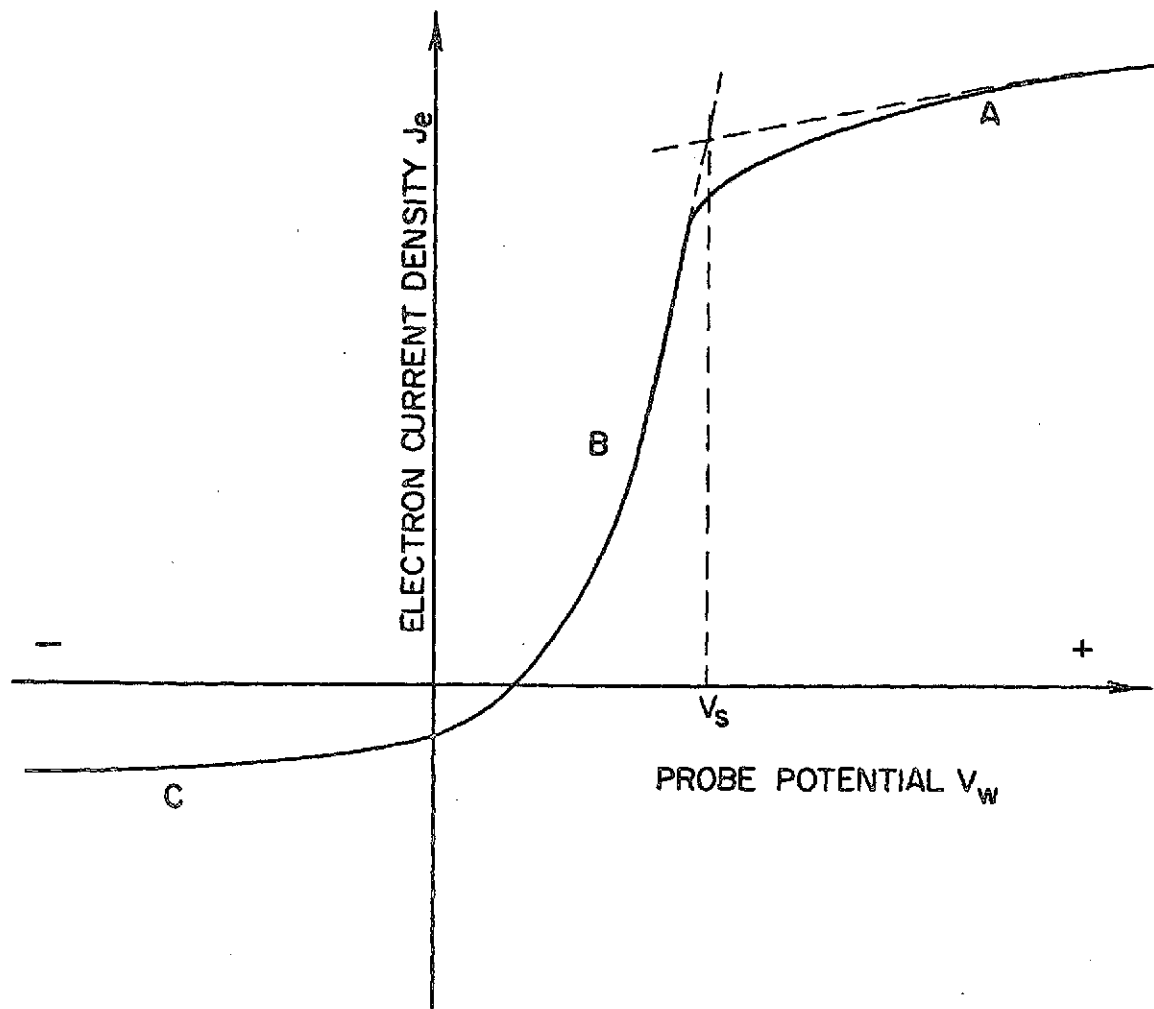


Figure 2. Typical Electrostatic Probe Current-Voltage Characteristics

If the probe is made negative relative to  $V_g$ , electrons will begin to be repelled and ions accelerated. The electron current falls drastically as  $V_w$ , the probe potential decreases. This region (portion B) is called the retarding-field region of the characteristic. Finally, at point  $V_f$ , called the floating potential, the probe is sufficiently negative to repel all electrons except a flux equal to the flux of ions, and, therefore, draws no net current. At large negative values of  $V_w$ , all electrons are repelled and an ion sheath is formed on the probe surface. The current collected is the saturation ion current (portion C).

The thickness of the sheath is an index of the effectiveness of the plasma shielding effect, and is measured to be typically on the order of a few Debye lengths,  $\lambda_D$ ; this parameter is normally drawn from an analysis when the body is stationary and its size is reduced to zero (9). Electric field distribution inside the sheath is governed by a Poisson equation. When the charge density is sufficiently low and applied potential is high enough, the space charge effect can be neglected and the sheath per se can be said to no longer exist. Theory based on this approximation is referred to as the zero space charge theory.

The exact relationship between the plasma parameters and the probe characteristic depends on the geometry of the probe, and the relative magnitudes of the collision length, the probe dimensions, and the Debye length. Clearly, the probe characteristic of a moving probe will differ from that of a stationary probe.



## 2.2 Theories Including Space Charge Effect

### 2.2.1 Stationary Probe

For the case of low pressure, the interaction problem of a stationary electrostatic probe was first treated in detail by Mott-Smith and Langmuir. Their solution can also be found in Chen (10). They assumed that the sheath layer surrounding the probe can be approximated by one which has a sharp outer edge, outside of which the potential is that of the plasma. When the sheath is thin compared to the probe radius ( $\lambda_D \ll R$ ), every attracted charged particle that enters the sheath will be collected, and current is given by

$$I = j_r A_s \quad (2.2.1)$$

where  $A_s$  is the area of the sheath,  $j_r$  is the random current density crossing a unit area in one direction. For a Maxwellian velocity distribution, this is given by

$$j_r = \frac{e}{4} n_0 \bar{c} \quad (2.2.2)$$

where  $\bar{c}$  is the random velocity of the attracted particles,  $n_0$  is its number density outside the sheath. Notice that  $j_r$  depends on  $n_0$  which is usually unknown, while  $A_s$  changes with different probe potential for a cylindrical or spherical probe. For a planar probe,  $A_s$  is a constant (see Eqs. 29, 30 and 31, p. 127, ref. 10).

When the sheath is thick compared to probe radius ( $\lambda_D > R$ ), not all particles entering the sheath will hit the probe because of the possibility of orbital motions. The law of conservation energy and angular momentum have to be included in the analysis. It was found that

the saturation electron current varies with  $V_w$  for spheres and as  $V_w^{1/2}$  for cylinders (Eqs. 52 and 53, p. 130, ref. 10); it does not change for planes since no orbits are possible and the sheath area is again constant.

The Langmuir theory mentioned above has two limitations. First, the collision length between the attracted charged particles and the neutrals must be larger than the sheath thickness or the probe radius, whichever is shorter. Otherwise, in the presence of collisions, the probe current will depend also on the transport coefficients of the plasma (e.g., diffusion coefficient). Second, the probe current is solved in terms of two unknowns, the ambient number density of the attracted charged particles and the sheath thickness. There is only one unknown ( $n_0$ ) in the thick sheath case (10). In the thin sheath case, the sheath thickness has to be determined independently. This problem was solved by Bettenger and Walker (11) for a spherical probe. In that case, the nondimensional sheath thickness ( $\Delta$ ) was given by

$$\Delta = 0.83 \rho_s^{1/3} \phi_w^{1/2} \quad (2.2.3)$$

$$\phi_w = \frac{eV_w}{kT} \quad (2.2.4a)$$

$$\rho_s = \frac{R}{\lambda_D} \quad (2.2.4b)$$

$$\Delta = \frac{S}{\lambda_D} \quad (2.2.4c)$$

where  $S$  is sheath thickness,  $\lambda_D$  is the Debye length,  $R$  is the probe radius,  $V_w$  is the probe potential,  $e$  is the electron charge,  $k$  is the Boltzman constant, and  $T$  is the temperature of the attracted particles.

At high pressure, the first limitation mentioned above relating to collisionless sheath is not satisfied. Here, the minimum practical probe radius (so that the probe will not melt) and the sheath thickness are both larger than the mean free path for the attracted particle-neutral collisions. Su and Lam (12) solved this problem and developed a continuum theory of a stationary spherical electrostatic probe. For the Debye length much less than the probe radius (thin sheath), their analysis identified four distinct regions, they are: the quasi-neutral, the transitional, the ion-sheath, and the ion-diffusion region. In the latter two regions, the Boltzman electron density distribution is not a valid description; as it was shown that the effects of electrons in these regions are completely negligible.

For probes of more moderate size compared to the Debye length, Su and Lam present a numerical solution. To remove an instability in the numerical integration, a third order term which was responsible for the existence of the ion-diffusion layer was neglected. The error introduced was estimated to be of order of  $T_e/T_i$  which is generally very small in many plasmas. In the D-region, however,  $T_e/T_i$  is of order unity. Cicerone and Bowhill (13) in their attempt to find a continuum probe theory in the D-region, repeated the numerical integration with the third order term mentioned above included. The result shows that the approximation introduced by Su and Lam appreciably affects the V-C characteristic of the probe.

In the transition regime (intermediate pressure), Talbot and Chow (14) gave an approximate analytic analysis of the effects of collisions on ion saturation and electron current for both cylindrical and

spherical negatively biased probes. This was accomplished by using the Bernstein-Rabinowitz (15) and Laframboise (16) results and the Su-Lam (12) and Cohen (17) results to evaluate certain integrals which appeared in the analysis in the collisionless and continuum limits, respectively. They then use an interpolation formula to span the transition regime between these limits. Their results have been found to compare favorably with experimental results (14).

### 2.2.2 Moving Probe

The superposition of a directed plasma motion toward a probe will destroy the symmetry of the plasma sheath with respect to the probe. The electric field of the sheath will no longer be a central force system. This undesirable feature allows solution only in very special cases.

Again, treatments for a moving collisional probe and a moving collisionless probe are completely different. By a collisional probe, one means that  $\lambda_{s-n} \ll L$ , where  $\lambda_{s-n}$  is the mean free path for species (s) - neutral collisions, and  $L$  is the characteristic length of the probe. This, of course, also includes the case where there is a collisionless sheath on the probe surface with a collisional region outside. A collisionless probe implies that  $\lambda_{s-n} \gg L$ . Notice that this does not include the possibility of having a viscous boundary layer of the neutral flow since usually  $\lambda_{n-n} \ll \lambda_{s-n}$ , where  $\lambda_{n-n}$  is the neutral-neutral mean free path. However, the fact that  $\lambda_{s-n} \gg L$  implies that the effect of the neutrals on the species (s) is small, the viscous boundary-layer effect on the charged particles do not have to be considered.

Using a wave mechanical approach, Chmielewski (18) solved the collisionless slowly drifting, spherical (both positively and negatively biased) probe problem by a perturbation method. The speed ratio  $(\bar{U}/C_1)$  is used as the small perturbation parameter. The result shows that only a small effect on the stationary probe characteristic is expected when a slow plasma drift is imposed (19). Physically, this is reasonable, since the electrostatic field effect on the sheath structure is large compared with a small flow perturbation. Also the current collected by the sphere is the average of the current to the upstream and downstream sides of the probe; the local current perturbation on both sides tend to cancel each other.

For the case of a collisional moving probe, a brief review of the present knowledge on this subject is as follows. For an ion collecting (negatively biased) probe moving in a collisional medium, two important parameters are involved. They are the nondimensional Debye length  $(\lambda_D/L)$  and Reynolds number  $(Re)$ , where  $\lambda_D = [kT_e / (4\pi n_{eo} e^2)]^{1/2}$ ,  $Re = \bar{U}L \nu^{-1}$ , and  $\nu$  is the kinematic viscosity of the neutral gas. These two parameters are associated with the relevant highest order derivatives (this will be shown in a later chapter) in the system of governing equations. It is, therefore, logical to expect that there will be two singular perturbations in the problem: one for the viscous layer, associated with the Reynolds number,  $Re$ , and another for the sheath, associated with the Debye length parameter  $\lambda_D/L$ .

The nature of the problem depends on the relative ordering of these two parameters. When  $\lambda_D L^{-1} \ll Re^{-1/2} \ll 1$ , physically the inequality implies that the sheath is thin compared with the viscous

boundary layer. This allows neglecting convection within the sheath. The resulting ion flow in the sheath can be treated as one dimensional, which is crucial in solving the sheath equation. Also, this condition will automatically only allow a moderate probe potential to be considered, since a strong probe potential will give a thick sheath. When the inequality is not satisfied, the sheath can be thick and the problem of convection within the sheath has to be properly taken into consideration.

First, the case when the sheath is imbedded inside the viscous boundary layer ( $\lambda_D L^{-1} \ll Re^{-1/2} \ll 1$ ) will be considered. Talbot (20) developed a theory for a collecting electrode placed at the stagnation point of a blunt body immersed in a supersonic partially ionized stream. He assumed a thin collisionless sheath inside the viscous stagnation boundary layer. Inside the sheath, the current density is given by the Langmuir probe theory. Outside, the ion-electron pairs diffuse together relative to the neutral gas. The behavior here is governed by an equation consisting of an ambipolar diffusion term (to be discussed later) and the convection term.

When there are a considerable number of collisions inside the sheath, Lam (21) developed a continuum, incompressible analytic solution to a blunt probe in a plasma which consists of positive ions and electrons. He assumed that the viscous boundary layer thickness  $(Re)^{-1/2}$  is much larger than the sheath thickness  $(\lambda_D/L)$ . Outside the electric boundary layer (a layer where electrical effects are dominant) and which is assumed to be of the same order of thickness as the viscous boundary layer, the number density of the charged particles is unperturbed.

Inside, it is further split up into two layers. The upper inner layer is an ambipolar diffusion layer where a quasi-neutral conditions ( $n_i = n_e$ ) holds. Here, physically the slower ions retard the diffusion of the electrons by setting up an electrostatic field. Thus electrons and ion diffuse together; this is called the ambipolar diffusion. In the lower inner layer, adjacent to the probe surface, free diffusion and field effects are dominant. Closed form analytical results were obtained for the floating potential and the current-voltage characteristic. It is interesting to compare the sheath thickness,  $S$ , found in Lam's work ( $S \sim \epsilon^{1/6} \lambda_D^{2/3}$ , where  $\epsilon = T_i/T_e$ ) to that found by Bettenger and Walker (11) for a collisionless stationary probe ( $S = 0.83 \lambda_D^{2/3} \phi_w^{1/2} R^{1/3}$ , where  $\phi_w = \frac{eV_w}{kT_e}$ , and  $R$  is the probe radius). The sheath thickness in two case bears the same relationship to the Debye length.

Lam's theory was extended to plasma consisting of positive ions, electrons and negative ions by Touryan and Chung (22). They concluded that only when the temperature of the electrons and the ions are the same can the sheath equation can be numerically integrated. The solution found for a flat plate shows that the electron saturation current is suppressed by the presence of negative ions while the positive ion saturation current is slightly increased. For a higher negative ion mobility, the above effects are increased.

The difficulty of unequal electron and ion temperatures was solved numerically by Bailey and Touryan (23) for a flat plate. Results were obtained for both electron attracting and retarding fields over a larger range of applied probe potentials. By working with the governing

equations for the entire region rather than two sub-regions (ambipolar and sheath), one could minimize problems in numerical instabilities (in computing the sheath) and avoid the cumbersome task of asymptotic matching of two regions with two or more parameters. The results show that for  $T_e/T_i > 1$ , the sheath plays a much greater role in determining the ion saturation current than when the flow is in thermal equilibrium with  $T_e = T_i$ .

Secondly, the case when the sheath is not thin compared to the viscous boundary layer is considered. Johnson and DeBoer (24) developed a theory for the electric boundary layers that form on flat-plate and cylindrical probes aligned parallel with a high speed flow, when the probe potential is large and negative. They assumed that the nondimensional potential ( $\phi_w$ ) and the parameter,  $R_i (\phi_w)^{1/2}$  were infinitely large, where  $R_i = \bar{U} \lambda_D D_i^{-1}$ , and  $D_i$  is the ionic diffusion coefficient. This assumption makes it possible to neglect derivatives with respect to flow direction, compared with corresponding derivatives with respect to normal direction,  $y$ . The expression obtained for the sheath thickness ( $S$ ) at sufficiently far downstream of a flat plate is

$$S = \left(\frac{9}{2}\right)^{1/4} x^{1/4} \lambda_D^{1/2} D_i^{1/4} \bar{U}^{-1/4} \phi_w^{1/2} \quad (2.2.5)$$

Thus the sheath thickness varies with  $\lambda_D^{1/2}$ , grows further downstream ( $x^{1/4}$ ) due to the ion supply by convection, and it is also a function of the nondimensional potential  $\phi_w^{1/2}$  since  $\phi_w$  is large in the present case. The sheath thickness for the cylindrical probe cannot be explicitly expressed. The numerical solution shows that for given flow conditions and electrode potentials, the flat plate sheath is thicker than



the equivalent axisymmetric sheath. This is due to the better shielding of the cylindrical case which results from the convergence of the ion streamlines on the probe.

### 2.3 Theories with No Space Charge Effect

Hoult (25) derived a continuum subsonic probe theory for the D-region where the charged particle density is very low. He made two physical assumptions. The first is that the charged particle density of the plasma is low enough that the space charge electric field is small compared with the applied field. The field then is simply the electrostatic field in a vacuum. This condition decouples the species conservation equations and allows each species to respond independently. Paired diffusion (ambipolar diffusion) naturally no longer exists. He further assumed that the convection term to be completely dominant until very near the probe surface. It was concluded that the charged particles density is perturbed only very near the wall; this layer was called the diffusion layer. Inside the diffusion layer, the free diffusion term and the mobility term govern the dynamics of each species. For a collecting disc, the positive current to a highly negatively biased probe was given by

$$I_p = (en_{+0} \bar{U} \pi r^2) \left(\frac{2}{\pi}\right) \left(\frac{eV_w}{kT_e}\right) \frac{1}{Rd_1} \quad (2.3.1)$$

where  $n_{+0}$  is the free stream positive ion density,  $\bar{U}$  is the free stream velocity,  $V_w$  is the probe potential,  $Rd_1$  is the ionic electrical Reynolds number ( $\bar{U}LD_1^{-1}$ ), and  $D_1$  is the ionic diffusion coefficient. A similar result is obtained for a highly positively biased probe.

Sonin (26) accepted the first assumption of Hoult, discarded the second, and did a complete analysis for ion collection of a supersonic rocket-borne blunt negatively biased probe. The details will be described in Appendix A. In two extreme cases, strongly attracting field and weak field, the current expression is identical to the expression derived by Hoult for the subsonic probe at a high electric field.

#### 2.4 Discussion

The review of the above theories leads to the conclusion that the solvability of the above mentioned plasma-probe interaction problems depend on two factors: the probe geometry, and the ability to predict, at least the order of magnitude of, the physical quantities like  $T_e$  and  $N_{eo}$  in the neutral plasma even before the problem is solved.

With the simple geometry like Walker and Bettinger's stationary collisionless spherical probe (11), Chmielewski's slowly drifting collisionless spherical probe (18), and Bailey's moving collisional infinite planar probe (23), all the physical quantities depend only on one coordinate (radial distance ( $r$ ) for the former two, and the boundary coordinate ( $\eta$ ) for the last case). This simplification allows a complete numerical solution without making any assumption.

When the geometry is not simple, a prior knowledge of the order of magnitude of the physical quantities in the neutral plasma is required. This is explained as follows. In the sheath-edge approach, the Debye length, the usual sheath thickness representative length scale, is needed to determine whether the sheath is thin (space-charge limited)

or thick (orbital limited), and whether the sheath is collisional or collisionless, so that the corresponding treatment is used. On the other hand, when a boundary layer analysis is possible and used, the ordering of the relative parameters ( $\lambda_D$ , Re, Rd) also require the knowledge of the Debye length. A prior estimation of the plasma's physical quantities is needed to determine the size of the Debye length.

With the nondimensional probe potential ( $\phi_w$ ), much smaller than unity or with local thermodynamic equilibrium (27), the sheath thickness for a collisionless infinite planar probe and spherical probe is well represented by the Debye length (28). Local thermodynamic equilibrium means that sufficient collisional interchange of kinetic energy takes place over a length that is small as compared with the local linear scale of field and medium. Thus Talbot's (20) collisionless sheath thickness can be represented by the Debye length only when  $\phi_w \ll 1$ . For a moving collisional probe, one can generally expect that the sheath thickness will not depend on the free stream velocity unless the sheath is thick compared with the viscous boundary layer. In general, the sheath thickness is a function of the free stream velocity,  $\bar{U}$ , the probe potential,  $\phi_w$ , and the Debye length,  $\lambda_D$ .

For a moving blunt probe operating in the D-region of the ionosphere, the analysis of Lam (21), and Touryan and Chung (22) cannot be used, simply because the assumption  $\lambda_D L^{-1} \ll (\text{Re})^{-1/2}$  is not satisfied. The neglect of the convection term in Hoult's zero space charge theory needs further justification. Hoult's tactful assumption that the perturbed region is confined to the thin diffusion layer, which is crucial for the application of his boundary layer analysis, is questionable in

general. For ion collection, Sonin's analysis included the convection term, and seems to be a more complete formulation of the problem. However, the absence of any sheath allows the electric field to extend a large distance from the probe surface. Regarding the present problem, this fact, together with the electron's small mass and high mobility, can be expected to result in a large effective collecting surface far away from the probe for electrons. Such an approach results in a large perturbed region, and an analysis completely different from Hoult's will be required. It is interesting to note that few laboratory experiments have been conducted for electron collection in a collisional plasma. This is simply due to the difficulty that a positively biased probe will greatly disturb the small volume of plasma generated in the laboratory.

Before proceeding with the solution of the problem at hand, it will be noted that a complete review of the electric probe theory has recently been made by Chung, et al. (29). They systematically discussed the past probe theories in continuum, transitional, and collisionless regime. Their work should be referred to for a better understanding of the present state-of-the-art of electric probes.

## CHAPTER III

## BASIC PARAMETERS AND EQUATIONS FOR A D-REGION BLUNT PROBE

## 3.1 The Composition of the D-Region

The charged particle constituents in the D-region are of interest here. In the normal day time D-region, the primary positive ions were theoretically expected to be  $\text{NO}^+$ ,  $\text{O}_2^+$ , and  $\text{N}_2^+$  (30). The  $\text{N}_2^+$  ion can be removed very rapidly by charge exchange with  $\text{O}_2$  to form  $\text{O}_2^+$ , which in turn charge exchanges with  $\text{NO}$  to form  $\text{NO}^+$ . Thus  $\text{NO}^+$  was suspected to be dominant in the D-region. However, recent in situ measurement (30, 31) of the D-region positive ion composition showed that water derived ions of mass 19 ( $\text{H}_3\text{O}^+$ ), 37 ( $\text{H}_5\text{O}_2^+$ ) and 55 ( $\text{H}_7\text{O}_3^+$ ) predominated below 82 km in the undisturbed D-region, while  $\text{NO}^+$  and  $\text{O}_2^+$  are the major ions above this altitude. To account for these hydrated ions, attempts to find a chain reaction starting with the primary ions  $\text{O}_2^+$  and  $\text{NO}^+$ , leading rapidly to the water clusters are underway. Considerable success in explaining  $\text{O}_2^+$  composition has been made, while  $\text{NO}^+$  is still under investigation. At present, it is generally accepted that the hydrated ions are the major positive ions in the D-region (32).

Initially, it was believed that  $\text{O}_2^-$  was the principal negative ion, since  $\text{O}_2$  is a major neutral constituent and  $\text{N}_2$  does not form a stable negative ion. Some doubt was introduced, when the early observation of the twilight variation of the "polar cap absorption" events showed that the primary response of the D-region was to UV, rather than visible light to which  $\text{O}_2^-$  will undergo photodetachment. Flowing afterglow studies (33, 34) led to the conclusion that  $\text{NO}_3^-$  and its hydrates should be the dominant negative ion and recent observation by Narcisi, et al.

(35), are consistent with this for a normal D-region. The rocket-borne radio wave absorption experiment by Aikin (36) shows that negative ions can be neglected above 70 km during the day in the D-region.

### 3.2 Physical Quantities of the Medium

Three quantities, the mean free path, thermal velocity, and the temperature are considered here.

The elastic cross sections,  $\sigma$ , listed in McDaniel (37), are used to compute the mean free path of neutral-ion collisions and neutral-neutral collisions. The lack of data for the hydrated positive ions ( $\text{H}_5\text{O}_2^+$ ) required the use of  $\sigma$  for  $\text{O}_2^+$ ; this is believed to be a good estimation since the difference of their masses is small. For the computation of the mean free path for electron-neutral collisions, Benson's (38) expression for the collision frequency of electron in the D-region is used. The resultant expressions are as follows:

$$\lambda_{i-n} = \frac{1.3 \times 10^4}{N} \quad (3.2.1)$$

$$\lambda_{n-n} = \frac{1.6 \times 10^{14}}{N} \quad (3.2.2)$$

$$\lambda_{e-n} = \frac{\bar{C}_e}{8.4 \times 10^7 p} \quad (3.2.3)$$

where  $\lambda_{s-n}$  (cm) is the mean free path of the collision between the species, s, and neutral, n, N is the neutral gas density ( $\text{cm}^{-3}$ ), p is the neutral gas pressure (mm Hg, and  $\bar{C}_e$  is the thermal velocity of the electron ( $\text{cm sec}^{-1}$ ). The results are presented in Table 1.

Due to the scarcity of charged particles in D-region, collisions between these species are rare. The mean free path,  $\lambda_{e-i}$ , is estimated to vary between  $10^5$  cm to  $10^7$  cm in the D-region.

Table 1

The Mean Free Path of Charged Particles in the D-Region

Altitude km	The Mean Free Path for Collisions between		
	Electron-Neutral cm	Neutral-Neutral cm	Ion-Neutral cm
90	90	2	1.6
80	20	.56	.455
70	4.2	.082	.067
60	1.2	.024	.020
50	.32	.0082	.0067
40	.08	.0032	.0026

The abundance of collisions between charged particles and neutrals results in good thermal contact between species. Thus, all charged particles and neutrals are taken to have the same temperature. The temperature varies between 200°K to 270°K in the D-region. Using an average temperature of 230°K, the average thermal velocity,  $\bar{C}_s$  which is defined as  $[8kT / (\pi m_s)]^{1/2}$  are  $\bar{C}_n \approx \bar{C}_i = 4.7 \times 10^4 \text{ cm sec}^{-1}$ , and  $\bar{C}_e = 9.5 \times 10^6 \text{ cm sec}^{-1}$ , where  $\bar{C}$  is the thermal velocity, subscripts n, i, and e denote neutrals, ion, and electron, respectively.

### 3.3 Magnetic Field Effect on Probe

The influence of the earth's magnetic field on different processes in a plasma is characterized by the Larmor radius,  $\gamma_L$ , which is defined by  $\gamma_L = m_s v_{\perp s} (eB)^{-1}$ , where  $m_s$  is the mass of the species, s, and  $v_{\perp s}$  is the velocity in the plane perpendicular to the magnetic induction, B. When the magnetic field is weak enough so that the Larmor radius is large compared to length scale of the plasma region perturbed by the probe, the current to the probe is not affected. On the contrary, when the Larmor radius is comparable to or smaller than the relevant dimensions, the current to the probe is affected. Usually, the rms speed  $(3kT m_s^{-1})^{1/2}$  is a good approximation for  $v_{\perp s}$ . According to Alpert et al. (39), B is approximately 0.5 Oersteds below 100 km, thus the Larmor radius of electrons and ions are as follows:  $\gamma_{Le} \sim 1 \text{ cm}$ , and  $\gamma_{Li} \sim 200 \text{ cm}$ . For ion collection, both the probe diameter and the perturbed length scale (which is later found to be  $L R_d^{-1/2}$ ) for a negatively biased probe is smaller than  $\gamma_{Li}$ , so that the magnetic effect can be neglected. However, this conclusion is not so obvious for electron collection (positively biased probe). Above the altitude 60 km, the Larmor radius



is shorter than both the mean free path of electron-neutral collisions and the perturbed characteristic length (which is later found to be  $\phi_w L (8Rd)^{-1/2}$ ); thus the electron current process would be expected to be affected by the magnetic field. Below 60 km, the Larmor radius is larger than the mean free path of electron-neutral collisions, and it is questionable that the Larmor radius is still a characteristic length scale in the same sense noted above; thus this effect will be neglected here.

### 3.4 Interaction of a Biased Probe with the D-Region Plasma

A charged body in a plasma attracts charges of opposite sign; thus, the net active charge is reduced with distance away from the probe and this effect leads to screening. The Debye length is generally used to represent this screening distance, within which the electric field is significant. The usual derivation of the Debye length is outlined as follows:

Consider a sphere of radius,  $R$ , and charge,  $Z_e$ , at rest with respect to a plasma containing, per unit volume, in its undistributed state:  $n_{eo}$  electrons of charge,  $-e$ , and  $n_{io} = n_{eo} Z_i^{-1}$  ions of charge,  $Z_i e$ . The potential distribution is governed by the Poisson equation in spherical coordinates as

$$\frac{1}{\gamma^2} \frac{d}{d\gamma} \left( \gamma^2 \frac{dV}{d\gamma} \right) = 4\pi e^2 (n_e - Z_i n_+) \quad (3.4.1)$$

where  $\gamma$  is the radial distance,  $V$  is the potential and  $n_e$  and  $n_+$  are respectively the electron and ion density at distance,  $\gamma$ . Now assuming local thermodynamic equilibrium, the distribution of particles in the potential field is given by

$$n_e = n_{eo} \exp(\phi) \quad (3.4.2)$$

$$n_i = (n_{eo} / Z_i) \exp(-Z_i \phi) \quad (3.4.3)$$

where  $\phi$  is the nondimensional potential defined as  $eV/(kT_e)$ . For  $Z_i = 1$ , the exponential functions in Eqs. (3.4.2) and (3.4.3) are expanded in series. Combining Eqs. (3.4.1 - 3.4.3), Eq. (3.4.1) becomes

$$\frac{1}{\gamma^2} \frac{d}{d\gamma} \gamma^2 \frac{dV}{d\gamma} = 4\pi e^2 n_{eo} \left[ 2 \left( \frac{eV}{kT_e} \right) + \frac{1}{3} \left( \frac{eV}{kT_e} \right)^3 + \frac{1}{60} \left( \frac{eV}{kT_e} \right)^5 + \dots \right] \quad (3.4.4)$$

with the boundary conditions

$$V(\gamma = \infty) = 0 \quad (3.4.5a)$$

$$V(\gamma = R) = V_w = \frac{1}{4\pi R} \quad (3.4.5b)$$

Consider the special case when we have

$$\frac{1}{6} \phi^2 \ll 1 \quad (a)$$

With the exception of the first term, other terms in the R.H.S. of Eq. (3.4.4) can be neglected and its solution is

$$V = V_w \frac{R}{\gamma} \exp[-2^{1/2} (\gamma - R) \lambda_D^{-1}] \quad (3.4.6)$$

where

$$\lambda_D = \left( \frac{kT_e}{4\pi e^2 n_{eo}} \right)^{1/2} \quad (\text{cgs}) \quad (3.4.7)$$

Now, at the distance of one Debye length from the surface, the potential is given by

$$V(R + \lambda_D) = V_w \frac{R}{R + \lambda_D} \exp(-2^{1/2}) \quad (3.4.8)$$

Combining the inequality (a) and Eq. (3.4.8), we have

$$\frac{R}{R + \lambda_D} << \frac{kT_e}{eV_w} \exp(2^{1/2}) \quad (b)$$

The inequality (b) and the local thermodynamic equilibrium are two prerequisite conditions for Eq. (3.4.6) to be a valid description of the potential distribution. To satisfy the inequality (b), it requires either the size of the sphere ( $R$ ) is infinitesimally small or  $\phi_w << 1$  for a sphere of arbitrary size. According to Öpik (27), the requirement of having local thermodynamic equilibrium over the decay length has a bearing only for large values of  $\phi$ ; for small values the state of equilibrium is irrelevant. It is obvious that the Coulomb field is essentially damped for  $(\gamma - R) > \lambda_D$ . For this reason, the Debye length is used as the screening distance of a charged body. Assuming the electron number density in the D-region is about  $1000 \text{ cm}^{-3}$  at 80 km and  $100 \text{ cm}^{-3}$  at 50 km, the Debye length is 3 cm at 80 km and 12 cm at 50 km.

In the D-region, the average temperature of the electrons is approximately 230°K; this is one order of magnitude less than the plasma electron temperature (3000°K) usually considered in analysis. With this low temperature, and the available data on potential at which blunt probe measurements were made, it is found that the assumption  $\phi_w << 1$  cannot be satisfied throughout the D-region. Accordingly, the use of the Debye length as an indicator of screening (sheath) thickness is at

best approximate here, since the experiment does not meet the assumption of the derivation. It is natural, at this stage, to speculate that the screening distance will be a function of  $\lambda_D$  and  $\phi_v$ . However, a basic question to investigate, as will be done in section 3.6, is whether the concept of a screening distance (sheath) is appropriate in the present problem.

In the study of the transport of the particles to the biased probe at rest, the concepts of drift velocity and diffusion are involved. For a weakly ionized plasma, each species of charged particles independently diffuses through the neutral gas. The diffusive motion is retarded by random collisions with the gas molecules. This diffusive flow, which due to a gradient in a composition, can be superimposed on other types of flow which might be produced by external fields or by gradients in the total pressure. The diffusive flow velocity  $w$  is given by

$$w = \frac{-D_s}{n} \nabla n \quad (3.4.9)$$

where  $\nabla n$  is the gradient of the number density,  $n$ , of the diffusing particles, and  $D_s$  is the diffusion coefficient of species  $s$ , which is a joint property of the particles and the medium through which they are diffusing.

When an ion moves through a gas under the influence of a static uniform electric field,  $E$ , the ionic motion consists of a slow uniform drift in the field direction superimposed on the much faster random motion. For  $E/P$  small and constant, the drift velocity of the ion,  $V_D$ , is

$$V_D = \mu E \quad (3.4.10)$$

where  $\mu$ , the constant of proportionality, is called the mobility of the ions.

Now, consider a cloud of charged particles diffusing through a uniform gas, and we apply an electric field in the opposite direction of a strength to balance the tendency of diffusion. Thus, equating the two velocities ( $w$ ,  $V_D$ ) and assuming that the ions are in thermal equilibrium with gas, one obtains the Einstein relation

$$\frac{\mu}{D_s} = \frac{e}{kT} \quad (3.4.11)$$

This relation should not be used indiscriminantly. It is valid only for ions at low  $E/P$ , but not for electrons and ions at high  $E/P$ . The very capability of the electron to be accelerated rapidly by the electric field and to lose relatively small energy in elastic collisions, results in the electron drift velocity no longer being a linear function of the applied electric field intensity.

### 3.5 Similarity Parameters

For any probe-plasma interaction problem, the physical process is characterized by a set of nondimensional parameters. These parameters are obtained by reducing the governing equations (continuity, momentum, energy, and charge conservation) to dimensionless form. For similar processes, these parameters will have the same numerical values. Only those pertinent to the present problem are discussed here.

For the neutral gas, the usual fluid mechanical parameters which appear in the continuity and momentum equations are the Mach number,  $M$ ,

and the Reynolds number,  $Re$ . The Mach number is defined as  $|v|/c$ , where  $v$  is the flow velocity, and  $c$  is the local sonic speed. For  $M \rightarrow 0$ , the fluid is incompressible, i.e.,  $\nabla \cdot q = 0$ . In fact, appreciable effects of compressibility are rarely encountered in a steady state in which  $M$  does not exceed 0.5. (The main exception is free convection, in which buoyancy is the very cause of the motion.) For a typical ARCAS rocket payload drifting down with a parachute drag system, the free stream velocity,  $\bar{U}$  is 100 m/sec,  $L \sim 10$  cm, so the free stream Mach number,  $M_0$ , is estimated (7) to be 0.3. Thus in the present case, the neutral gas flow is effectively incompressible. The Reynolds number characterizes the viscosity and the inertial force and is defined as  $Re = VL \nu^{-1}$  where  $\nu$  is the kinematic viscosity. For a body immersed in a flow, the reciprocal of the square root of the Reynolds number is a measure of the thickness of the surface boundary layer where viscosity is significant. This parameter can also provide an indication of the degree of turbulence in the boundary flow. In the present problem, the Reynolds number is estimated to be 500 at 50 km and 10 at 80 km. Thus, for such a small number, the neutral gas flow over the blunt probe is laminar.

For the charged particles, the parameters involved are the Schmidt number,  $Sc_s$ , and the electrical Reynolds number,  $Rd_s$ , where suffix,  $s$  denotes the species. Schmidt number for each species is defined as  $Sc_s = \nu D_s^{-1}$  where  $D_s$  is the coefficient of diffusion of that species. It is the ratio of transport of momentum by viscosity and the transport of charge particles. For electrons, the diffusion coefficient can be found from McDaniel (37). It has been estimated (7) that  $Sc_1 \sim 2$  at 50 km

and 1 at 80 km. Electrical Reynolds number is the product of the Reynolds number and the Schmidt number. For a negatively biased probe immersed in a plasma flow,  $(Rd^{-1/2})$  is a measure of the thickness of the surface layer where diffusion (ambipolar when the motion of charged particles is coupled, free when they are uncoupled) is significant.

As a summary to the above discussions, various length scales and parameters with altitudes are plotted in Table 2.

### 3.6 Zero Space Charge Theory

We shall consider a parachute-borne, subsonic, electrostatic blunt probe at a specified (positively and negatively biased) potential, in a steady, incompressible flow with frozen chemistry and singly ionized plasma. The motion of the neutral gas is assumed unaffected by the charged particles, and any geomagnetic effects are not considered.

The potential distribution is determined by Poisson's equation as

$$\nabla^2 V = -4\pi e (n_+ - n_- - n_e) \quad (3.6.1)$$

where  $V$  is the potential,  $n_s$  is the number density of species  $s$ , and subscripts  $(+, -, e)$  denotes positive ion, negative ion, and electron respectively. The nondimensional variables are defined as

$$\tilde{V} = V/L \quad (3.6.2)$$

$$\tilde{n} = n/n_{eo} \quad (3.6.3)$$

$$\lambda_D = kT_e / (4\pi n_{eo} e^2) \quad (3.6.4)$$

$$\phi = eV / (kT_e) \quad (3.6.5)$$

Table 2

Dimensionless Parameters and Various Length Scales in the D-Region

	80 km	50 km
Altitude		
Mach number	0.3	0.3
Viscous Reynolds number	10	500
Electrical Reynolds number	10	1000
Viscous boundary layer thickness	3.16 cm	0.45 cm
Electric boundary layer thickness	3.16 cm	0.316 cm
Debye length	3 cm	12 cm
Electron-neutral mean free path	20 cm	.32 cm
Ion-neutral mean free path	1.6 cm	0.0067 cm



$$\alpha = \lambda_D / L \quad (3.6.6)$$

$$\tilde{q} = q / \bar{U} \quad (3.6.7)$$

where  $\nabla \cdot$  is the divergence operator,  $n_{eo}$  is the ambient electron density,  $\lambda_D$  is the Debye length,  $T_e$  is the electron temperature,  $L$  is the probe diameter,  $q$  is the flow velocity, and  $\bar{U}$  is the free stream velocity. The nondimensional potential,  $\phi$ , is normalized by wall potential,  $\phi_w$ . We have

$$\phi = \phi_w \quad u \quad (3.6.8)$$

where  $u = V/V_w$ . Substituting Eqs. (3.6.2 - 3.6.8) into Eq. (3.6.1), dropping the tilde, we have

$$\alpha^2 \phi_w \nabla^2 u = n_- + n_e - n_+ \quad (3.6.9)$$

For a blunt probe diameter of 10 cm, and the Debye length varying between 3 cm at 80 km and 12 cm at 50 km, the nondimensional Debye length,  $\alpha$ , is 0.3 at 80 km and 1.4 at 50 km. Notice here that the parameter  $\alpha$  is affected by the probe diameter. For a probe potential of 1 Volt,  $\phi_w \sim 43$  at 50 km, 58 at 80 km. Thus  $\alpha^2 \phi_w$  is a large parameter. The potential,  $u$  can then be written as an expansion in  $\alpha^2 \phi_w$ , that is

$$u = u_0 + \frac{1}{\alpha^2 \phi_w} u_1 + \frac{1}{(\alpha^2 \phi_w)^2} u_2 + \dots \quad (3.6.10)$$

where  $u_n$  is the  $n$ th order correction of the potential,  $u$ . Substituting Eq. (3.6.10) into Eq. (3.6.9), dividing by  $\alpha^2 \phi_w$ , and equating the same order term, the zeroth order term is

$$\nabla^2 u_0 = 0 \quad (3.6.11)$$

So, with an error of order  $(\alpha^2 \phi_w)^{-1}$ , Eq. (3.6.11) can be written as

$$\nabla^2 u = 0 \quad (3.6.12)$$

Thus the potential field is given to the first order approximation, by the Laplace equation, Eq. (3.6.12). This simplification is due to the low number density of charged particles ( $\alpha \sim 0(1)$ ) and the high wall potential ( $\phi_w \gg 1$ ).

Another way to look at this approximation is to make use of the superposition principle of the field. The field at any location in the plasma is actually the sum of the field due to the applied field in a vacuum,  $\nabla u_{app}$ , and the field due to the spatial distribution of the charged particles,  $\nabla u_{sp}$ . We have

$$\nabla u = \nabla u_{app} + \nabla u_{sp} \quad (3.6.13)$$

where

$$\nabla^2 u_{app} = 0 \quad (3.6.14)$$

$$\nabla^2 u_{sp} = n_- + n_e - n_+ \quad (3.6.15)$$

Now, if  $\nabla u_{app} \gg \nabla u_{sp}$ , we have

$$\nabla u \approx \nabla u_{app} \quad (3.6.16)$$

Taking the divergence of Eq. (3.6.16), we have

$$\nabla^2 u = 0 \quad (3.6.17)$$

With the electrostatic field described by the Laplace equation, the field will extend naturally to infinity, and it is no longer

confined only to a thin region adjacent to the probe, as it is in most probe-plasma interaction cases of interest. Physically, this is due to the fact that the low charged particle density in the D-region inadequately shields the plasma from the probe potential. This results in the field influenced region being large in comparison with the probe diameter. Outside the viscous boundary layer, the electrons with lighter masses, higher mobility will be dominated by the field effect, while the ions which are heavier, and less mobile, are governed by the flow mechanics. The fact that these two species are governed by entirely different forces in this case will exclude any ion-electron paired motion; thus, an ambipolar diffusion is not possible here. With this same line of reasoning, an alternate explanation is now provided to explain the existence of that ambipolar diffusion region found by Lam (21). The main point in that case is that the thin sheath assumed by Lam shields the outer region from the probe's potential. Thus, outside the sheath, electrons and positive ions are governed by the same neutral flow and the same diffusion process (see Lam's Eq. (4.1)). Being governed by the same processes, the positive ions and electrons will behave similarly despite their different polarity. Thus, the neutrality condition still holds outside the sheath which is often referred to as the ambipolar diffusion region.

Using the Laplace equation, Lam's (21) nondimensional species mass conservation equations become

$$Rd \, q \cdot \nabla n_+ - \nabla n_+ \cdot \nabla \phi - \nabla^2 n_+ = 0 \quad (3.6.18)$$

$$Rd \, q \cdot \nabla n_- - \nabla n_- \cdot \nabla \phi - \nabla^2 n_- = 0 \quad (3.6.19)$$

$$\beta Rd \, q \cdot \nabla n_e - \nabla n_e \cdot \nabla \phi - \nabla^2 n_e = 0 \quad (3.6.20)$$

with

$$\beta = \frac{D_i}{D_e} \approx \left( \frac{m_e}{m_i} \right)^{1/2}, \quad Rd = \frac{\bar{U}L}{D_i} \quad (3.6.21)$$

where  $m_e$  and  $m_i$  denotes the mass of electron and ion respectively. The mobility of ion and electron have been related to their diffusion coefficients by means of the Einstein relation. Notice that the species equations (Eqs. (3.6.18 - 3.6.21)) are decoupled, and each species will behave independently. The boundary conditions on charge density and potential far away from the probe are

$$n_+ (\infty) = 1 + \lambda \quad (3.6.22)$$

$$n_- (\infty) = \lambda \quad (3.6.23)$$

$$n_e (\infty) = 1 \quad (3.6.24)$$

$$\phi (\infty) = 0 \quad (3.6.25)$$

where  $\lambda$  is the ratio of negative ion density to the electron density at infinite distance from the probe. Assuming a perfectly absorbing probe surface, the boundary conditions at the probe surface are:

$$n_+ (0) = 0 \quad (3.6.26)$$

$$n_- (0) = 0 \quad (3.6.27)$$

$$n_e (0) = 0 \quad (3.6.28)$$

$$\phi(o) = \phi_w \quad (3.6.29)$$

It is interesting to note that, by combining Eqs. (3.6.18 - 3.6.20) one can obtain Touryan and Chung's (22) set of ambipolar equations, Eqs. (16-18), which was based on the assumption of a thin sheath on the probe surface. The difference of the charged particle dynamics in present case and that in Touryan's ambipolar region is obvious. In the present case, charged particles, being independent of each other's motion, move according to their own transport properties ( $\mu$ ,  $D$ ) and the influence of the neutral gas flow. Charged particles in the ambipolar diffusion region, however, have to satisfy the neutrality condition, i.e.,  $n_+ = n_- + n_e$ ; thus charged particles of opposite charge are, relatively speaking, attached to each other, and they travel together. Their motion depends on the influence of the neutral gas flow and a joint transport coefficient (ambipolar diffusion coefficient) of both species. Furthermore, the quasi-neutrality condition of the ambipolar diffusion region cannot be satisfied very near the wall where the sheath concept is needed to remove this singularity. Whereas, in the present case, the same set of equations, Eqs. (3.6.18 - 3.6.20), can be used for all locations.

## CHAPTER IV

## SUBSONIC CONTINUUM BLUNT PROBE THEORY

## 4.1 Introduction

It is appropriate to start the analytic problem with a discussion of the general method of treating the equations. The governing linear differential equation, the species conservation equation, is nondimensionalized to reveal the similarity parameters; similar processes have the same numerical parameters. A limiting (very small) numerical value of the parameter preceding the highest derivative term will serve to define a length scale, and hence the thickness of the perturbed region; the medium will be divided into two distinct regions. The outer region, with the order of the governing partial differential equation (PDE) lowered, is unperturbed. The species number density in the outer region is the same as that at an infinite distance away from the probe. The inner region, governed by the same order PDE as the original equation, but with fewer terms, is perturbed.

When the body length (diameter) is much larger than the perturbed characteristic length, the mathematics is simplified, and a boundary layer problem presents itself. In the inner region, with the exception of the convection term, all variation of physical quantities with the coordinate normal to the body surface is relatively negligible. Despite this simplification, the PDE is still difficult to solve due to the presence of the convection term which is still a function of all coordinates considered. The equation can be simplified further if the system considering has similarity. Mathematically, this means that a transformation can be found to reduce the PDE to an ordinary differential

equation. The resultant equation can, of course, be solved readily.

#### 4.2 Ion Collection Theory

The electric field distribution of the blunt electrostatic probe is first considered. The collector is mounted on the forward facing end of a right circular cylinder; the return electrode is at the rear and the side wall surfaces are insulator. With the space charge effect neglected, the electric potential field of a circular disc will be a very good approximation for the present probe potential distribution; the solution is readily available (40).

For a circular disc of radius,  $a$ , wall potential,  $V_w$ , and coordinates  $(y, d, r)$  as shown in Figure 3, the electric field,  $E$ , in two interested cases, are as follows:

$$|E| = \frac{2aV_w}{\pi r^2} \quad \text{for } r \gg a \quad (4.2.1)$$

$$E_y = \frac{-2V_w}{\pi a} \quad \text{for } r \ll a \quad (4.2.2a)$$

$$E_d = 0 \quad (4.2.2b)$$

where  $E_d$  and  $E_y$  are the electric fields in the  $d$  and  $y$  direction respectively.

##### 4.2.1 Attracted Ions

A positively biased probe is first considered. Negative ions and electrons are attracted to the probe; positive ions are repelled, but will find their way to the other (return) electrode where they lose

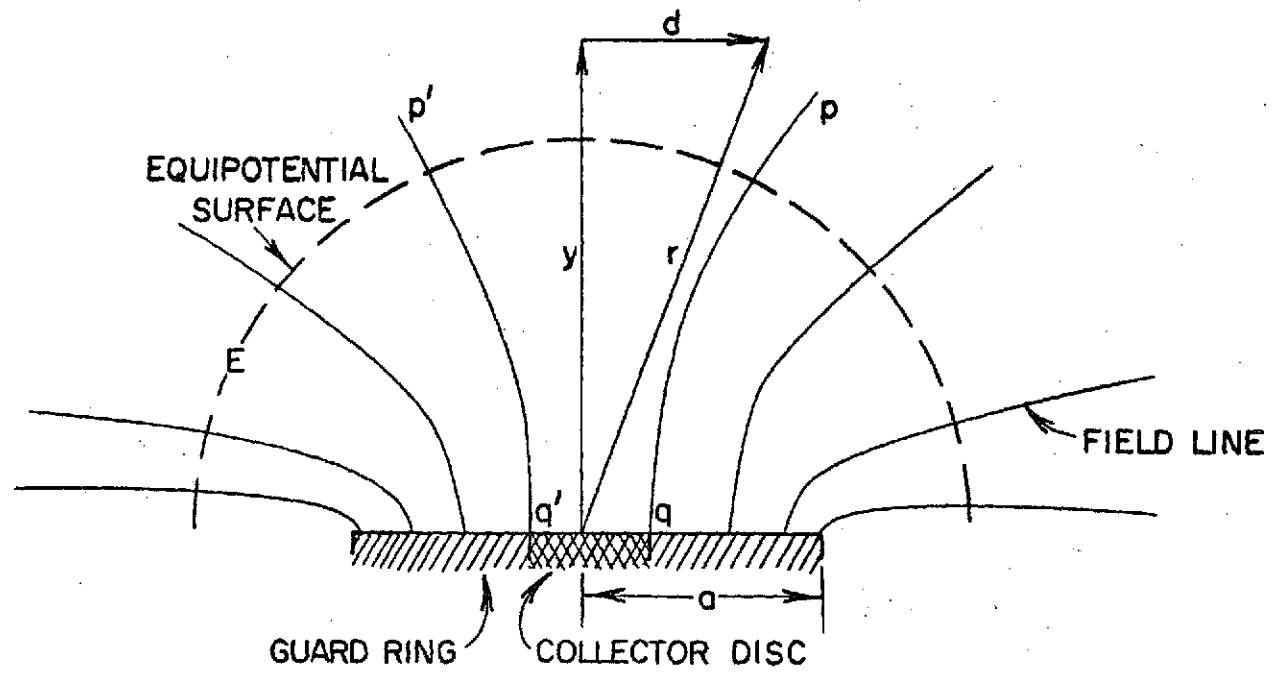


Figure 3. Electric Field of a Charged Circular Disc



their charges. The mass conservation equation of the negative ion is

$$Rd \, q \cdot \nabla n_- + \nabla \phi \cdot \nabla n_- - \nabla^2 n_- = 0 \quad (4.2.3)$$

with boundary conditions

$$n_-(\infty) = \lambda \quad (4.2.4a)$$

$$n_-(0) = 0 \quad (4.2.4b)$$

In the D-region,  $Rd \gg 1$ , so we can represent  $n_-$  by an asymptotic expansion as

$$n_- = n_{0-} + Rd^{-1} n_{1-} + Rd^{-2} n_{2-} + \dots \quad (4.2.5)$$

where  $n_{n-}$  is the  $n^{\text{th}}$  order correction. Substitute Eq. (4.2.5) into Eq. (4.2.3), divide by  $Rd$ , and equating the zeroth order term, we have

$$q \cdot \nabla n_{0-} = 0 \quad (4.2.6)$$

With an error of order  $(Rd^{-1})$ , we rewrite Eq. (4.2.6) as

$$q \cdot \nabla n_- = 0 \quad (4.2.7)$$

Note that the flow velocity,  $q$ , has been assumed of order 1 when equating various order terms. Naturally, this is correct only when the thickness of the electric boundary layer is larger or comparable to the viscous boundary layer thickness as in the present case. Eq. (4.2.7) implies that the negative ions here are not affected by probe potential and diffusion process can be neglected. Furthermore, the neutral flow

velocity,  $q$ , does not interact with the density gradient,  $\nabla n_-$ . Therefore, negative ion density is not perturbed and remains as a constant. That is, outside the electric boundary layer,

$$n_- = \lambda = n_{-0}/n_{e0} \quad (4.2.8)$$

The physical picture changes near the wall. The negative ion boundary condition of zero number density at the wall requires a large negative ion density gradient very near the wall. This region is investigated by stretching the normal coordinates with a dimensionless length scale,  $\delta_1$ . Let  $\bar{y} = y/\delta_1$ , and assume  $\delta_1 \ll 1$ . Substitute  $\bar{y}$  into Eq. (4.2.3), and in terms of the coordinates shown in Figure 4, we have

$$\begin{aligned} \text{Rd} \left( u \frac{\partial n_-}{\partial x} + v \frac{\partial n_-}{\partial y} \right) + \left( \frac{\partial \phi}{\partial x} \frac{\partial n_-}{\partial x} + \frac{1}{\delta_1^2} \frac{\partial \phi}{\partial y} \frac{\partial n_-}{\partial y} \right) - \\ \left( \frac{\partial^2 n_-}{\partial x^2} + \frac{1}{\delta_1^2} \frac{\partial^2 n_-}{\partial y^2} \right) = 0 \end{aligned} \quad (4.2.9)$$

The  $y$ -derivative of the convection term is not scaled because it is of the same order of the corresponding  $x$ -derivative term in all locations. To balance the convection term with the highest derivative term, it requires that

$$\delta_1 = \text{Rd}^{-1/2}$$

which is identified as the dimensionless thickness of the electric boundary layer. Neglecting terms of order  $(\text{Rd}^{-1/2})$ , we have

$$\left( u \frac{\partial n_-}{\partial x} + v \frac{\partial n_-}{\partial y} \right) + \frac{\partial \phi}{\partial y} \frac{\partial n_-}{\partial y} - \frac{\partial^2 n_-}{\partial y^2} = 0 \quad (4.2.11)$$

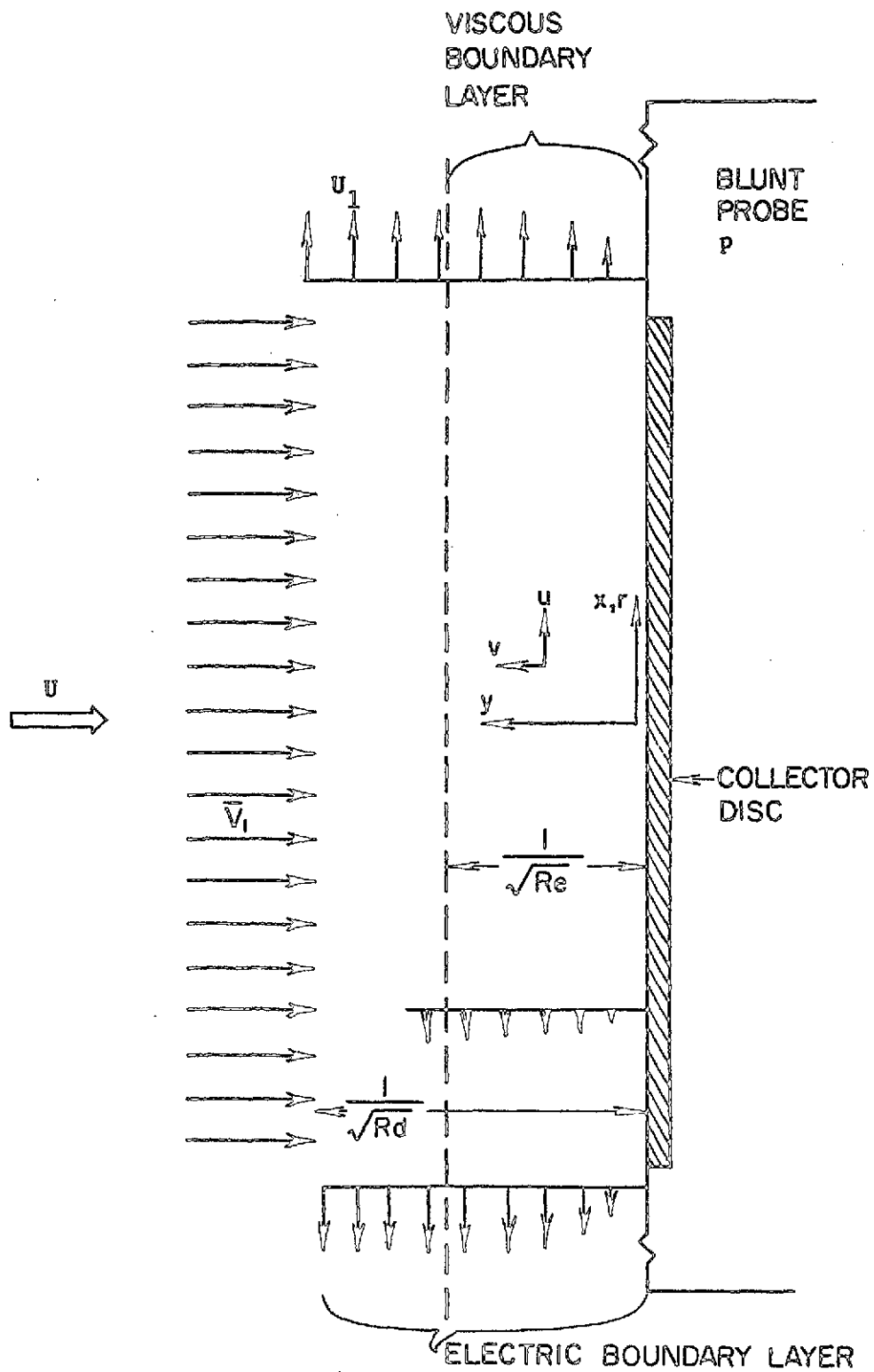


Figure 4. Axisymmetric Stagnation Flow Over the Blunt Probe

which is called the electric boundary layer equation. When equation (4.2.11) is rewritten in dimensional form (except  $n_-$ ), we have

$$\rho u \frac{\partial n_-}{\partial x} + \rho v \frac{\partial n_-}{\partial y} = \rho D \frac{\partial^2 n_-}{\partial y^2} - \left( \frac{De}{kT} \rho \frac{\partial v}{\partial y} \right) \frac{\partial n_-}{\partial y} \quad (4.2.12)$$

with boundary conditions

$$n_- (y = 0) = 0 \quad (4.2.13a)$$

$$n_- (y = \infty) = \lambda \quad (4.2.13b)$$

It must be noted that Eq. (4.2.12) is valid only inside the thin electric boundary layer of  $Re^{-1/2}$  thick, and when  $y \rightarrow \infty$  in Eq. (4.2.13b), the boundary condition merely corresponds to the outer edge of the electric boundary layer. Since the electric boundary layer is thin, the electric field,  $E_y$ , is essentially constant inside this layer. From Eq. (4.2.2), we have

$$E_y = \frac{-2V_w}{\pi a} \quad (4.2.14)$$

The physical picture for the migration of negative ions to a moving positively biased blunt probe is as follows. Negative ions coming to the probe by entrainment in the neutral flow are unperturbed until they enter the electric boundary layer. Inside the electric boundary layer, convection, mobility and diffusion all contribute to the flux, and hence to the spatial distribution of the negative ions. The neutral gas flow velocity ( $u, v$ ) governed by the neutral gas momentum equation (4.2.12) is the same as Eq. (7) in Sonin's (26) work, the only exception is that the present case is simpler due to the assumed constancy of the

neutral gas density. Sonin's solution is outlined in Appendix A. The solution obtained for a negative-ion density gradient at the surface of the probe is

$$\left( \frac{\partial n_-}{\partial \eta} \right)_{\eta=0} = \left( \frac{2Sc}{\pi} \right)^{1/2} \frac{\exp \left[ - \frac{\hat{E}^2 / 4ScRes}{1 + \operatorname{erf} \left[ \hat{E} / (4ScRes)^{1/2} \right]} \right]}{1 + \operatorname{erf} \left[ \hat{E} / (4ScRes)^{1/2} \right]} \quad (4.2.15)$$

with

$$\hat{E} = \frac{ea}{kT_e} E_y \quad (4.2.16)$$

and

$$Res = \frac{ga^2}{\nu} \quad (4.2.17)$$

where  $\eta$  is a boundary layer coordinate (see Appendix A),  $Sc$  is the Schmidt number of the negative ion which is approximately the same as that of the positive ion,  $Res$  is the Reynolds number based on the stagnation condition,  $g$  is the stagnation point inviscid flow velocity gradient, and  $\nu$  is the kinematic viscosity of the neutral gas.

The negative current density,  $dI_-$ , to the collector disc is

$$dI_- = (n_{-0} e n_- v_-)_y = 0 \quad (4.2.18)$$

where  $v_-$  is the negative ion velocity due to diffusion and mobility, that is,

$$v_- = \frac{D \nabla n_-}{n_-} - \mu E \quad (4.2.19)$$

Therefore, substituting Eq. (4.2.19) into Eq. (4.2.18), and dividing both sides by  $en_{-0}a$ , we have

$$\frac{dI_-}{en_{-0}ga} = \frac{D}{ga} \left( \nabla n_- \right)_{\eta=0} \quad (4.2.20)$$

$$\frac{dI_-}{en_{-0}ga} = \left( \frac{2}{Res} \right)^{1/2} \frac{1}{Sc n_{-0}} \left( \frac{\partial n_-}{\partial \eta} \right)_{\eta=0} \quad (4.2.21)$$

Combining Eqs. (4.2.21) and 4.2.15), we have

$$\frac{dI_-}{en_{-0}ga} = 2 \left( \frac{1}{\pi Sc Res} \right)^{1/2} \frac{\exp \left[ -(\hat{E}^2/4ScRes) \right]}{1 + \operatorname{erf} \left[ \hat{E}/(4ScRes)^{1/2} \right]} \quad (4.2.22)$$

Following Sonin (26), when the strong field condition is satisfied, i.e.,  $\hat{E} (4ScRes)^{-1/2} \gg 1$ , Eq. (4.2.22) can be written as

$$\frac{dI_-}{en_{-0}ga} = \frac{-\hat{E}}{ScRes} \quad (4.2.23)$$

Using the Einstein relation, Eq. (4.2.23) can be reduced to

$$dI_- = -en_{-0} \mu E \quad (4.2.24)$$

Thus when the attracting field in the electric boundary layer satisfies the strong field condition, the electric field effect will overshadow the flow effects and become the governing factor in ion collection.

Notice that Eq. (4.2.24) is exactly the same expression for ion current predicted by Hoult's theory.

The above analysis is done for a positively biased probe. When instead, the response of the positive ions to a negatively biased probe is considered, the negative sign in Eq. (4.2.12) will change to positive,  $n_-$  to  $n_+$ , and the resultant equation corresponding to Eq. (4.2.24) is

$$dI_+ = en_{+0} \mu E \quad (4.2.25)$$

#### 4.2.2 Repelled Ions

For a positively biased probe, the mass conservation equation for positive ions is

$$Rd \, q \cdot \nabla n_+ - \nabla \phi \cdot \nabla n_+ - \nabla^2 n_+ = 0 \quad (4.2.26)$$

with boundary conditions

$$n_+(\infty) = 1 + \lambda \quad (4.2.27a)$$

$$n_+(0) = 0 \quad (4.2.27b)$$

With the exact same procedure as outlined the previous section, we have

$$\frac{dI_+}{en_{+0}ga} = \frac{2}{(\pi ScRes)^{1/2}} \frac{\exp[-(\hat{E}^2/4ScRes)]}{1 - \operatorname{erf}[\hat{E}/(4ScRes)^{1/2}]} \quad (4.2.28)$$

For strong field condition, Eq. (4.2.28) can be reduced to

$$\frac{dI_+}{en_{+0}ga} = 2 \frac{\exp[-\hat{E}^2/4ScRes]}{(\pi ScRes)^{1/2}} \quad (4.2.29)$$

Notice that the current density  $dI$  is negligibly small for

$$\hat{E} (4ScRes)^{-1/2} \gg 1.$$

The corresponding solution for the negative ions to a negatively biased probe is

$$\frac{dI_-}{en_{-0}ga} = \frac{2}{(\pi ScRes)^{1/2}} \frac{\exp[-(\hat{E}^2/4ScRes)]}{1 + \operatorname{erf}[\hat{E}/(4ScRes)^{1/2}]} \quad (4.2.30)$$

$$\frac{dI_-}{en_0ga} = \frac{2 \exp [-(\hat{E}^2/4ScRes)]}{(\pi ScRes)^{1/2}} \quad (4.2.31)$$

To satisfy the strong field condition, a higher probe potential is required at lower altitudes, where the electric Reynolds number is larger. For a strong probe potential, the current of the repelled ions to the probe is negligibly small.

#### 4.2.3 Justification of Hoult's Ionic Theory in the D-Region

Hoult's (7) ion collection blunt probe theory has been widely used for the D-region ionic data interpretation. This theory is based on a bold assumption that the convection is completely dominant until very close to the wall where mobility and diffusion abruptly dominate the transport of the charge particles. Hoult's prediction of the linear variation of the current with voltage is well supported by blunt probe data in the D-region (41).

The previous section has shown that Sonin's ionic theory is equivalent to Hoult's theory provided the strong field condition,  $\hat{E} (4 ScRes)^{-1/2} \gg 1$ , is satisfied. To explain the capability of Hoult's oversimplified model giving an experimentally verified prediction, it is logical to see whether the strong field condition is satisfied in the D-region. The available blunt probe data, which gives the potential of the negatively biased probe at which measurements were made, is the Eclipse data (42). The radius of the probe,  $a$ , is 10.3 cm, the free stream velocity,  $U$ , is 100 m/sec.

With

$$D_e = \frac{kT_e}{m_e v_e} \quad (4.2.32)$$



and

$$\beta = (m_e/m_-)^{1/2} \quad (4.2.33)$$

The strong field parameter is reduced to

$$\frac{\hat{E}}{\sqrt{4ScRes}} = e \frac{a}{4UkT_e \sqrt{m_e m_-}}^{1/2} \frac{E_y}{(\nu_e)^{1/2}} \quad (4.2.34)$$

where  $\nu_e$  is the electron collision frequency with the neutrals, and  $m_-$  is the mass of the negative ion. By substituting the constants, we obtain

$$\frac{\hat{E}}{\sqrt{4ScRes}} = 3.36 \times 10^3 \frac{E_y}{(\nu_e)^{1/2}} \quad (4.2.34)$$

This measuring probe potential,  $V_w$ , is approximately the middle point of the range of the potential at which the negatively biased probe is collecting positive ion current. The following computation is done for the data obtained from the launch (D16) on 12 Nov 1966, and the launch (Cert) on 5 Nov 1966, during a solar eclipse (42). The results are tabulated in Table 3 and Table 4.

The result clearly shows that the strong field condition  $(\hat{E} (4ScRes)^{-1/2} \gg 1)$  is satisfied throughout all altitude of interest. Hoult's ionic collection theory, thus is an adequate theoretical model to be used for ionic data interpretation in the D-region.

### 4.3 Electron Collection Theory

#### 4.3.1 Stationary Blunt Probe Theory

Before proceeding directly to the moving blunt probe analysis, the limiting solution of a zero velocity blunt probe is first discussed here. The governing equations are as follows:

Table 3

Evaluation of the Strong Field Parameter for Data from "D-16"

	Altitude (km)							
	45	50	55	60	65	71	77	80
Range of probe potential (Volt)	-20 0	-20 0	-20 0	-20 0	-15 0	-15 0	-15 0	-15 0
Probe potential during measurement $V_w$ (Volt)	-10	-10	-10	-10	-7.5	-7.5	-7.5	-2.5
Wall electric field $E_y$ (Volt/m)	62	62	62	62	46	46	46	15
Electron-neutral collision frequency $\nu_e$ (sec <sup>-1</sup> )	$6.3 \times 10^7$	$3.2 \times 10^7$	$1.6 \times 10^7$	$8.4 \times 10^6$	$4.6 \times 10^6$	$2.2 \times 10^6$	$8 \times 10^5$	$5 \times 10^5$
Strong field parameter $E/(4ScRes)^{1/2}$	26.2	36.8	52	72	72	104	173	171

Table 4

Evaluation of the Strong Field Parameter for Data from "Cert"

	Altitude (km)							
	45	50	55	60	67	70	76	80
Range of probe potential (Volt)	-20 0	-20 0	-16 0	-14 0	-17 0	-17 0	- 7 0	- 4 0
Probe potential during measurement $V_w$ (Volt)	-10	-10	- 8	- 7	- 8.5	- 8.5	- 3.5	- 2
Wall electric field $E_y$ (Volt/m)	64	64	51	45	54	54	22	13
Electron-neutral collision frequency $\nu_e$ (sec <sup>-1</sup> )	$6.3 \times 10^7$	$3.2 \times 10^7$	$1.6 \times 10^7$	$8.4 \times 10^6$	$3.4 \times 10^6$	$2.4 \times 10^6$	$8.2 \times 10^5$	$5 \times 10^5$
Strong field parameter $E/(4ScRes)^{1/2}$	27	38	43	52	98	122	83	148

$$\nabla^2 n_e - \nabla \phi \cdot \nabla n_e = 0 \quad (4.3.1)$$

$$\nabla^2 \phi = 0 \quad (4.3.2)$$

with the boundary conditions

$$\begin{aligned} n_e(\infty) &= n_{eo}, & n_{e \text{ surface}} &= 0 \\ \phi(\infty) &= 0, & \phi_{\text{surface}} &= \phi_w \end{aligned}$$

where the subscript, surface, denotes conditions at the probe surfaces. The corresponding boundary configuration is shown in Figure 5a. Notice that this configuration does not form a closed boundary surface.

The basic requirement for the solvability of the above two elliptic, linear, second order partial differential equation is knowing the conditions on closed boundary surface such as the one shown in Figure 5b. In view of this difficulty of the present problem, the blunt probe is represented by an oblate spheroid. Letting the spheroid thickness go to zero, the blunt probe becomes a two-sided disc as shown in Figure 6a. This model, crude as it is, will give a first-order approximation of the real voltage-current characteristics of the blunt probe.

In the special case when a thin sheath exists on the probe surface, physical quantities will be independent of the coordinate normal to the probe surface. The governing equations will be two coupled, second order ordinary differential equations and these have been solved by Su and Kiel (43).

The present problem in its reduced form as shown in Figure 6a, has been analyzed by Stahl and Su (44). An analytic solution was

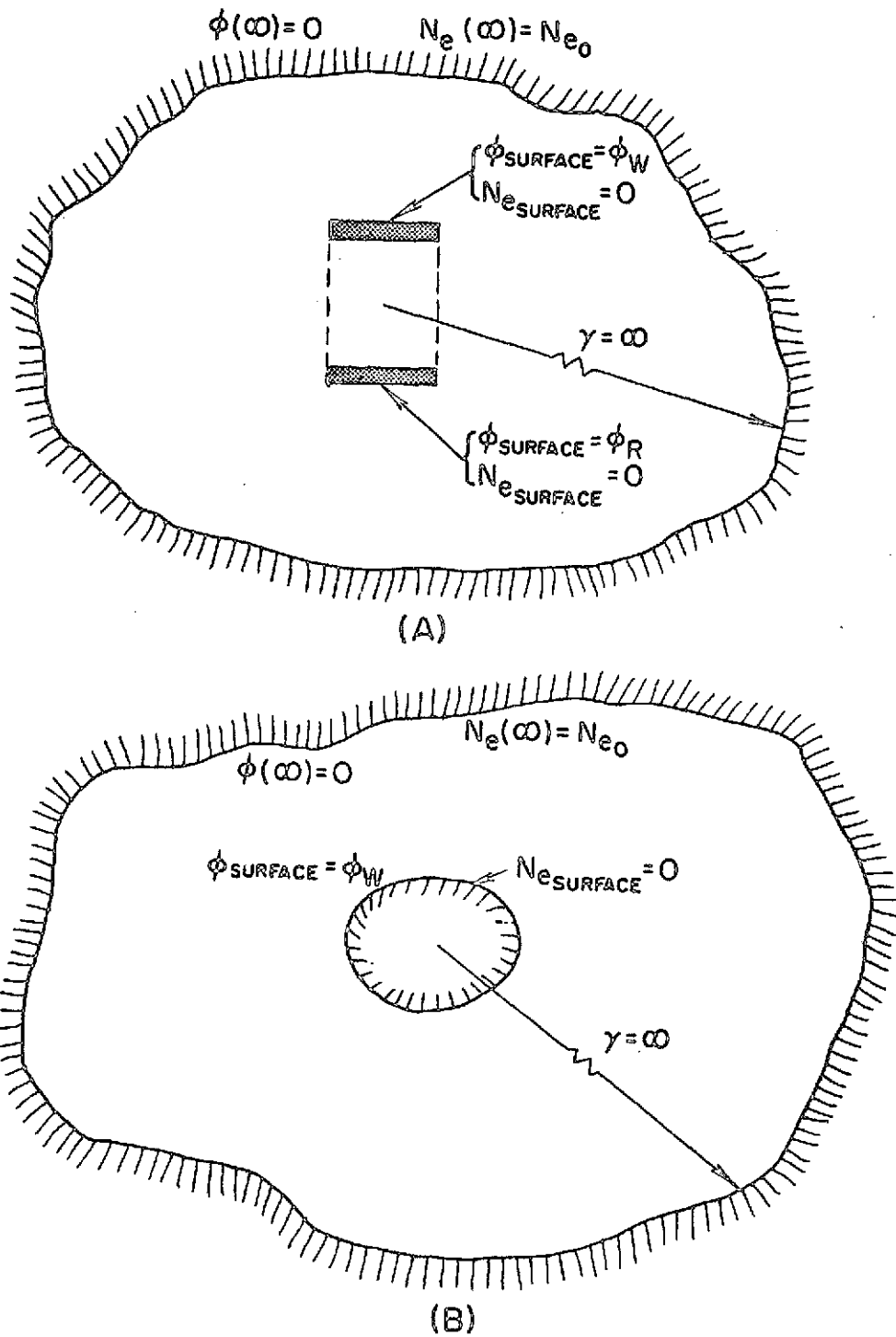


Figure 5. Boundary Surfaces of the Perturbed Plasma:  
 (A) Open Boundary Surface, (B) Closed Boundary Surface

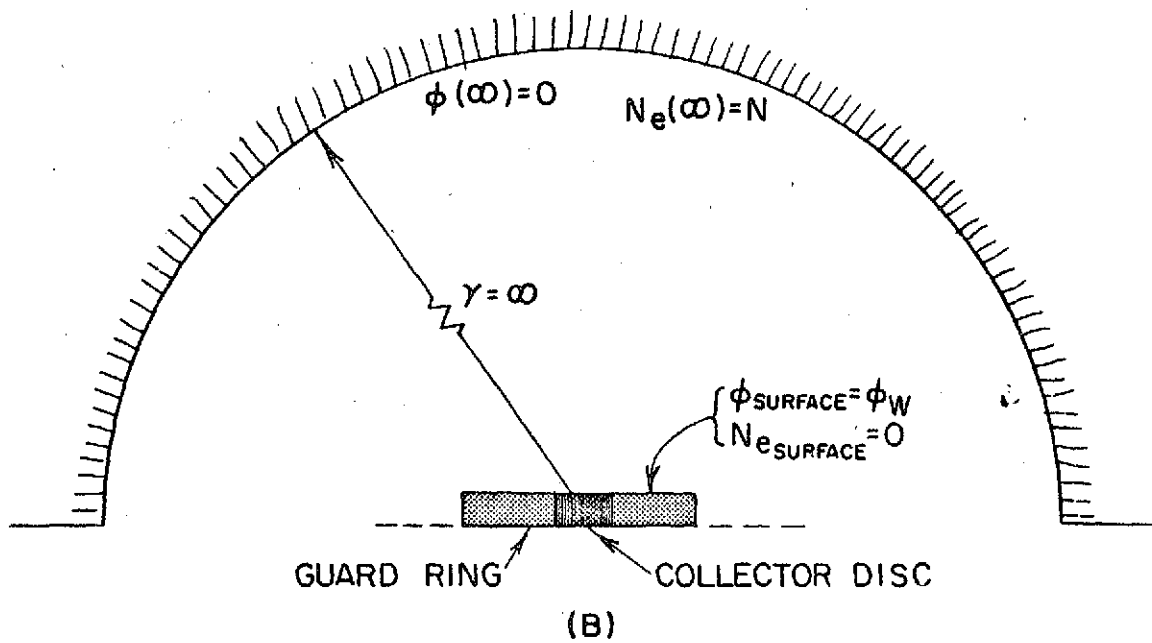
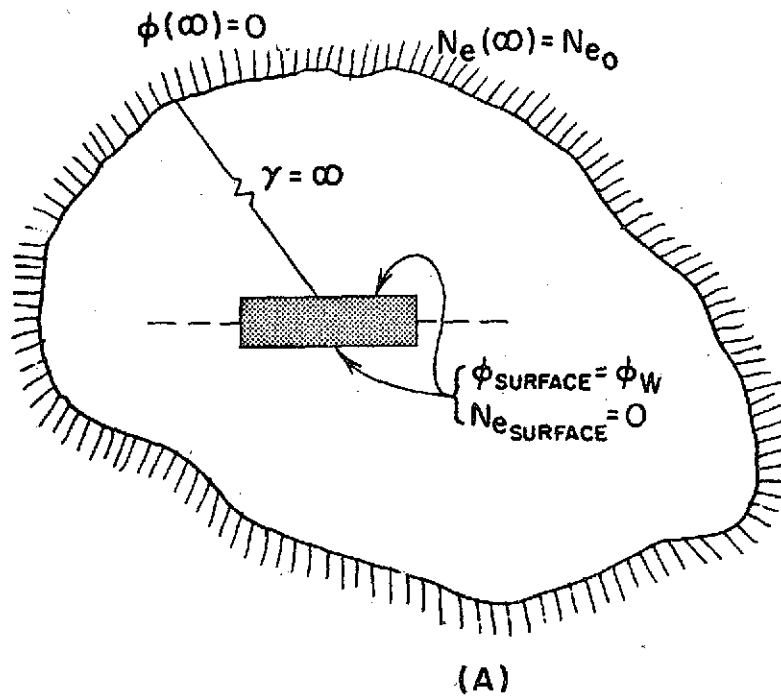


Figure 6. Boundary Configurations of the Blunt Probe:  
 (A) Two-Sided Disc, (B) One-Sided Disc

found by assuming that the electron density gradient will vary linearly with distance from the probe when far away from the probe surface. An Einstein relation was used, though invalid for electrons. In the present work, none of the above assumptions are made. A simple model, based solely on data of electron drift velocity, is proposed.

Only the upper half of the disc, shown in Figure 6b, where the collector disc is imbedded, is considered here. The electric field expressions used here for this one-sided disc are the same as that used by previous workers (43, 44) and have been listed in the beginning of this chapter. The electrons, while bouncing around in collisions with neutrals, have a net drift velocity along electric field lines. The field lines normal to a given surface on the probe will form a stream tube. In particular, the stream tube,  $pqq'p'$  to the collector disc as shown in Figure 3, is of interest here. The flux of electron through the tube is governed by Gauss' law as

$$AE = \text{constant}_1 \quad (4.3.3)$$

where A and E is the local stream tube cross-sectional area and the magnitude of the electric field respectively. Mass conservation also gives

$$n_e A v_D = \text{constant}_2 \quad (4.3.4)$$

Combining Eqs. (4.3.3) and (4.3.4), we have

$$n_e \frac{v_D}{E} = \text{constant}_3 \quad (4.3.5)$$

For a given altitude and hence pressure  $p$ , we have

$$n_e \frac{v_D}{E/p} = \text{constant}_4 \quad (4.3.6)$$

Since the drift velocity for electron is no longer assumed to be linearly dependent on  $E$ , the experimental results of the electron drift velocity versus electric field and pressure listed in McDaniel (45) are used. The curve for data taken at gas temperature of 300°K is shown in Figure 7. The curve has a constant slope,  $v_{Dp}/E$ , of about  $10^7 \text{ cm}^2 \text{ sec}^{-1} \text{ volt}^{-1} \text{ mm Hg}$  at portion AB, and  $5.5 \times 10^5 \text{ cm}^2 \text{ sec}^{-1} \text{ volt}^{-1} \text{ mm Hg}$  at CD. The slope at the saddle BC varies at values much smaller than the above values.

The point  $E_w/p$  on the curve (Figure 7) is first considered. In view of the fact that the velocity of the descending probe in the D-region is small, the moving blunt probe data,  $E_w/p$  is used in the present analysis. Data (46) consistently shows that the point  $E_w/p$  is located on the portion CD of the curve. Values in one case are presented in Table 5. At a given altitude,  $E/p$  will start with a value,  $E_w/p$ , on portion CD; as distance away from the probe surface increases,  $E/p$  decreases. Portion AB on the curve will now be replaced by a straight line (Figure 8). Eq. (4.3.6), when combined with the fact that the slope,  $v_{Dp}/E$ , is a constant at field values below B, shows that the electron density is constant at  $n_{eo}$  (ambient electron density) for all locations outside a position,  $\gamma_o$ , as shown in Figure 8. This distance,  $\gamma_o$ , thus can be regarded as the perturbed thickness of the stationary probe. The electron density is a constant,  $n_{eo}$ , outside  $\gamma_o$ ; within the distance  $\gamma_o$ ,



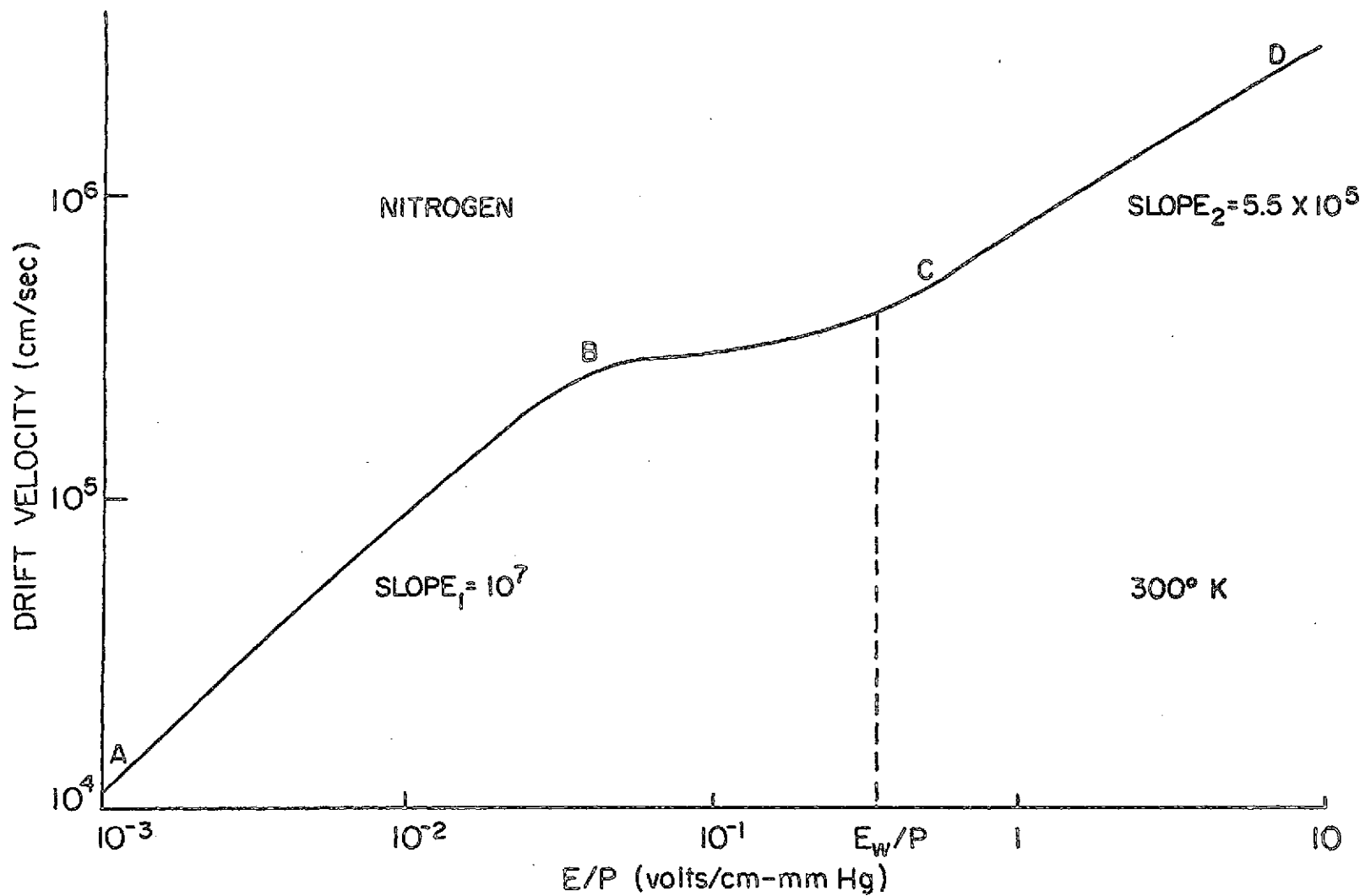


Figure 7. Experimental Data Obtained by Park, Voshall and Phelps on the Drift Velocity of Electrons in Nitrogen (Figure 11-3-11 D of Ref. 45)

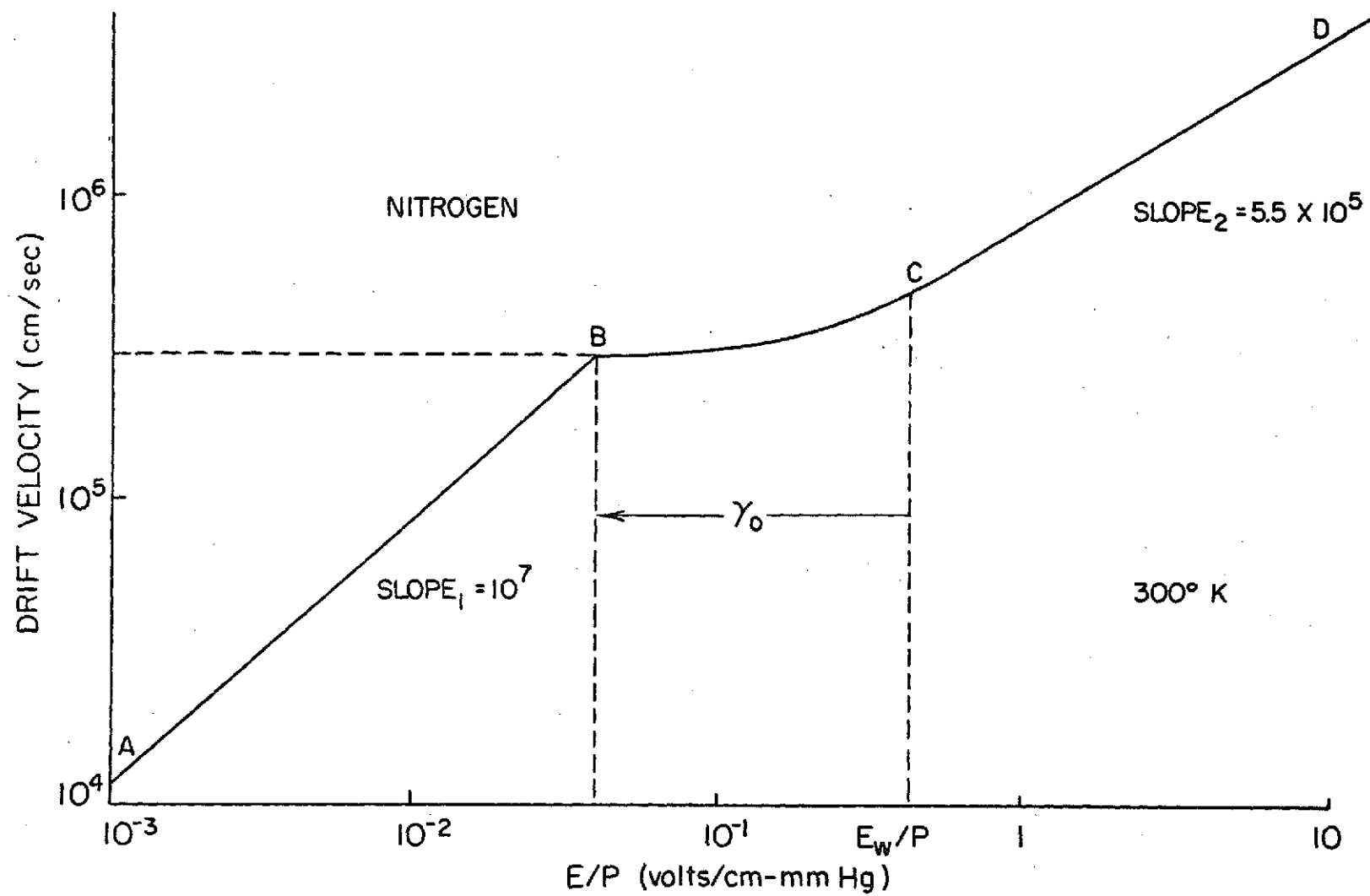


Figure 8. The Approximate Electron Drift Velocity versus  $E/p$  Plot for Stationary Blunt Probe Theory

the density changes according to Eq. (4.3.6). At B,  $E_o/p = 4 \times 10^{-2}$  volt  $\text{cm}^{-1}$  mm Hg $^{-1}$  and  $v_{Do} = 3 \times 10^5$  cm sec $^{-1}$ . With Eqs. (4.2.1) and (4.2.2a), we have

$$\frac{E}{p} = \frac{E_w}{p} \frac{a^2}{\gamma^2} \quad (4.3.7)$$

Thus at B, we have

$$\gamma_o = 5a \left( \frac{E_w}{p} \right)^{1/2} \quad (4.3.8)$$

With Eq. (4.3.3), the electron collecting surface area,  $A_o$ , is given by

$$A_o = \pi \gamma_{col}^2 \frac{\gamma^2}{a^2}$$

For the data from the launch on December 5, 1972, the perturbed length  $\gamma_o$ , the collecting surface area  $A_o$ , and the free stream velocity are presented in Table 5.

While a near-surface diffusion layer is expected to exist, the current to the collector disc is determined by the condition on the surface at a distance  $\gamma_o$  away from the probe. It is

$$I_e = e v_{Do} A_o n_{eo} \quad (4.3.9)$$

where  $A_o$  is the cross-sectional area of the stream tube at distance  $\gamma_o$  from the probe surface. Using Gauss' law and Eqs. (4.3.8) and (4.3.9), we have

$$I_e = 25ev_{Do} n_{eo} A_{col} \left( \frac{E_w}{p} \right) \quad (4.3.10)$$

Table 5

Variation of the Parameter,  $E_w/p$ , the Electron Collecting Surface Area,  $(A_o)$  to the Collector Disc, the Perturbed Length Scale,  $\gamma_o$ , and the Free Stream Velocity,  $\bar{U}$ , for the Launch on December 5, 1972.

Altitude (km)	$E_w/p$ $\frac{\text{Volt}}{\text{cm-mm Hg}}$	$A_o$ (cm <sup>2</sup> )	$\gamma_o$ (cm)	$\bar{U}$ (m/sec)
82	1.85	227	25.2	350
74.2	0.5	62.4	13.2	310
65.2	0.44	54.2	12.3	225
58.6	0.31	38.0	10.3	123
47	0.26	30.4	9.2	63
37	0.25	29	9	25

Substituting numerical values, we have

$$I_e = 2.4 \times 10^{-12} \frac{\gamma_{col}^2}{a} \frac{n_{eo} V_w}{p} \quad (4.3.11)$$

Thus the electron current to the collector disc is proportional to the area of the collector disc, ambient electron density and probe potential. The current decreases for a larger guard ring and lower gas pressure. Taking the derivative of Eq. (4.3.11), we have

$$\frac{dI_e}{dV_w} = 2.4 \times 10^{-12} \frac{\gamma_{col}^2}{a} \frac{n_{eo}}{p} \quad (4.3.12)$$

Now,  $\frac{dI_e}{dV_w}$  is related to the term  $\sigma_-$  usually referred to as the negative conductivity by

$$\frac{dI_e}{dV_w} = \frac{2\gamma_{col}^2}{a} \sigma_- \quad (4.3.13)$$

Combining Eqs. (4.3.12) and (4.3.13), we have the virtual relationships,

$$n_{eo} = 8.35 \times 10^{11} p \sigma_- \quad (4.3.14)$$

This model, which does not specifically include diffusion processes, is based purely on a dominant mobility concept. The diameter of the area,  $A_o$ , is the characteristic length of this problem. Its value compared with the electron-neutral mean free path is an indication of the validity of a continuum description of the system. Comparisons of the drift velocity at the point B, ( $v_{Do} = 3 \times 10^5$  cm sec<sup>-1</sup>) and the free stream velocity,  $\bar{U}$ , of the descending probe reveal a very interesting result, the former being much larger than the latter. This

seems to demean the contribution of convection to the electron flux as compared with that by mobility. Thus it seems to imply that the present stationary blunt probe theory may be used for a subsonically descending probe. At this stage, however, it is not clear how the convection effect will perturb the electron density at distance from the probe further away than the perturbed thickness  $\gamma_0$ . The convection effect will be investigated in the following sections.

#### 4.3.2 Identification of Characteristic Layers for a Moving Blunt Probe

For a positively biased probe, the electron conservation equation in a continuum medium is

$$\beta R_d \mathbf{q} \cdot \nabla n_e - \nabla \cdot (\nabla n_e - \phi_w n_e \nabla U) = 0 \quad (4.3.15)$$

with

$$n_e(\infty) = 1 \quad (4.3.16a)$$

$$n_e(0) = 0 \quad (4.3.16b)$$

In the D-region,  $R_d$ , the electrical Reynolds number is  $10^3$  at 50 km, 10 at 80 km, with  $\beta \approx 5 \times 10^{-3}$ . It will be noted for the purpose of comparison that the characteristic thickness for ion collection as noted earlier, is  $\delta_1 = (R_d)^{-1/2}$ . Notice that all physical lengths have been nondimensionalized by the probe diameter,  $L$ . The presence of the term  $\beta$  in Eq. (4.3.15), which is not found in the equations for ions, makes the analysis for electron collection completely different from the ion collection theory. The following analysis will be based on the assumption that  $\phi_w \gg \beta R_d$ , which is appropriate in the D-region.

The fact that  $\phi_w$  is the largest parameter in Eq. (4.3.15) clearly reveals that the mobility term,  $(\nabla n_e \cdot \nabla \phi)$ , is dominant in the nondimensional length scale of order 1. This implies that the electron, moving in region of approximately  $L$  cm away from the probe, is mainly governed by the mobility (a combined effect of electric field and collisions). Physically, the existence of this mobility dominant region is due to the small inertia and high mobility of the electrons.

For smaller or larger length scale (nearer to or further away from the probe), the physical picture changes. A smaller dimensionless length scale  $\delta_2$  will first be considered. In terms of the coordinates shown in Figure 4, Eq. (4.3.15) becomes

$$\begin{aligned} \frac{\beta R d}{\phi_w} \left( u \frac{\partial n_e}{\partial x} + v \frac{\partial n_e}{\partial y} \right) + \left( \frac{\partial n_e}{\partial x} \frac{\partial \psi}{\partial x} + \frac{\partial n_e}{\partial y} \frac{\partial \psi}{\partial y} \right) \\ - \frac{1}{\phi_w} \left( \frac{\partial^2 n_e}{\partial x^2} + \frac{\partial^2 n_e}{\partial y^2} \right) = 0 \end{aligned} \quad (4.3.17)$$

The small parameter  $\left(\frac{1}{\phi_w}\right)$  in front of the highest order derivative term (singularly perturbation problem) predicts we have a boundary layer behavior of the electron density near the probe. The coordinate is stretched by letting  $\eta = \frac{y}{\delta_2}$  where  $\delta_2 \ll 1$ , Eq. (4.3.17) becomes

$$\begin{aligned} \frac{\partial^2 n_e}{\partial \eta^2} + \delta_2 \frac{\partial^2 n_e}{\partial x^2} - \phi_w \delta_2 \frac{\partial n_e}{\partial x} \frac{\partial \psi}{\partial x} - \phi_w \delta_2 \frac{\partial n_e}{\partial \eta} \frac{\partial \psi}{\partial y} \\ \text{(A)} \qquad \qquad \qquad \text{(B)} \qquad \qquad \qquad \text{(C)} \end{aligned}$$

$$-\beta R d \delta_2^2 \left( u \frac{\partial n_e}{\partial x} + \frac{v}{\delta_2} \frac{\partial n_e}{\partial \eta} \right) = 0 \quad (4.3.18)$$

Notice that  $\frac{\partial U}{\partial y}$  is not scaled. This is because the potential is decreasing slowly (algebraic decay), and a boundary layer behavior (exponential decay) of the potential is not possible. To balance the highest derivative term (A), and to satisfy the condition that  $\delta_2 \ll 1$ , the only candidates are (B) and (C).

The term (B) is first chosen, giving  $\delta_2 = \phi_w^{-1/2}$ . This, however, when substituted into Eq. (4.3.18), dropping terms smaller than order 1, will give

$$\frac{\partial^2 n_e}{\partial \eta^2} - \frac{\partial n_e}{\partial x} \frac{\partial U}{\partial x} + \phi_w^{1/2} \frac{\partial n_e}{\partial \eta} \frac{\partial U}{\partial y} = 0 \quad (4.3.19)$$

The last term, which is of order  $\phi_w^{1/2}$ , is larger than the other two order 1 terms. So, with an error of order  $\phi_w^{-1/2}$ , we have

$$\frac{\partial n_e}{\partial \eta} \frac{\partial U}{\partial y} = 0 \quad (4.3.20)$$

However, a constant magnitude for potential or electron number density is not reasonable. This contradictory conclusion implies the initial assumption is incorrect.

So, instead, the term (C) is used to balance (A). This gives  $\delta_2 = \frac{1}{\phi_w}$ , and the resultant equation is

$$\frac{\partial^2 n_e}{\partial \eta^2} - \frac{\partial n_e}{\partial \eta} \frac{\partial U}{\partial y} = 0 \quad (4.3.21)$$

$$n_e(\eta \rightarrow \infty) = n_{ec} \quad (4.3.22)$$

$$n_e(0) = 0 \quad (4.3.23)$$



The scaling factor,  $\frac{1}{\phi_w}$ , is identified as the nondimensional thickness of this layer, which we will refer to as the diffusion layer. The fact that this layer is thin  $\left(\frac{L}{\phi_w}\right)$  allows the electrical field,  $\frac{\partial \psi}{\partial y}$ , to be treated as a constant. The solution of Eq. (4.3.21) is

$$n_e = n_{eC} \left[ 1 - \exp \left( \frac{\partial \psi}{\partial y} \eta \right) \right] \quad (4.3.24)$$

where  $n_{eC}$  is the electron density at the edge of the diffusion layer.

The mechanism is clearly shown in Figure 9. For any control volume inside this layer, the diffusion process and the mobility together determine the number density inside this volume. For diffusion, since the electron number density increases exponentially with distance from the wall, the density gradient is smaller further away from the probe, and thus results in a loss of electrons inside this control volume due to diffusion. On the other hand,  $\frac{\partial \psi}{\partial y}$  decreases algebraically with distance away from the probe. Thus the product term,  $n_e \frac{\partial \psi}{\partial y}$ , is larger further away from the probe surface. This results in a net gain of electrons in the control volume from the undisturbed plasma due to mobility. The combined effect of the diffusion and mobility, of course, will leave the number density in the control volume unchanged.

Diffusion, a phenomenon due to the electron's thermal motion, can be observed independently if the electron and ion densities are so low that the space charge field can be neglected. From a physical standpoint, the gradient appearing at a point in the field is the result of a process of creation or loss of plasma, and in particular, it results from the zero concentration boundary condition imposed at the surface of the probe.

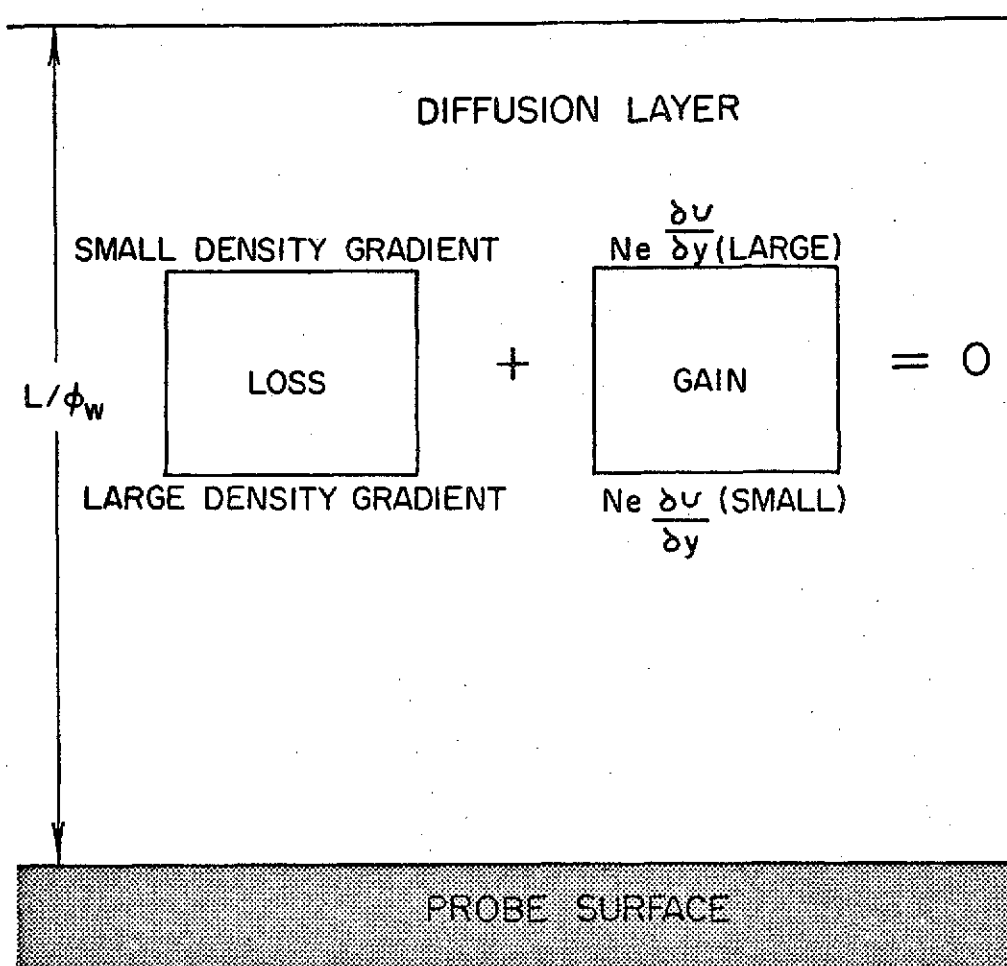


Figure 9. Schematic Representation of Loss and Gain of Electron in the Diffusion Layer

It is important to note that the diffusion layer is predicted by the continuum equation, Eq. (4.3.15). It is appropriate only when this layer can be treated as a continuum. Otherwise, the density gradient and the drift velocity artifices are not defined, and diffusion and mobility mechanisms can no longer be taken to exist since they are collisional processes. The criterion for having a continuum inside the diffusion layer is that the diffusion layer  $\left(\frac{L}{\phi_w}\right)$  is thicker than the mean free path of the electron-neutral collisions,  $\lambda_{e-n}$ . When this criterion is not satisfied, the diffusion layer is no longer a relevant concept. This will be further discussed in the next section.

Next, a large dimensionless length scale,  $\delta_3 \gg 1$  is considered. Here, at such a far distance away from the probe, the x-direction variations of the physical quantities ( $n_e, u$ ) will be comparable to the variations in y-direction. So, both coordinates are scaled as  $(\bar{x}, \bar{y}) = (x, y)/\delta_3$ , where  $\delta_3 \gg 1$ .

Substituting into Eq. (4.3.17), we obtain

$$\begin{aligned} & \frac{\beta R d}{\phi_w} \left( u \frac{\partial n_e}{\partial \bar{x}} + v \frac{\partial n_e}{\partial \bar{y}} \right) + \frac{1}{\delta_3} \left( \frac{\partial n_e}{\partial \bar{x}} \frac{\partial u}{\partial \bar{x}} + \frac{\partial n_e}{\partial \bar{y}} \frac{\partial u}{\partial \bar{y}} \right) \\ & - \frac{1}{\phi_w} \delta_3 \left( \frac{\partial^2 n_e}{\partial \bar{x}^2} + \frac{\partial^2 n_e}{\partial \bar{y}^2} \right) = 0 \end{aligned} \quad (4.3.25)$$

It is not possible to balance the highest order derivative term

$$\left( \frac{\partial^2 n_e}{\partial \bar{x}^2} + \frac{\partial^2 n_e}{\partial \bar{y}^2} \right) \text{ while simultaneously satisfying the condition, } \delta_3 \gg 1.$$

Thus, the boundary layer analysis using the length scale,  $\delta_3$ , to balance the highest order derivative term fails in this case. This failure is

expected since all boundary layer analyses are based on the requisite assumption that the perturbed region is a thin layer on the body.

However, useful information is gained when the first two terms, convection and mobility, in Eq. (4.3.25) are allowed to balance each other; this gives  $\delta_3 = \phi_w (\beta R d)^{-1}$ . Dropping the term of order  $\beta R d \phi_w^{-2}$ , we have

$$\left( u \frac{\partial n_e}{\partial x} + v \frac{\partial n_e}{\partial y} \right) + \left( \frac{\partial n_e}{\partial x} \frac{\partial u}{\partial x} + \frac{\partial n_e}{\partial y} \frac{\partial u}{\partial y} \right) = 0 \quad (4.3.26)$$

Hence convection and mobility will determine the spatial distribution of electrons between the region at  $\phi_w L (\beta R d)^{-1}$  cm away from the probe and the next inner layer. Physically this is reasonable since there must be an intermediate distance away from the probe surface where both convection and mobility are both of the same order of magnitude. Notice also that when  $\delta > \phi_w (\beta R d)^{-1}$ , the convection term in Eq. (4.3.25) dominates, which implies that for regions at distance greater than  $\phi_w L (\beta R d)^{-1}$  cm from the probe, convection alone dominates. In this outer region, ( $\delta > \phi_w (\beta R d)^{-1}$ ), as has been also observed in ion collection theory, the electron number density is unperturbed and is the same value as the density at an infinite distance away from the probe.

As a result, the analysis predicts four distinct regions for electron collection in continuum flow. They are:

1.  $0 < \delta < \phi_w^{-1}$  diffusion-mobility dominant region
2.  $\phi_w^{-1} < \delta < 1$  mobility dominant region
3.  $1 < \delta < \phi_w (\beta R d)^{-1}$  mobility-convection dominant region
4.  $\phi_w (\beta R d)^{-1} < \delta$  convection dominant region

where  $\delta$  is a nondimensional length away from the probe surface. The physical picture can be summarized as follows. With respect to the probe, the electrons are moving with a constant velocity  $\bar{U}$  (the free stream velocity). When outside the sphere of influence of the probe, the electron density is unperturbed and is the same as the ambient electron density. When inside the sphere, which is approximately of radius  $\phi_w L (\beta R_d)^{-1}$  cm, the electrons begin to feel the pull of the probe potential and converge toward the probe. Here convection and mobility dominate the dynamics of the electrons. This stage continues until the electrons are near enough to the probe ( $\delta < 1$ ) that the electric field alone, completely determines the motion of the electrons. This process persists until the electrons are very close to the probe ( $\delta < \phi_w^{-1}$ ). Here, the converging effect increases the electron density, but not high enough for the space charge effect to be included. This high number density, together with the zero electron density boundary condition at the wall set up a density gradient, which balances the mobility by the diffusion process.

#### 4.3.3 A Simple Model Based on Particle Convection

Attempts to obtain an analytic solution to the Eq. (4.3.15) will be very difficult if not impossible. This is explained as follows: Previous analysis shows that the perturbed region, for electron collection, is large compared with the probe size. Thus the whole fluid domain (not just a thin layer on the probe surface) as shown in Figure 6b has to be considered. Furthermore, the superposition of a flow on the probe destroys the symmetry of the system which is now crucial for any

analytic solution. Thus, the system is too complex to allow an analytic solution. The only consolation is that the electric field is uncoupled from the species density and hence the flow effect. The electric field over a one-sided biased disc can still be used for the present problem. This last assumption, together with some observed characteristics of the system, allows the present problem to be solved in a control volume fashion.

A simple consistent model is now developed in order to relate the current collected to the probe voltage and ambient quantities for electron collection. In view of the result of the previous section, the perturbed region is divided into three distinct regions.

#### 1. Diffusion layer

This is a very thin layer adjacent to the probe surface. Diffusion and mobility are the dominant processes governing the transport of electrons, and hence the spatial distribution of electron density; it is shown in Figure 10a. Due to the edge effect, only the central portion of the probe is governed by the diffusion equation, Eq. (4.3.22), and the electron number density is given by Eq. (4.3.24). The electron current to the collector disc is

$$\begin{aligned} I_e &= en_{eC} D_e \left( \frac{\partial n_e}{\partial y} \right)_{\text{wall}} A_{\text{col}} \\ &= -en_{eC} D_e \left( \frac{\partial \phi}{\partial y} \right)_{\text{wall}} A_{\text{col}} \end{aligned} \quad (4.3.27)$$

where  $n_{eC}$  is the electron density at the edge of the diffusion layer,  $D_e$  is the diffusion coefficient of the electron, and  $A_{\text{col}}$  is the area of

the collector disc on the probe. Since the diffusion layer is thin  $\left(\frac{L}{\phi_w}\right), \left(\frac{\partial\phi}{\partial y}\right)_{\text{wall}}$  is a constant and given by

$$\left(\frac{\partial\phi}{\partial y}\right)_{\text{wall}} = \frac{-2V_w}{\pi a} \quad (4.3.28)$$

where  $V_w$  is the probe potential,  $a$  is the radius of the probe. Notice that only portions of the electrons entering the diffusion layer will be collected by the collector disc, while the rest go to the guard ring.

## 2. Mobility Layer

Immediately above the diffusion layer, the electron dynamics are determined only by the electric field as the field induced velocities dominate convection velocity here. This region is referred to as the mobility layer and is shown in Figure 10b.

Near the outer edge of the region, the electric field is given by

$$E_B = \frac{-2aV_w}{\pi\gamma_B^2} \quad (4.3.29)$$

where  $E_B$  is the electric field at the outer edge of the mobility layer, and  $\gamma_B$  is the radial distance from the outer edge to the probe. Notice that Eq. (4.3.29) is correct only when  $\gamma_B \gg a$ . The negatively charged (return) electrode on the other end of the probe can influence the electron density below the level line AB. However, on the basis of rocket experiments, only those electrons entering through the upper hemisphere shown in Figure 10b need to be considered. Electrons enter

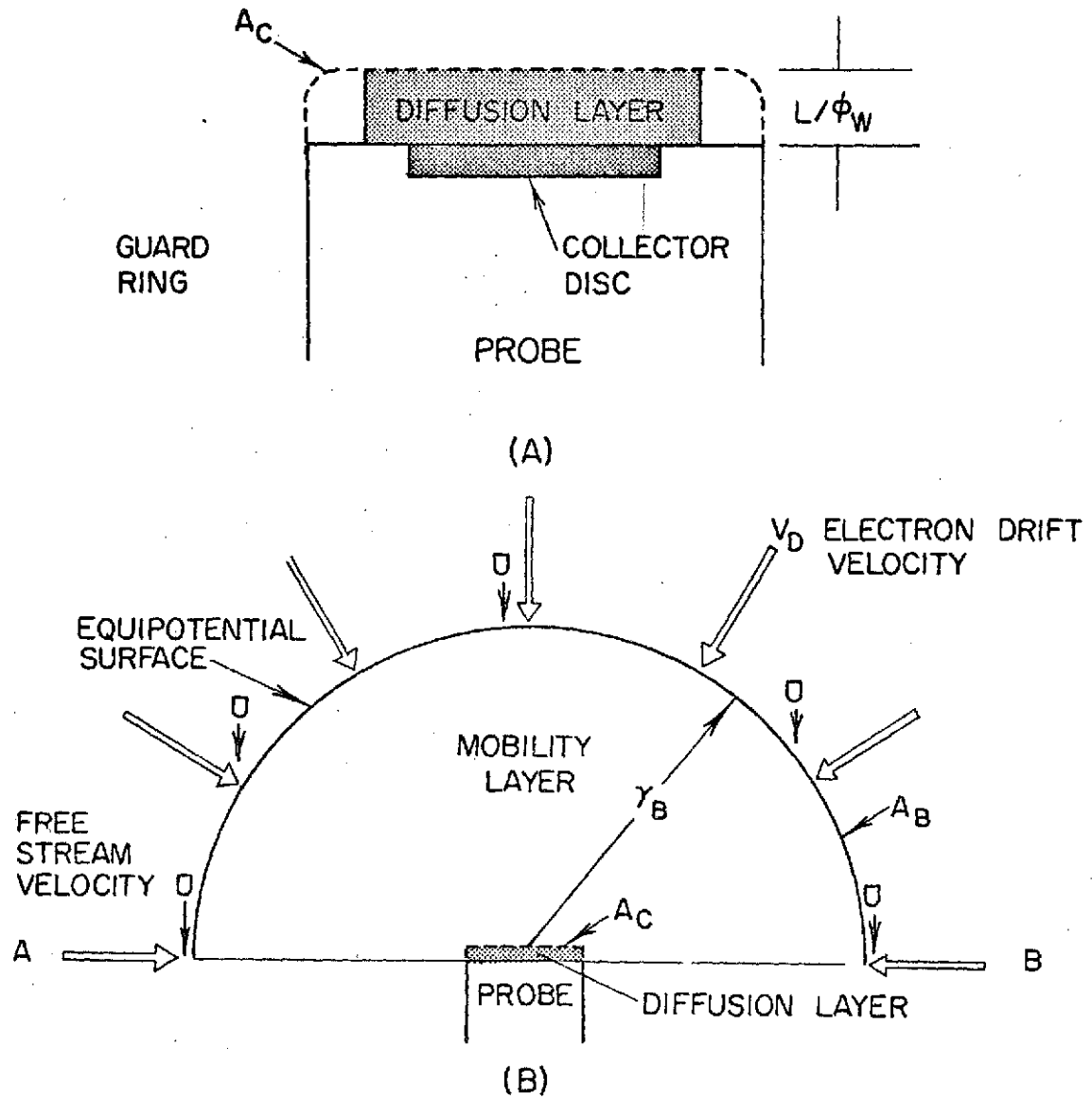


Figure 10 (A) Diffusion Layer on the Probe

(B) Mobility Layer on the Probe



the mobility region with two velocity components, the convection velocity which is the same as the free stream velocity, and a drift velocity. The electric drift velocity as a function of the electrical field  $E$  and the neutral gas pressure, can be found in McDaniel (45). The drift velocity is smaller further away from the probe.

In view of the fact that convection is neglected in the mobility layer, the outer edge of the mobility layer can be defined as a surface where the drift velocity is much larger than the convection velocity. To estimate orders of magnitude,  $v_{DB} = 10 \bar{U}$  is a criterion that will be used to approximately locate the outer edge of the mobility layer in this model. There is an upper limit in choosing  $v_{DB}$ . For a too large  $v_{DB}$ , the outer edge of the mobility layer will be too close to the probe for  $\gamma \gg a$  to be valid; and, hence, Eq. (4.3.29) cannot be used for electric field evaluation at the outer edge of the mobility layer.

The criterion,  $v_{DB} = 10 \bar{U}$ , used to include the characteristics of a mobility layer ( $v_D \gg \bar{U}$ ) is an ad hoc assumption. Thus, the corresponding length,  $\gamma_B$ , where this velocity occurs is not a natural length scale derived from the governing equations. At a given altitude knowing the neutral gas pressure,  $p$ , and the probe velocity,  $\bar{U}$ , and hence the electron drift velocity,  $v_{DB}$ , the electric field  $E_B$  can be found in McDaniel (45). Knowing the probe potential, and with the help of Eq. (4.3.29), the radial distance,  $\gamma_B$ , can be computed. It will be recalled that the above analysis of the governing equations indicated that the thickness of the mobility layer is of order  $L$ . These length scales together with the stationary probe mobility layer

thickness,  $\gamma_0$ , are presented in Table 6. It is noted that  $\gamma_B$  which is roughly twice as large as  $L$ , is of the same order as  $L$ . Thus the mobility layer thickness predicted by the above ad hoc criterion generally agrees with the prediction based on analysis on the governing equation. The use of the radial distance  $\gamma_B$  instead of  $L$  has the advantage that a hemispheric mobility layer outer edge is physically more realistic than an infinite planar edge at distance  $L$  from the probe surface predicted by the two-dimensional species equation analysis.

It will be noted here that the above criterion, which is crucial for the analysis that follows, will be irrelevant when the probe is stationary. The present model would predict an infinitely large mobility layer for zero convection velocity. The question of consistency of the present theories for moving and stationary blunt probe naturally arises. Does the finite mobility layer (thickness  $\sim \gamma_0$ ) predicted by the stationary probe theory proposed previously contradict the infinite mobility dominant domain implied by the moving probe theory here in the zero velocity limit? The stationary probe theory is based on the observation that the current to the probe can be evaluated approximately at a distance  $\gamma_0$  from the probe surface due to the nonlinear variation of the electron drift velocity with electric field. Any stationary probe theoretical model, not considering the nonlinearity of the electron drift velocity would also predict an infinitely large mobility region. This is obvious since the Laplace equation predicts an electric field extending to infinite distance from the probe and hence the electron drift velocity. This undeniably is a bad feature of the present convection model in the zero velocity limit. However, a

Table 6

Comparison of Various Length Scales for the Mobility Layer

Altitude (km)	$\gamma_o$ (cm)	L (cm)	$\gamma_B$ (cm)
82	25.2	7.4	15
74.2	13.2	7.4	12
65.2	12.3	7.4	14
58.6	10.3	7.4	15
47	9.2	7.4	18

latter discovery turns out that convection is negligible and a comparison of  $\gamma_A$  and  $\gamma_O$  in Table 6 shows that these two lengths are approximately of the same magnitude. Thus the singular behavior of the convection model in the zero velocity limit is irrelevant.

Electrons entering through surface B will also hit surface C. Thus electron density at surface B and C are related by the following equation expressing mass conservation,

$$n_{eB} (A_B v_{DB} + \pi \gamma_B^2 \bar{U}) = n_{eC} (A_C v_{DC} + \pi a^2 \bar{U}^1) \quad (4.3.30)$$

where  $n_e$  is the electron density,  $v_D$  is the drift velocity,  $A$  is the area,  $a$  is the probe radius. The suffixes B and C denote quantities at surface B and C respectively.  $\bar{U}^1$  is the convection velocity at the diffusion layer's outer edge which is much smaller than  $\bar{U}$ .

The question of the sensitivity of the current predicted by the model to the choice of a larger drift velocity, say  $v_{DB} = 100 \bar{U}$ , is raised. The mobility layer affects the current to the probe by predetermining the electron number density at the outer edge of the diffusion layer through Eq. (4.3.30). Since  $v_{DC} > v_{DB} \gg \bar{U} > \bar{U}^1$ , approximately Eq. (4.3.30) becomes

$$n_{eB} A_B v_{DB} = n_{eC} A_C v_{DC} \quad (4.3.31)$$

$$\frac{n_{eB}}{n_{eC}} = \frac{(\pi a^2)}{(2\pi \gamma_B^2)} \frac{v_{DC}}{v_{DB}} \quad (4.3.32)$$

For a given probe potential and pressure, Eq. (4.3.32) becomes, with (4.3.29)

$$\frac{n_{eB}}{n_{eC}} = \text{const} \frac{E_B}{v_{DB}} \quad (4.3.33)$$

A glance on Figure 8 clearly reveals that the ratio  $E_B/v_{DB}$  is relatively constant on the portion CD of the curve; thus a higher drift velocity,  $v_{DB}$ , will not appreciably affect the ratio  $n_{eB}/n_{eC}$  and hence the current to the probe.

### 3. Convection and Mobility Region

Above the mobility layer, is the region where the electric field becomes weaker, and both mobility and convection determine the trajectory, and density of electrons. At such a large distance away from the probe, it is appropriate to assume the convection velocity of the electron does not change throughout this region, while the drift velocity directed toward the probe is increasing steadily. The outer edge of this region is defined as the location where the convection velocity,  $\bar{U}$ , is much greater than the drift velocity,  $v_D$ . Specifically, for this model  $v_{DA} = 0.1 \bar{U}$  is chosen to be the criterion for determining the position of this outer edge. The minimum allowable  $v_{DA}$  depends on the availability of the experimental data for  $v_D$ . Notice in McDaniel (45) that the lowest value of  $v_D$  reported is approximately  $10^3$  cm/sec. The structure of the convection and mobility region, and inner layers are sketched in Figure 11.

Only the electrons which entered through the central portion of the hemisphere at  $\gamma_A$ , as shown in Figure 11, will arrive at the mobility layer. To estimate the magnitude of this electron collecting surface  $A_A$ , the trajectory of electron has to be evaluated inside

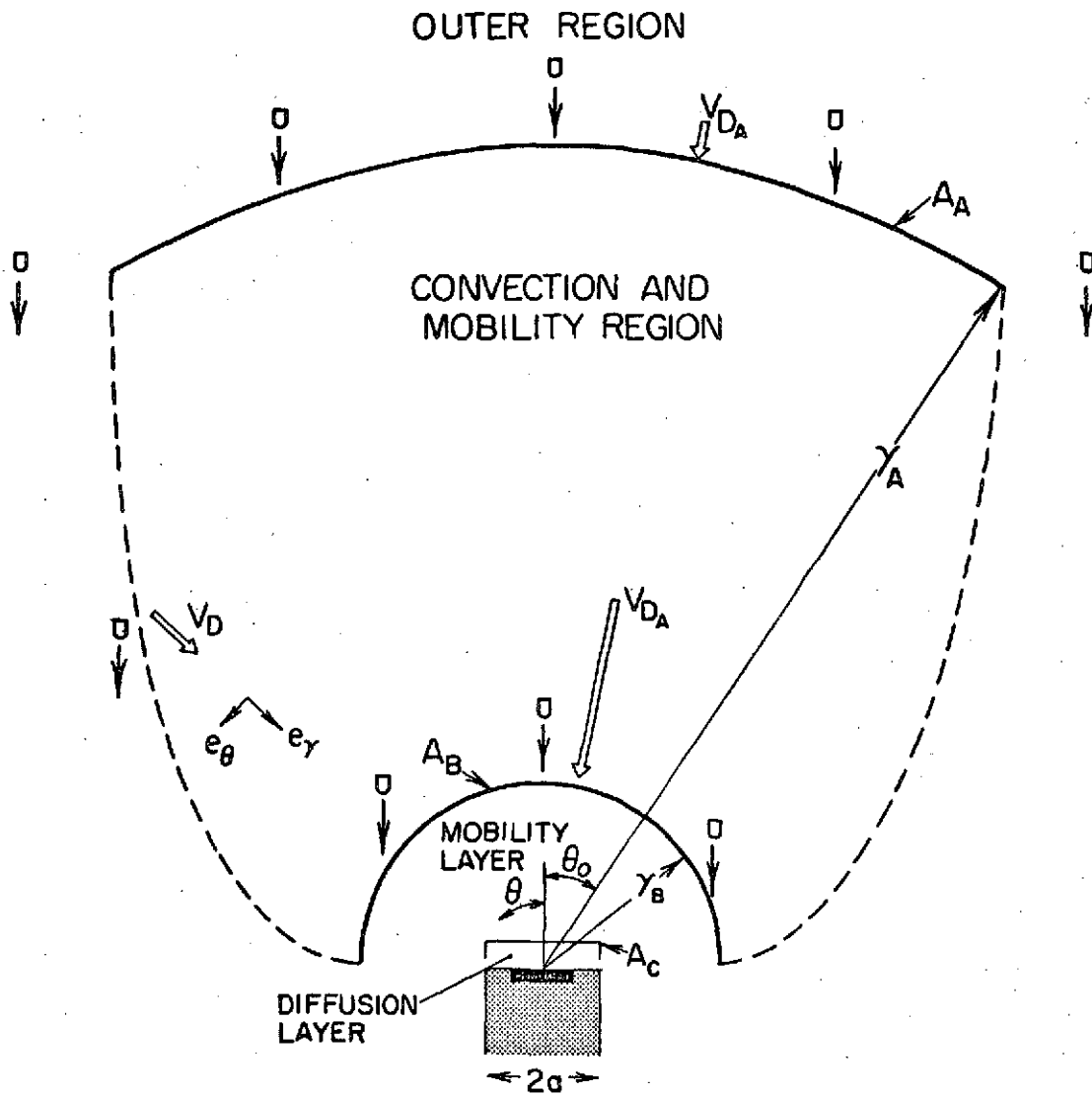


Figure 11. Perturbed Regions Surrounding a Positively Biased Probe

the convection and mobility region. With the convection velocity,  $\bar{U}$  being a constant, and the drift velocity,  $v_D$  a function of  $|E/p|$ , the velocity vector  $\bar{v}$  of the electron at any location inside the convection and mobility region is given by

$$\bar{v} = \bar{e}_r (\bar{U} \cos \theta + v_D) + \bar{e}_\theta \bar{U} \sin \theta \quad (4.3.34)$$

where  $\bar{e}_r$  and  $\bar{e}_\theta$  are radial and tangential limit vectors respectively, and  $\theta$  is the angle as shown in Figure 11. Knowing  $\gamma_A$ ,  $\gamma_B$ , and the drift velocity at any location, the minimum angle,  $\theta_0$ , for collection can be easily found by a simple numerical routine.

Again, by conservation of electrons, the electron number density at surface A and surface B are related by

$$\frac{n_{eB}}{n_{eA}} = \frac{\pi(\gamma_A \sin \theta)^2 \bar{U} + 2\pi\gamma_A^2 (1-\cos \theta) v_{DA}}{\pi\gamma_B^2 \bar{U} + 2\pi\gamma_B^2 v_{DB}} \quad (4.3.35)$$

Now, outside surface A, the electric field is so weak that the number density of electrons is relatively unperturbed. Thus, it is a fair assumption to say that

$$n_{eA} = n_{eo} \quad (4.3.36)$$

Combining Eqs. (4.3.27), (4.3.30) and (4.3.35), we have

$$I_e = -en_{eo} D_e \left( \frac{\partial \phi}{\partial y} \right)_{\text{wall}}^{A_{\text{col}}} \frac{\gamma_A^2 [\sin^2 \theta \bar{U} + 2 (1-\cos \theta) v_{DA}]}{[a^2 v_{DC} + \gamma_C^2 \bar{U}]} \quad (4.3.37)$$

Notice that  $D_e$ ,  $\gamma_A$ ,  $\gamma_B$ ,  $v_{DC}$  and  $v_{DA}$  are all dependent on the wall potential  $V_w$ . Thus, the current  $I_e$  may no longer be a linear function of the wall potential as found by Hoult (7).

To see how the number density in different layers varies with the probe voltage and altitude, we assume  $\bar{U} = 100$  m/sec,  $a = 10$  cm and compute  $n_{eB}/n_{eA}$  and  $n_{eC}/n_{eB}$  as follows. At a given probe potential and altitude (hence  $p$ ), and the fact that  $v_{DB} = 10 \bar{U}$  and  $v_{DA} = 0.1 \bar{U}$ ,  $\gamma_A$  and  $\gamma_B$  can be found. The drift velocity inside the convection and mobility region can be approximated as

$$v_D = 10 (\log_{10} E/p + 7.065) \quad (4.3.38)$$

which is a good representation for drift velocity below  $10^5$  cm/sec as shown in McDaniel (45). Thus, knowing  $E$ ,  $p$  and  $v_D$  inside this region, the trajectory of the electron can be numerically computed and the minimum angle  $\theta_0$  and hence  $A_A$  can be found. The time increment used in the numerical computation is  $10^{-8}$  sec. Having  $\theta_0$ ,  $\gamma_A$  and  $\gamma_B$ , the electron density ratio  $n_{eB}/n_{eA}$  and  $n_{eC}/n_{eB}$  can be found. The results are plotted in Figure 12 and Figure 13, for the mobility layer radius,  $\gamma_B$ , and  $n_{eC}/n_{eo}$ .

As expected, at any altitude, it was found that an increase of probe potential perturbs the plasma further. Thus the collecting surface,  $A_A$ , is larger, further away from the probe, and the ratio  $n_{eC}/n_{eB}$  is greater. When the potential is held fixed, as the probe goes higher altitude, the gas will be less dense, and the electrons have fewer collisions with the neutral gas molecules. Thus a smaller electric field is required to accelerate the drift velocity of the electron to meet the requirement  $v_D = 10 \bar{U}$ , and the distance from the probe where having this



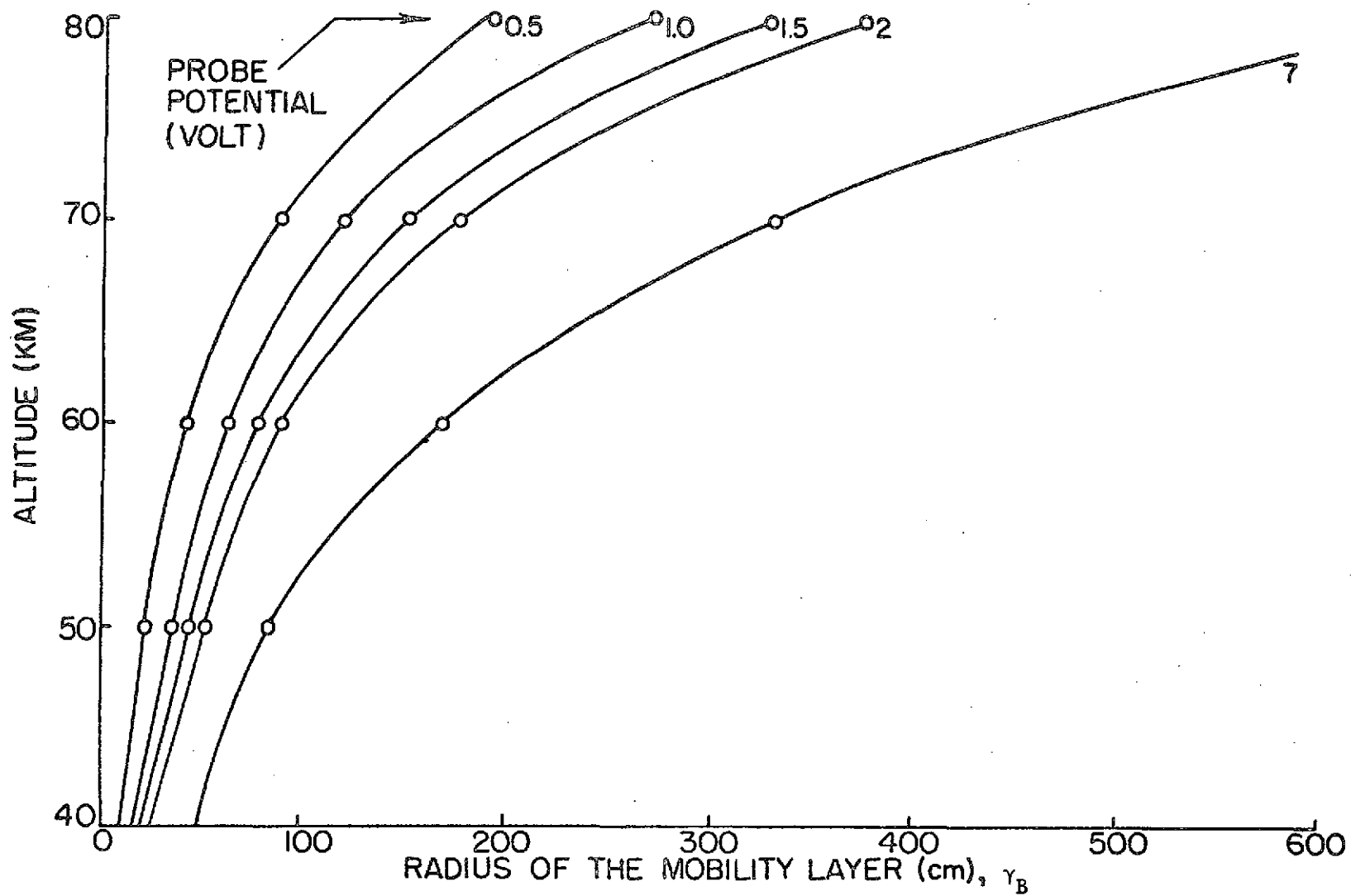


Figure 12. The Influence of the Altitude on the Mobility Layer Radius with Varying Probe's Potential

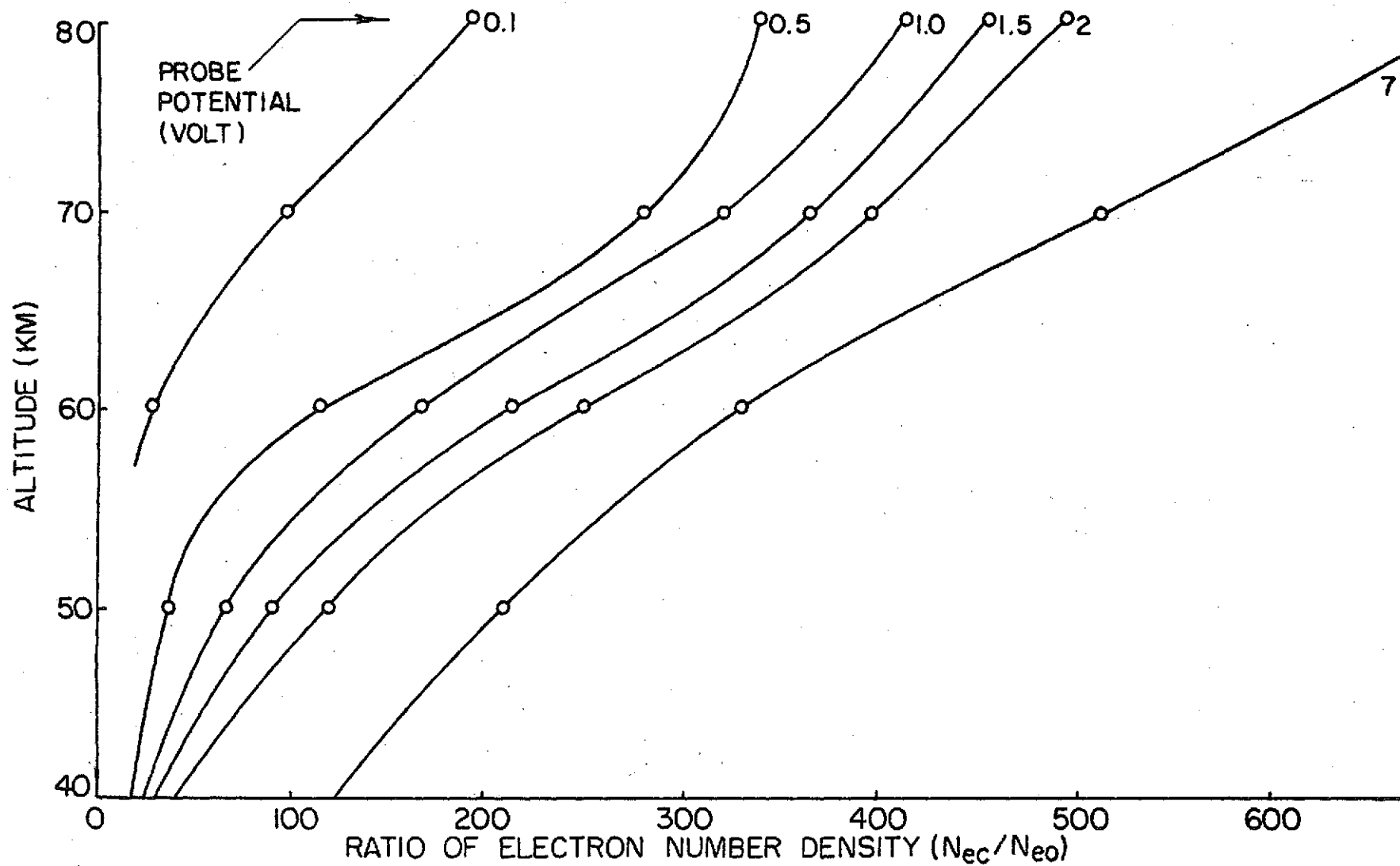


Figure 13. The Influence of Altitude on the Ratio of Electron Number Density at the Outer Diffusion Layer Edge to the Ambient Electron Density with Varying Probe Potential

electric field, of course, will be longer. Therefore, the collecting surface,  $A_A$ , will be larger and further away from the probe.

Unexpectedly, the numerical result shows that the collecting angle  $\theta_0$  is approximately constant at  $28^\circ$ . The ratio  $n_{eB}/n_{eA}$  was also found to be approximately constant at 1 for altitudes and voltages considered. Thus, it appears that the convection and mobility region only explains the mechanism how the mobility layer gets its electrons; the region does not, however, change the electron number density and essentially the electron density at the outer edge of the mobility layer is the electron ambient density.

Notice that the probe radius is the typical size of earlier rocket launches (Cert, D-16), which is two or three times larger than the size of more recent launches. Even with this large radius and at the extreme condition (80 km, 7 volt), the ratio  $n_{e0}/n_{eo}$  is only about 70 which is low enough for the space charge effect to be neglected. The zero space charge approximation is even better for smaller probe radius and lower altitudes.

#### 4.3.4 Collisionless Surface Layer

The fact that the diffusion of electrons is a collisional phenomenon requires that the mean free path of electron-neutral collisions,  $\lambda_{e-n}$ , should be much smaller than the estimated thickness of the diffusion layer ( $L/\phi_w$ ). When this requirement is not satisfied, the diffusion layer is not a relevant concept. This difficulty is removed by replacing the diffusion layer with a collisionless surface layer.

For the case  $\lambda_{e-n} < a$ , one mean free path ( $\lambda_{e-n}$ ) from the probe, a closed surface is drawn as shown in Figure 14a. The electrons inside this layer experience no collision with the neutrals. This layer is referred to as the collisionless surface layer. Above this layer, we still have the mobility layer, and the convection and mobility layer. Inside this collisionless surface layer, electrons move at thermal velocity and the current to the collector disc is the thermal flux times the area of the collector disc. Thus, the electron current and electron density ratio are

$$I_e = \frac{e}{4} n_{e\lambda} \bar{C}_e A_{col} \quad (4.3.39)$$

$$n_{eB} A_B v_{DB} = n_{e\lambda} (\pi a^2) \bar{C}_e \quad (4.3.40)$$

Combining Eqs. (4.3.35), 4.3.39) and (4.3.40), we have

$$I_e = \frac{1}{4} n_{eo} e \bar{C}_e A_{col} H \quad (4.3.41)$$

$$H = \frac{\pi (\gamma_A \sin \theta)^2 \bar{U} + 2\pi \gamma_A^2 (1 - \cos \theta) v_{DA}}{\pi a^2 \bar{C}_e} \quad (4.3.42)$$

Remembering that  $v_{DA} \ll \bar{U}$  and  $\theta \approx 28^\circ$ , we have

$$H = \frac{\gamma_A^2 (\sin^2 \theta) \bar{U}}{a^2 \bar{C}_e} \quad (4.3.43)$$

The radius of the convection-mobility region,  $\gamma_A$ , is found as follows: The drift velocity,  $v_{DA}$ , which has been chosen to be  $0.1 \bar{U}$ ,

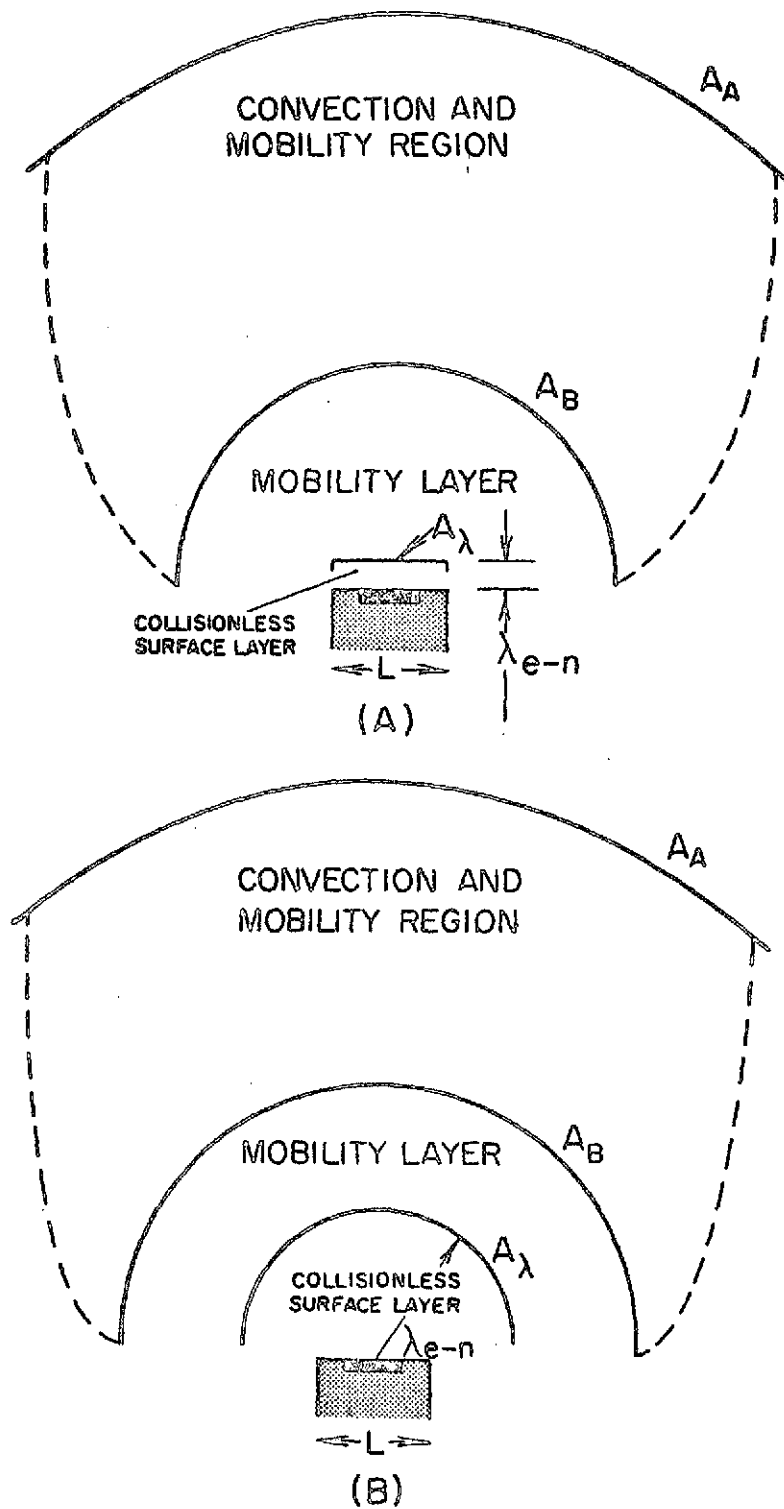


Figure 14. Perturbed Regions around a Positively Biased Probe for  
 (A)  $\lambda_{e-n} \ll L$ , (B)  $\lambda_{e-n} \gtrsim L$

has a maximum value of  $3.5 \times 10^3 \text{ cm sec}^{-1}$  at 82 km. Data in McDaniel (45) shows that for drift velocity below  $10^5 \text{ cm sec}^{-1}$ , we have

$$v_D = 10^7 \frac{|E|}{p} \quad (4.3.44)$$

So, at the outer edge of the convection-mobility region, we have

$$|E_A| = 10^8 \bar{U} p \quad (4.3.45)$$

Recall the relation

$$E_A = \frac{-2aV_w}{\pi \gamma_A} \quad (4.3.46)$$

we then have

$$\gamma_A^2 = 10^8 \frac{2a}{\pi} \frac{V_w}{p\bar{U}} \quad (4.3.47)$$

Now combining Eqs. (4.3.43) and (4.3.47), and recalling that the angle  $\theta$  has been found to be relatively constant at  $28^\circ$  for all altitudes and probe potentials considered, we have

$$H = 1.4 \times 10^7 \frac{V_w}{ap \bar{C}_e} \quad (4.3.48)$$

Taking the derivative of Eqs. (4.3.43) and (4.3.48) with respect to  $V_w$ , and combining with Eq. (4.3.13), we have

$$n_{eo} = 1.137 \times 10^{12} p \sigma_- \quad (4.3.49)$$

Notice that Eq. (4.3.49) is value only when  $\lambda_{e-n} \ll a$ . For other value of  $\lambda_{e-n}$ , the collisionless surface layer would be represented by

a hemisphere as shown in Figure 14b when  $\lambda_{e-n} \gg L$  and by a disc when  $\lambda_{e-n} \sim L$ . The electron number density in the mobility layer will now be given by.

$$n_{eB} A_B v_{DB} = n_{e\lambda} (\pi a^2 + 2\pi a \lambda_{e-n}) \bar{C}_e \quad (4.3.50)$$

$$\text{for } \lambda_{e-n} \sim L \quad (4.3.50)$$

$$n_{eB} A_B v_{DB} = n_{e\lambda} (2\pi \lambda_{e-n}^2) \bar{C}_e$$

$$\text{for } \lambda_{e-n} \gg L \quad (4.3.51)$$

Thus, the equations correspond to Eq. (4.3.49) for larger  $\lambda_{e-n}$  are

$$n_{eo} = 1.137 \times 10^{12} \left( \frac{a^2 + 2a\lambda_{e-n}}{a^2} \right) p\sigma_-$$

$$\text{for } \lambda_{e-n} \sim a \quad (4.3.52)$$

$$n_{eo} = 1.127 \times 10^{12} \left( \frac{2\lambda_{e-n}^2}{a^2} \right) p\sigma_-$$

$$\text{for } \lambda_{e-n} > a \quad (4.3.53)$$

Comparisons of Eqs. (4.3.41) and (4.3.48) and (4.3.11), and Eq. (4.3.49) with (4.3.14) show that the current collected by the collector disc predicted by the stationary probe theory is approximately the same as that by the present moving probe theory. The stationary probe theory is based on a purely mobility concept with the cut-off distance (perturbed region thickness) determined by electron drift velocity data. The moving probe theory begins with the

inclusion of convection, diffusion and mobility in the analysis. However, computations based on rocket data (Chapter V) shows that the diffusion layer is an irrelevant concept and hence does not physically exist for electron. Also, the convection effect perturbs the convection-mobility dominant region very little and thus can be neglected. Now, since mobility is the only dominant process in both stationary and flowing theories, it is thus not too surprising to find that they predict the same current to the collector disc. In the work below, rocket data will be reduced by the convection theory, though it must be remembered the stationary probe theory is equivalently accurate at low altitudes.

#### 4.3.5 Validity of the Electron Collection Theory in the D-Region

Two conditions have to be satisfied before the continuum equation Eq. (4.3.15) can be used. First, both the neutral gas and the electron gas must be a continuum. This requires  $\lambda_{n-n} \ll l_p$  and  $\lambda_{e-n} \ll l_p$ , where  $l_p$  is the characteristic length of the plasma-probe interaction problem. Now, since  $\lambda_{e-n} > \lambda_{n-n} > \lambda_{i-n}$ , the criterion to be met is

$$\lambda_{e-n} \ll l_p \quad (c)$$

Second, the mobility must be defined. This requires that the ratio of the velocity increment induced by the field,  $E$ , within one mean free path, to the thermal velocity, is small. With the time between collisions,  $\Delta t$ , represented by  $\lambda_{e-n}/\bar{C}_e$  and  $\bar{C}_e = (8 kT_e/\pi m_e)^{1/2}$ , we have (7)



$$\left(\frac{\Delta v}{v}\right)_{\max} \approx \frac{\pi}{8} \frac{eV_w}{kT_e} \frac{\lambda_{e-n}}{l_p} \ll 1 \quad (4.3.54)$$

Thus, we have

$$\frac{L_{\text{mob}}}{l_p} \ll 1 \quad (d)$$

where

$$L_{\text{mob}} = \frac{\pi}{8} \frac{eV_w}{kT_e} \lambda_{e-n} = \frac{\pi}{8} \phi_w \lambda_{e-n} \quad (4.3.55)$$

The above two conditions (c and d) ensure the legitimate use of the continuum equation and the mobility concept. In the process of analysis of the continuum equation, three further conditions are assumed. They are, (1)  $\phi_w \gg \beta R_d$  and  $\phi_w \gg 1$ , (2)  $\alpha^2 \phi_w \gg 1$ , (3)  $L_p / \phi_w \gg \lambda_{e-n}$ . The first condition allows the division of three distinct perturbed regions. The second allows the use of the Laplace equation, and the last made the diffusion layer concept a valid description of the electron dynamic very near the probe surface.

For electron collection theory in the D-region, there are three lengths which can be used for the characteristic length  $l_p$  of the plasma-probe interaction problem. They are the probe diameter  $L$ , the mobility layer radius  $\gamma_B$ , and the convection and mobility radius  $\gamma_A$ . The length  $L$  and  $\gamma_A$  are not chosen because the former is not a representative length scale for the perturbed region, while the latter does, but the variation of electron density in the convection and mobility region was found to be negligibly small in earlier sample computation. So the remaining one,  $\gamma_B$ , should be the characteristic length scale for this plasma-probe interaction problem. That is

$$l_p = \gamma_B \quad (4.3.56)$$

Notice that  $\gamma_B$  is a function of the radius,  $a$ , potential,  $V_w$ , altitude,  $h$ , and the velocity,  $\bar{U}$ , of the electrostatic blunt probe.

Based on the blunt probe data obtained from the launch on December 5, 1972, at Wallops Island, the mobility radius,  $\gamma_B$ , the electron's electrical Reynolds number,  $Rd_e$  ( $\beta Rd$ ), the mobility concept length scale,  $L_{mob}$ , and the diffusion layer's thickness,  $L/\phi_w$ , were evaluated and are plotted in Figure 15 with  $\lambda_{e-n}$ . It is concluded that the diffusion layer is not a relevant concept, since  $L/\phi_w < \lambda_{e-n}$  for all altitudes considered. The continuum assumption,  $\lambda_{e-n} \ll \gamma_B$ , fails above 70 km. Regarding the mobility concept, the length scale,  $L_{mob}$ , was found to be much greater than the characteristic length scale,  $\gamma_B$ , only below 60 km. However, according to Hoult (7), the requirement that  $L_{mob}/l_p \ll 1$  is conservative by a factor of  $10^2$  due to the clustering effect of the charged particles. Hoult concluded that the concept of diffusion is appropriate up to 80 km. The assumption  $\phi_w \gg \beta Rd$  was found to be good for all altitudes considered while the assumption  $\phi_w \gg 1$  is correct only below 70 km. In conclusion, the present electron collection theory is valid below the altitude 70 km. Above it, the result predicted by the theory is questionable.

#### 4.3.6 Electron Current to a Negatively Biased Probe

The present electron collection theory will not be complete without a discussion of the electron current to a negatively biased probe. Notice that the electron collection theory discussed

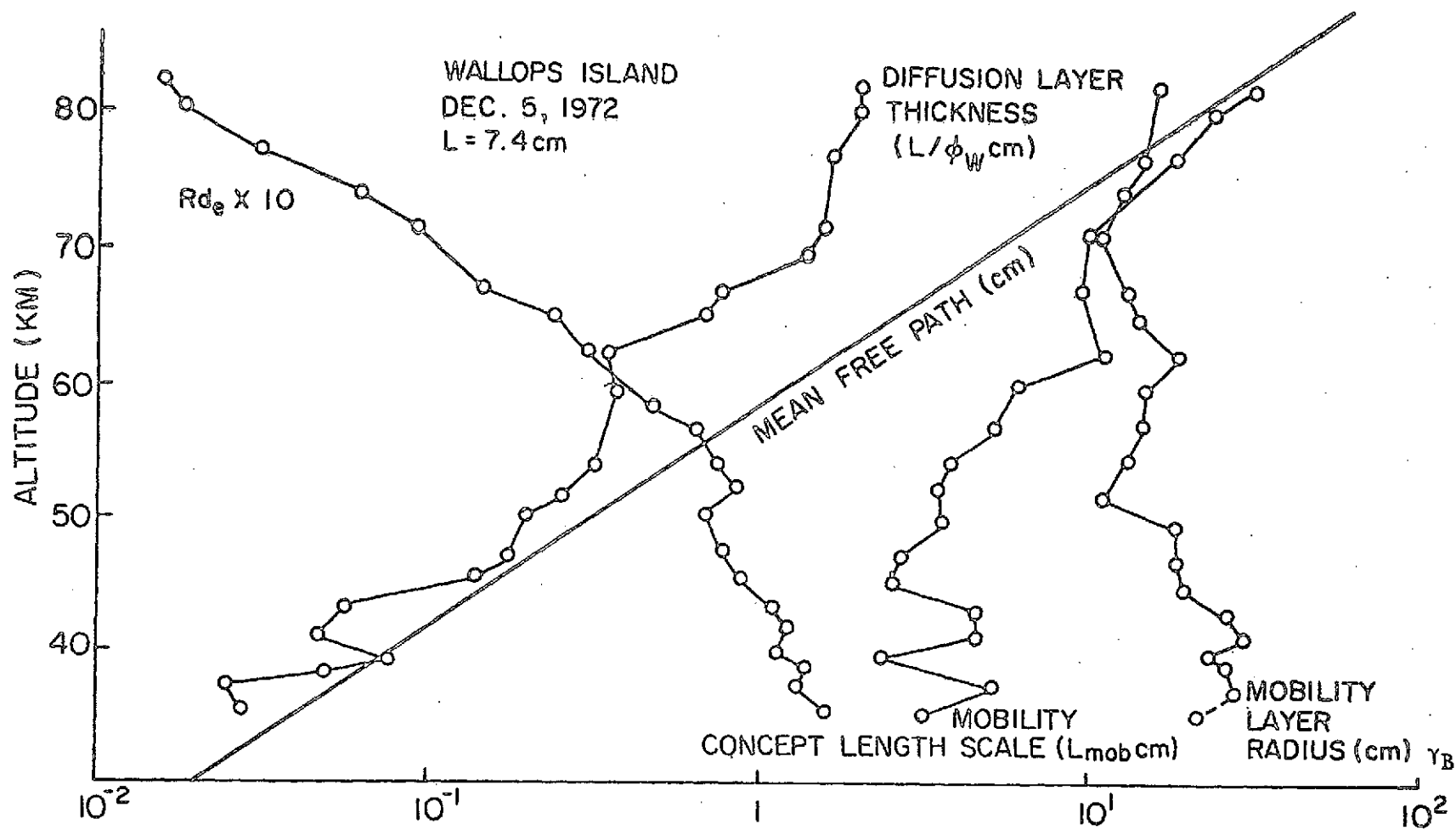


Figure 15. Various Length Scale in the D-Region

above is for a positively biased probe. The dynamics of electrons to a negatively biased probe is governed by the mass conservation equation as follows:

$$\nabla \cdot (\beta R d n_e q - n_e \nabla \phi - \nabla n_e) = 0 \quad (4.3.57)$$

It is a good assumption to assume that the electrons in the vicinity of the negatively biased probe are not dense enough to have a significant diffusion process. So, neglecting the diffusion term, we have

$$\nabla \cdot (\beta R d n_e q - n_e \nabla \phi) = 0 \quad (4.3.58)$$

or 
$$\beta R d n_e q - n_e \nabla \phi = K$$

where  $K$  is a constant. To satisfy the boundary condition  $n_e(o) = 0$ , it requires that  $K = 0$ . We have, then,

$$q = \frac{\nabla \phi}{\beta R d} \quad (4.3.59)$$

In the direction perpendicular to the probe surface,  $v \sim y$  for a stagnation flow, and  $\frac{\partial \psi}{\partial y} \sim 1$  near the wall. We then have

$$y_o \sim \frac{\phi_w}{\beta R d} \quad (4.3.60)$$

At this distance from the probe, the tendency for the electron to be carried toward the probe by the neutral gas is cancelled by the repulsion force of probe potential. This distance,  $y_o$ , is a representative thickness for the forbidden zone on the probe surface where electrons are prohibited. Throughout the D-region, this distance is very large,

thus, electron current to a negatively biased probe can be neglected as compared to be ionic current.

## CHAPTER V

## COLLISIONLESS BLUNT PROBE THEORY

The altitude of interest where the blunt probe will function in a collisionless regime is between 70 km and 300 km. Above 70 km, the collection continuum theory previously described begins to fail due to the rapid decrease of collision between electrons and neutrals. The kinetic theory based on statistical particle dynamics should be used in order to obtain a better microscopic picture of the physical processes involved in the interaction. The altitude of 300 km is chosen as the upper limit of the present discussion solely because the altitude corresponds to the F2 peak, where the electron density is highest in the ionosphere. For the purpose of estimating various relevant parameters, the typical variation of the electron temperature and density variation between these altitudes are included as shown in Figure 1 and Figure 16. It should be noted that both the neutral and electron temperature rise for higher altitudes, but with the latter rising more rapidly than the former.

## 5.1 Theory: 82 km to 300 km

The lack of any blunt probe data above 82 km requires discussion of this region to be based on some realistic assumption. The following is a discussion on the pros and cons of using the thin sheath theory to predict the probe characteristic above 82 km.

## 5.1.1 Applicability of Thin Sheath Concept

First, it is the intent here to show that a descending probe can be reasonably treated as a stationary probe. Above 82 km, all

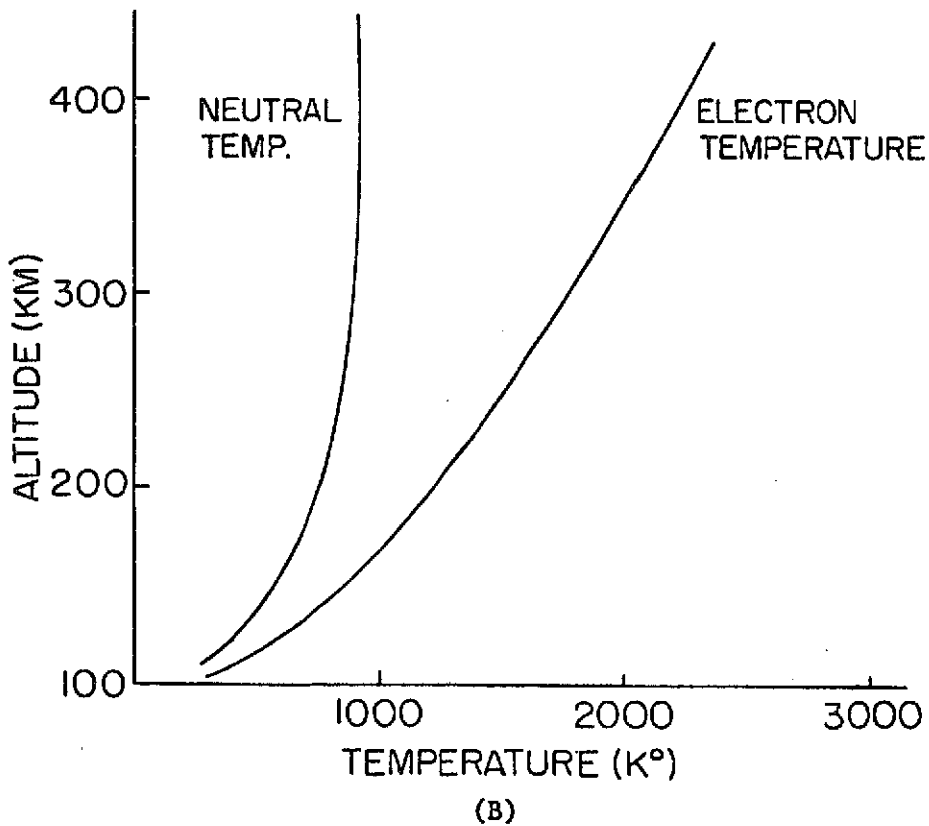
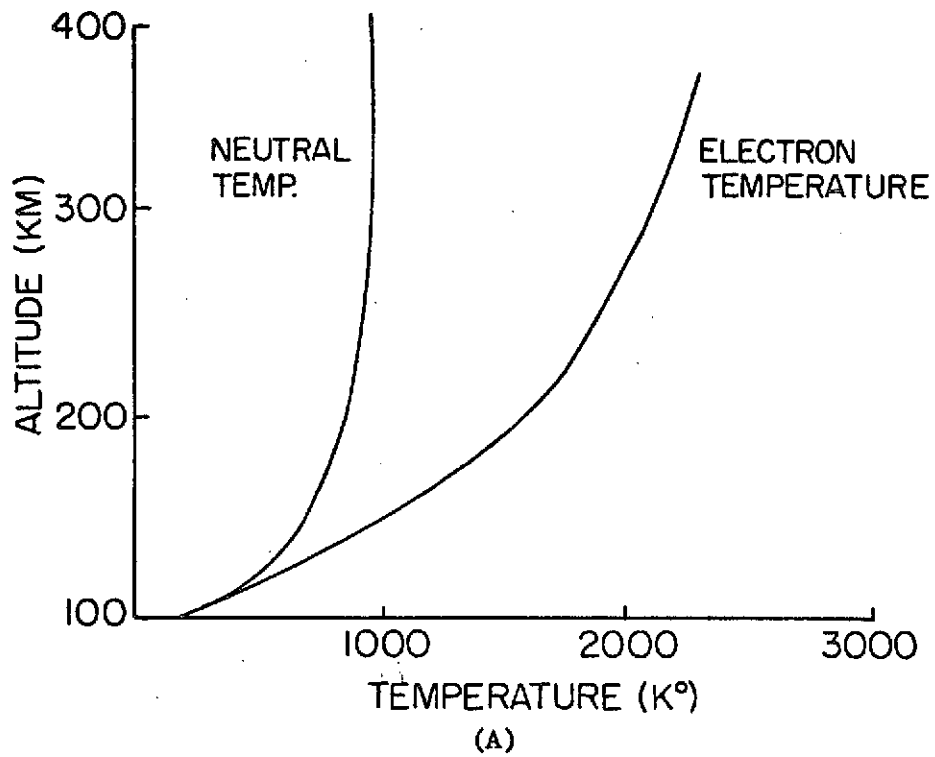


Figure 16. Variation of Measured Neutral and Electron Temperature with Altitude for (A) Puerto Rico in January 1967; (B) Millstone in December 1966 (from Stubbe (47))

charged particles whose mean free path is larger than all characteristic lengths of the plasma-probe interaction problem, are relatively free to move without collisions. Meanwhile, the very small numerical value of the parameter  $\alpha^2 \phi_w$  here, preceding the highest derivative term in the Poisson equation, indicates the presence of a sheath on the probe surface. Outside the sheath, charged particles unaffected by probe potential, are unperturbed, and enter the sheath as the vector sum of two velocities. They are the thermal velocity and the descending velocity of the probe,  $\bar{U}$ . Naturally, any probe theory neglecting the fact that the probe is actually descending at velocity,  $\bar{U}$ , will incur an error of order,  $\frac{\bar{U}}{\bar{C}_s}$ , where  $\bar{C}_s$  is the thermal velocity of the attracted charged particles.

For a parachute-borne probe descending from 300 km, the parachute will no longer be an effective drag inducing system. This failure is clearly revealed when comparing the relative size of the parachute diameter,  $d_{para}$ , and the neutral mean free path,  $\lambda_{n-n}$ , which can be used as an approximate separation distance between the neutral atoms. The very large ratio  $\lambda_{n-n}/d_{para}$  shows that the drag induced by the parachute is insignificant. Throughout most of the altitude range (82 km - 300 km), the probe will be descending at hypersonic speed which is estimated to be 1 km/sec. With the ionic thermal speed of approximately 500 m/sec, the error introduced by neglecting the descending velocity of a negatively biased probe is very large (200 percent). Whereas, for a positively biased probe, where electrons are attracted, the descending probe can be reasonably treated as a stationary probe with only an error of approximately 1 percent.



Second, the value of the nondimensional potential,  $\phi_w$ , between 82 km and 300 km, will be estimated with the guide-lines from lower altitude measurements. The electric field of the blunt probe at which measurements were made at lower altitudes are shown in Figure 17. At 82 km,  $E_w \sim 0.01$  volt/cm, and the corresponding probe potential for that probe configuration (radius  $\sim 3.7$  cm) is about 0.04 volt. Above 82 km, no blunt probe data has been obtained. For the sake of analysis, the probe potential above 82 km is assumed to be 0.04 volt. This is a conservative assumption, since the trend of the data shown in Figure 17 predicts that the field,  $E$ , will be even smaller for altitudes above 82 km. This, together with the electron temperature shown in Figure 16, allows an estimation of  $\phi_w$  which by definition is  $eV_w/(kT_e)$ . The computed value of  $\phi_w$  is 0.23 at 300 km and 0.3 at 175 km; it slowly increases to 3 at 82 km.

The magnitude of  $\phi_w$  between 175 km and 300 km found above satisfies the assumption of Öpik's analysis (4.8), and the screening distance of the biased probe at rest can be found on that basis. Öpik has examined the screening problem for a stationary finite size charged body (negative and positive) in medium where the general thermodynamic equilibrium holds (e.g., with a Maxwellian distribution of velocities). He found that the screening distance (sheath thickness) is exactly the Debye length when  $\phi_w < 0.3$ . This condition is satisfied between 175 km and 300 km, but fails in the altitudes ranging from 82 km to 175 km. The use of the Debye length as the sheath thickness between altitudes 82 km and 175 km is convenient, but not supported nor disapproved by any existing collisionless probe theory. In view of the fact that

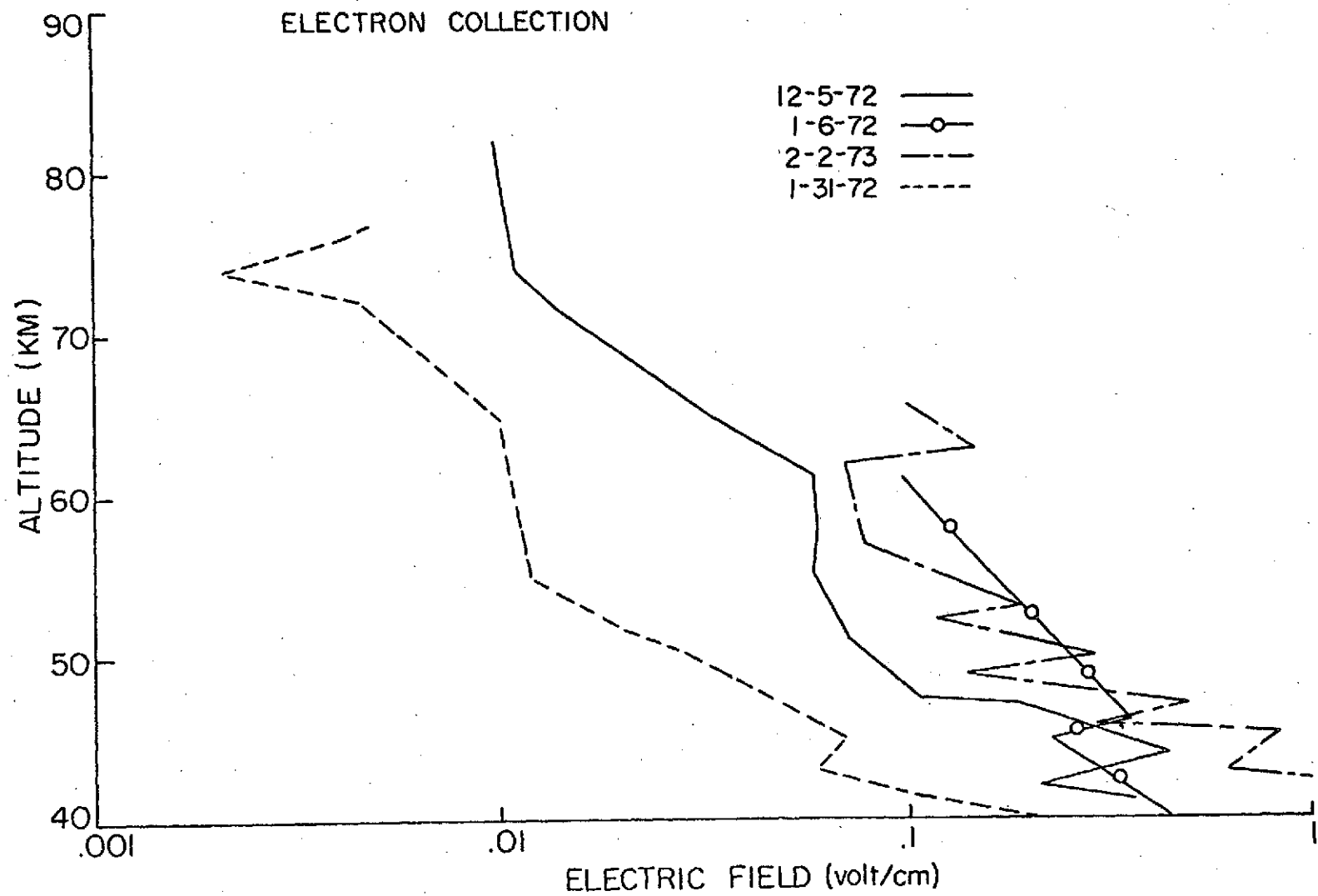


Figure 17. Variation of the Electric Field of the Probe at which Measurements were made with Altitude

$\phi_w \sim 1$  here, the sheath thickness will solely be a function of the Debye length and probably weakly depends on  $\phi_w$ . Thus, it is reasonable to use the Debye length as an indication of the sheath thickness throughout the entire range of altitudes considered here (82 km - 300 km).

The computed value of the Debye length based on the typical electron density shown in Figure 1 is 0.3 cm and 300 km and 3 cm at 82 km. For a typical probe diameter of 7.4 cm, the sheath on the probe is thin at 300 km and relatively thick at 82 km. The mean free path for charged particle-neutral collisions is larger than the thickness of the sheath; thus the sheath on the probe surface is collisionless. For a thin sheath, the streamlines of the attracted charged particles will be relatively straight and perpendicular to the probe surface. A one-dimensional analysis inside the sheath is thus applicable and will be listed in the next section. When the sheath is thick, the streamline will now narrow towards the center of the collector disc. To account for this converging effect of the streaming lines, the two-dimensional Poisson equation, which is elliptic in character, has to be solved. The mathematical equations involved are intractable. However, only those attracted charged particles entering through the central portion of the thick sheath will arrive at the collector disc, and be measured as the current to the probe. The converging effect here is probably small enough to allow the thin sheath solution to describe the probe characteristic. Naturally, the current will be underestimated by the thin sheath concept due to the converging effect of the stream lines.

In conclusion, the thin sheath concept will be used for the entire altitude range (82 km - 300 km) to determine the current voltage characteristic of the probe.

### 5.1.2 Thin Sheath Theory

The collisionless infinite flat plate stationary probe theory is well understood and available in text material (49). The planar probe is assumed to be cold and absorbing; both ions and electrons have a Maxwellian velocity distribution. Only the solutions are listed here.

For a positively biased probe ( $V_w > 0$ )

$$j = \frac{1}{4} n_{eo} e [\bar{C}_i \exp \left( -\frac{eV_w}{kT_i} \right) - \bar{C}_e] \quad (5.1.1)$$

$$\frac{\partial j}{\partial V_w} = -\frac{1}{4} n_{eo} e^2 \frac{\bar{C}_i}{kT_i} \exp \left( -\frac{eV_w}{kT_i} \right) \quad (5.1.2)$$

where  $j$  is the current density and  $T_i$  is the positive ion temperature.

For a negatively biased probe ( $V_w < 0$ )

$$j = \frac{1}{4} n_{eo} e [\bar{C}_i - \bar{C}_e \exp \left( -\frac{eV_w}{kT_e} \right)] \quad (5.1.3)$$

$$\frac{\partial j}{\partial V_w} = -\frac{1}{4} n_{eo} e^2 \frac{\bar{C}_e}{kT_e} \exp \left( -\frac{eV_w}{kT_e} \right) \quad (5.1.4)$$

Notice that the negative ion is not involved in the analysis since its concentration is negligibly small in these altitudes.

### 5.2 Discussion: 70 km to 82 km

A positively biased probe descending subsonically is considered here. Between 70 km and 82 km, the probe is operating in a double transitional regime, i.e.,  $L \approx \lambda_D \approx \lambda_{e-n}$ . In the absence of magnetic field, this is one of the most difficult plasma-body interaction problems one can encounter.

In this range of altitudes, neither the electron collection continuum theory described in the last chapter nor the present collisionless thin sheath solution will give a full description of the probe characteristic. However, their respective electron density predictions will be computed and compared in the next chapter.

## CHAPTER VI

## THE D-REGION ELECTRON DATA REDUCTION

## 6.1 Data Reduction by Continuum Theory

A proper reduction of the blunt probe electron data requires a knowledge of the probe potential at which measurements are made. This probe potential is needed in checking the applicability of a diffusion layer model, as compared to a collisionless surface layer. The potential is also needed in the investigation of whether various constraints posed in the derivation of the model is met at various altitudes.

Two measured quantities are first discussed. During the flight of the probe, the derivative of the electron current ( $I_e$ ) with respect to the applied potential ( $V_A$ ) between the collector disc and the return electrode is measured through a scheme using the following relation which is discussed by Mitchell (50).

$$\frac{dI_e}{dV_A} = \frac{1}{R_{cal}} \frac{(\Delta f / \Delta t)_{data}}{(\Delta f / \Delta t)_{cal}} \quad (6.1.1)$$

where  $R_{cal}$  is the resistance of the calibration resistor,  $(\Delta f / \Delta t)_{cal}$  is the slope of the straight line drawn through the preflight calibration ramp, and  $(\Delta f / \Delta t)_{data}$  is the corresponding slope of the in-flight data waveforms. The applied potential,  $V_A$ , when the  $(\Delta f / \Delta t)_{data}$  was obtained was also measured. It is related to the probe potential,  $V_w$ , as follows:

$$V_w = V_A \frac{1}{1 + \frac{\sigma_- L_p}{\sigma_+ L_r}} \quad (6.1.2)$$

where  $\sigma_-$  and  $\sigma_+$  is the negative and positive conductivity, respectively, and  $L_p$  and  $L_r$  are the length parameters of the probe and the return electrode. According to Hale, et al. (51), when the return electrode is several times larger than the collector plus guard ring, we have

$$V_w \approx V_A \quad (6.1.3)$$

In the display of the data thus obtained, instead of  $\frac{dI_e}{dV_w}$  and  $V_w$ , the negative conductivity,  $\sigma_-$ , and the wall electric field,  $E_w$ , are usually tabulated. The former two can be retrieved by the following equations [see (4.3.13) and (4.3.28)]

$$\sigma = \frac{a}{2\gamma_{col}^2} \left( \frac{dI_e}{dV_w} \right) \quad (6.1.4)$$

$$E_w = \frac{2V_w}{\pi a} \quad (6.1.5)$$

In this work, the data of five launches compiled by Burkhard (46) is recalculated here using the new continuum theory derived. The thickness of the diffusion layer and the corresponding electron-neutral mean free path are computed and plotted in Figure 18. A comparison clearly reveals that the diffusion layer concept is irrelevant and the layer is replaced by a collisionless surface layer as has been discussed last in Chapter IV.

With Eqs. (4.3.50) - (4.3.52) the ambient electron density, the old and new electron profiles are computed and plotted in Figures 19 to 23. The probe's descending speed, and the pressure of the D-region for the launch on December 5, 1972, are plotted in Figures 24 and

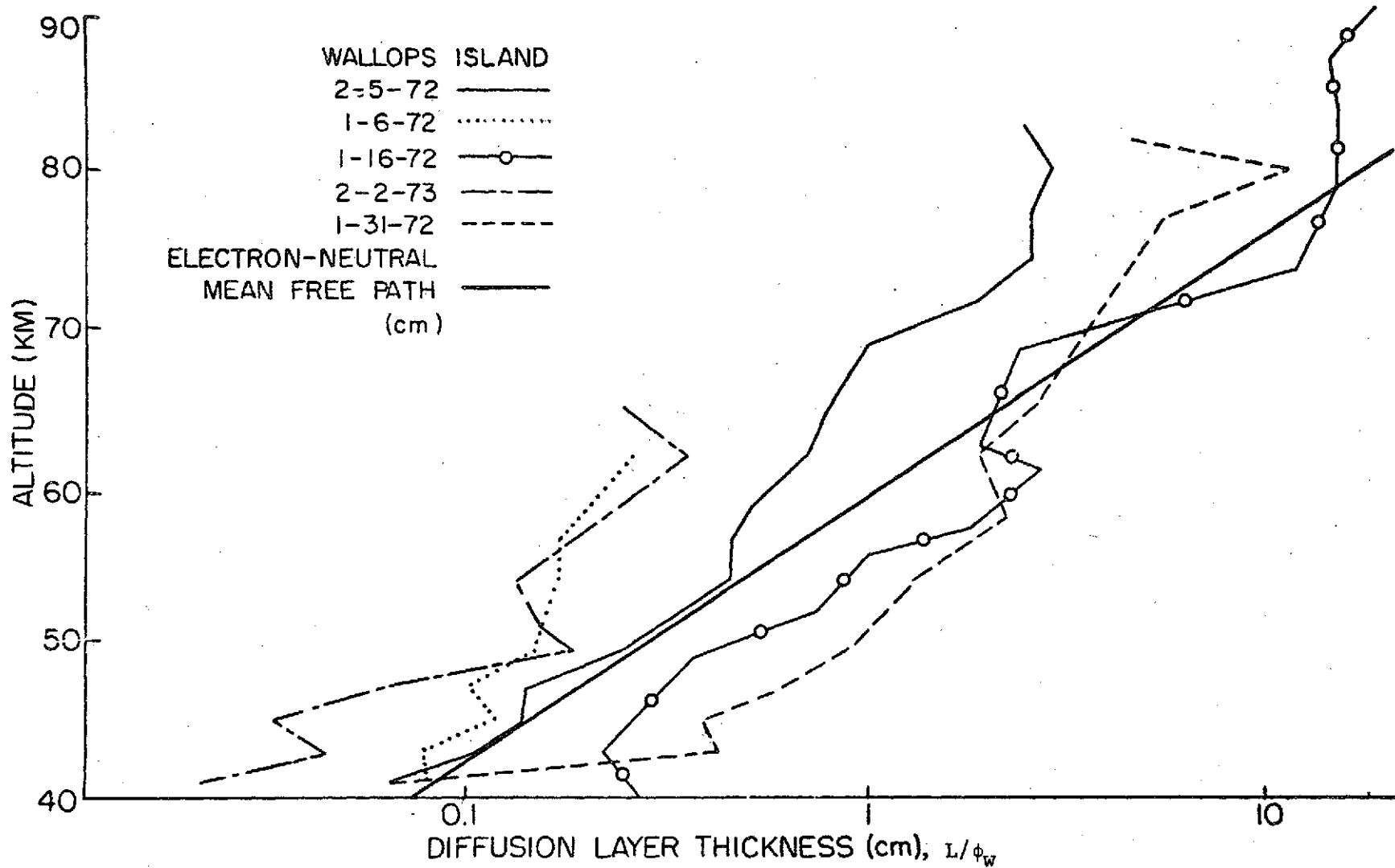


Figure 18. Electron Diffusion Layer Thickness with Varying Altitudes



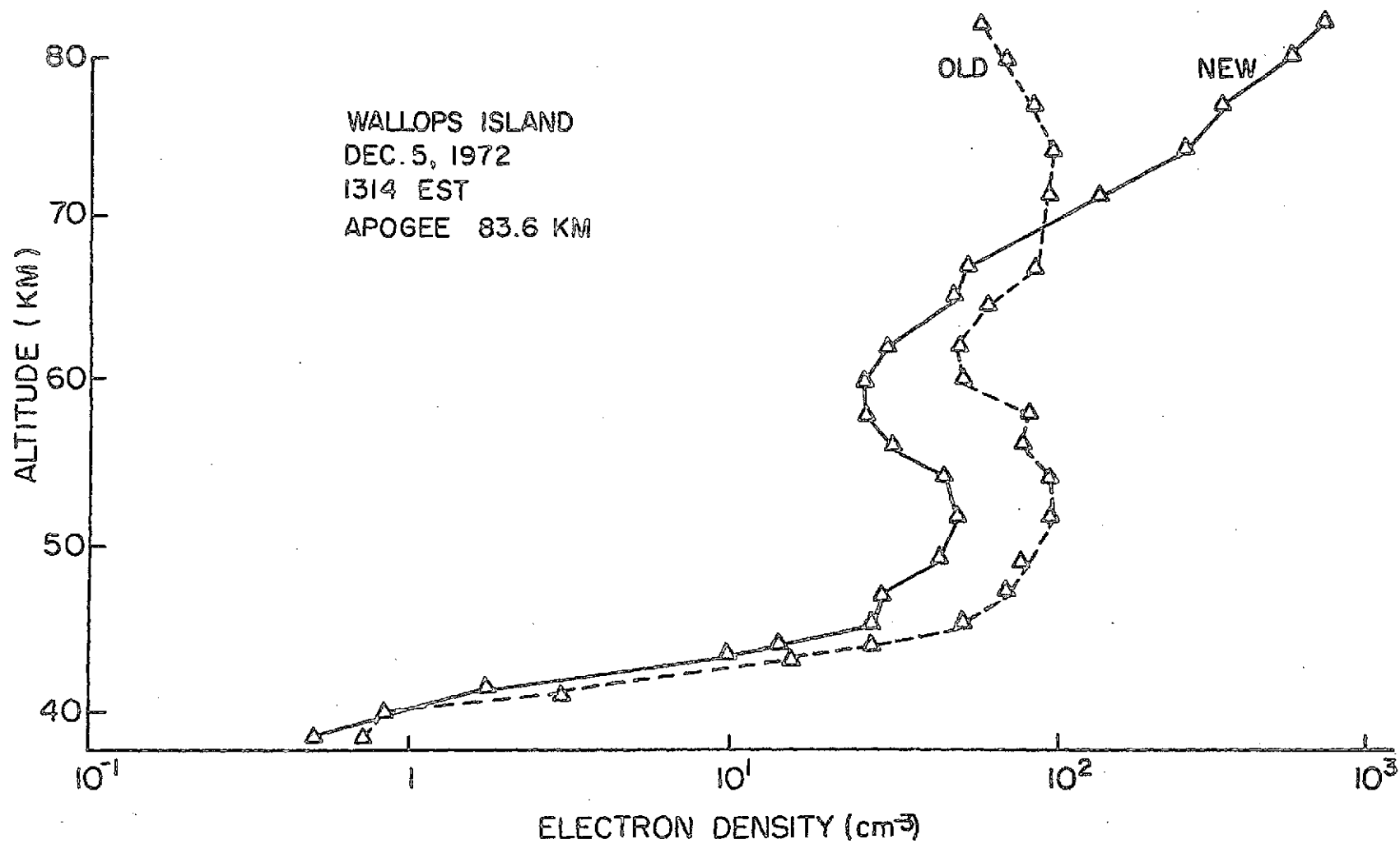


Figure 19. Electron Density Profile for December 5, 1972

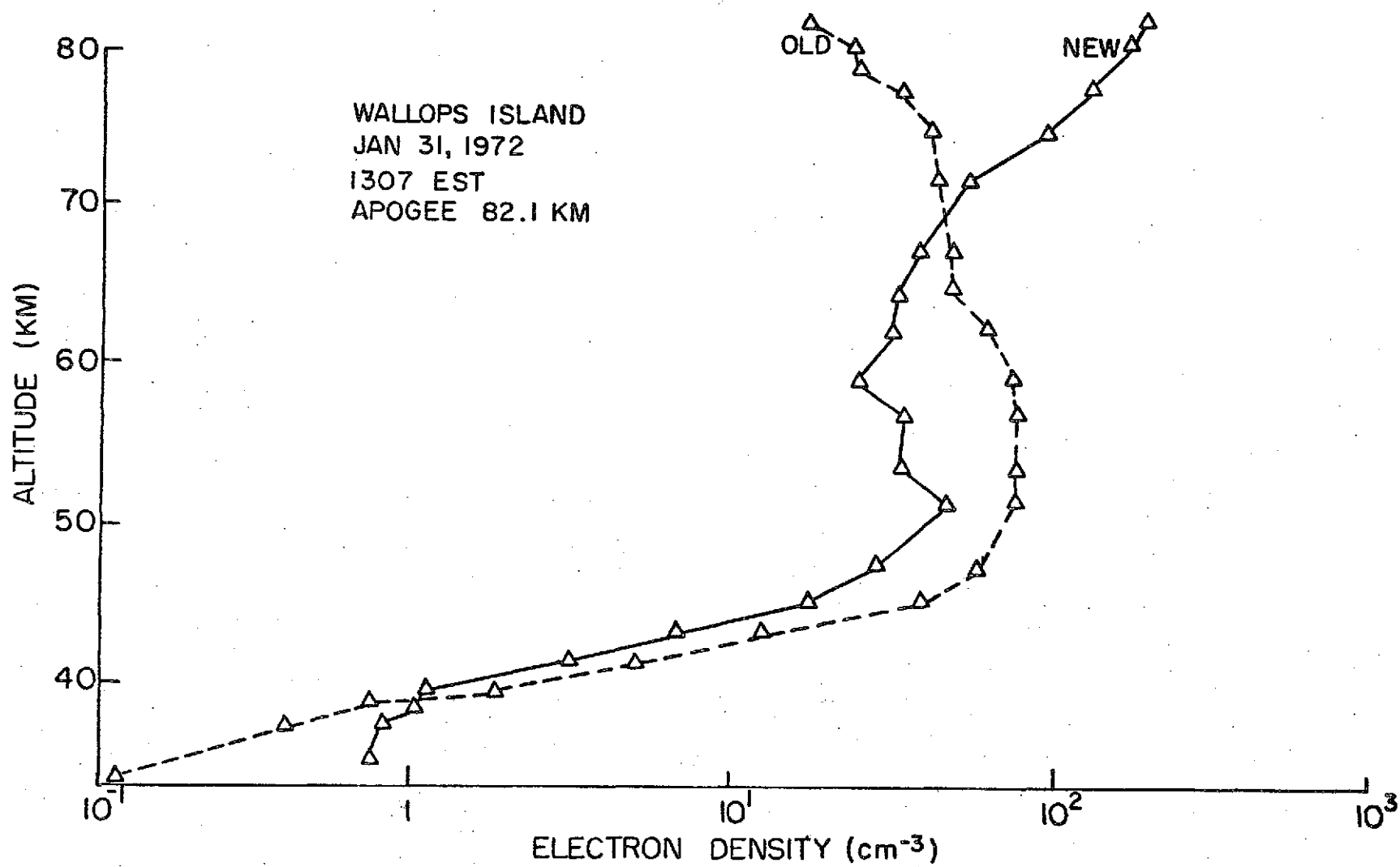


Figure 20. Electron Density Profile for January 31, 1972

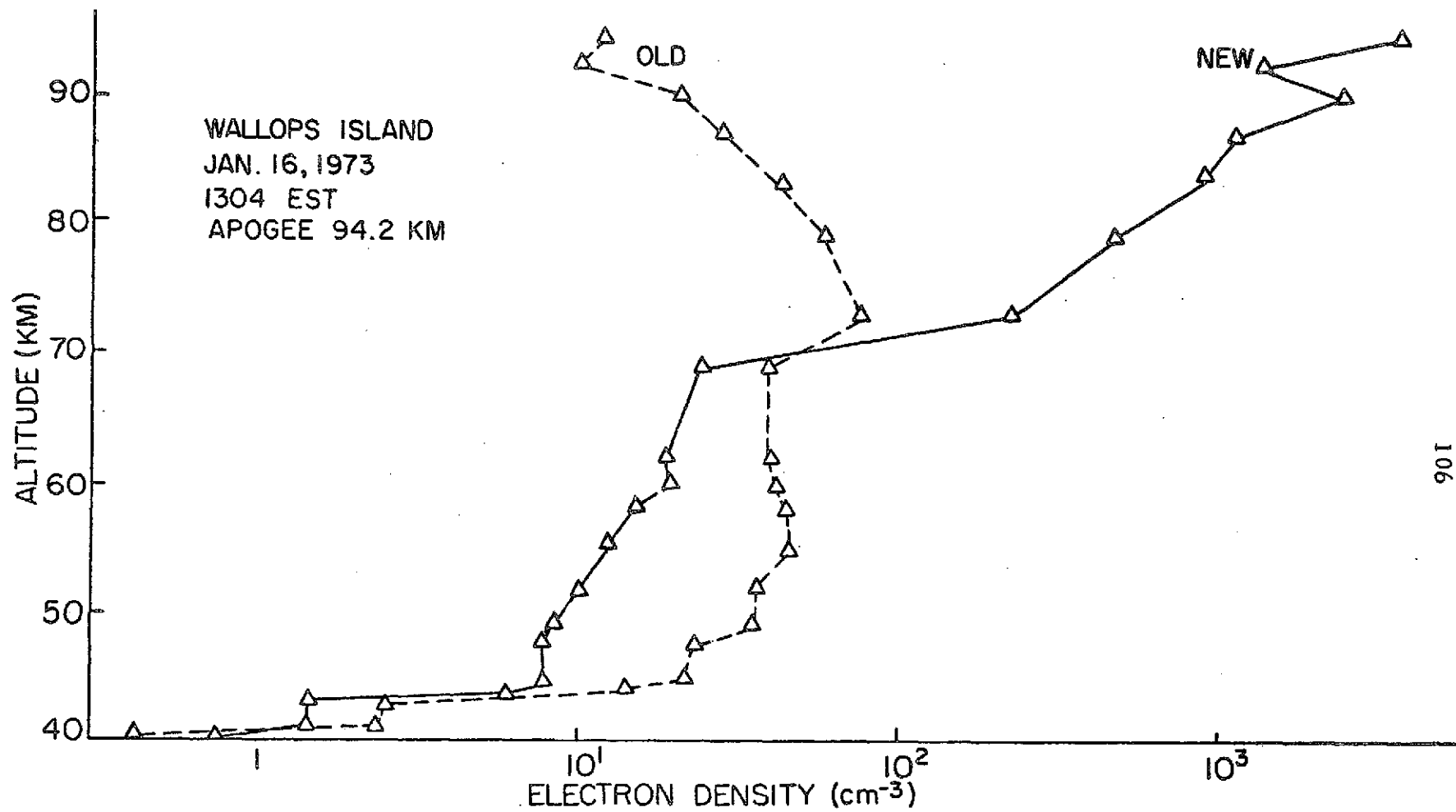


Figure 21. Electron Density Profile

January 16, 1973

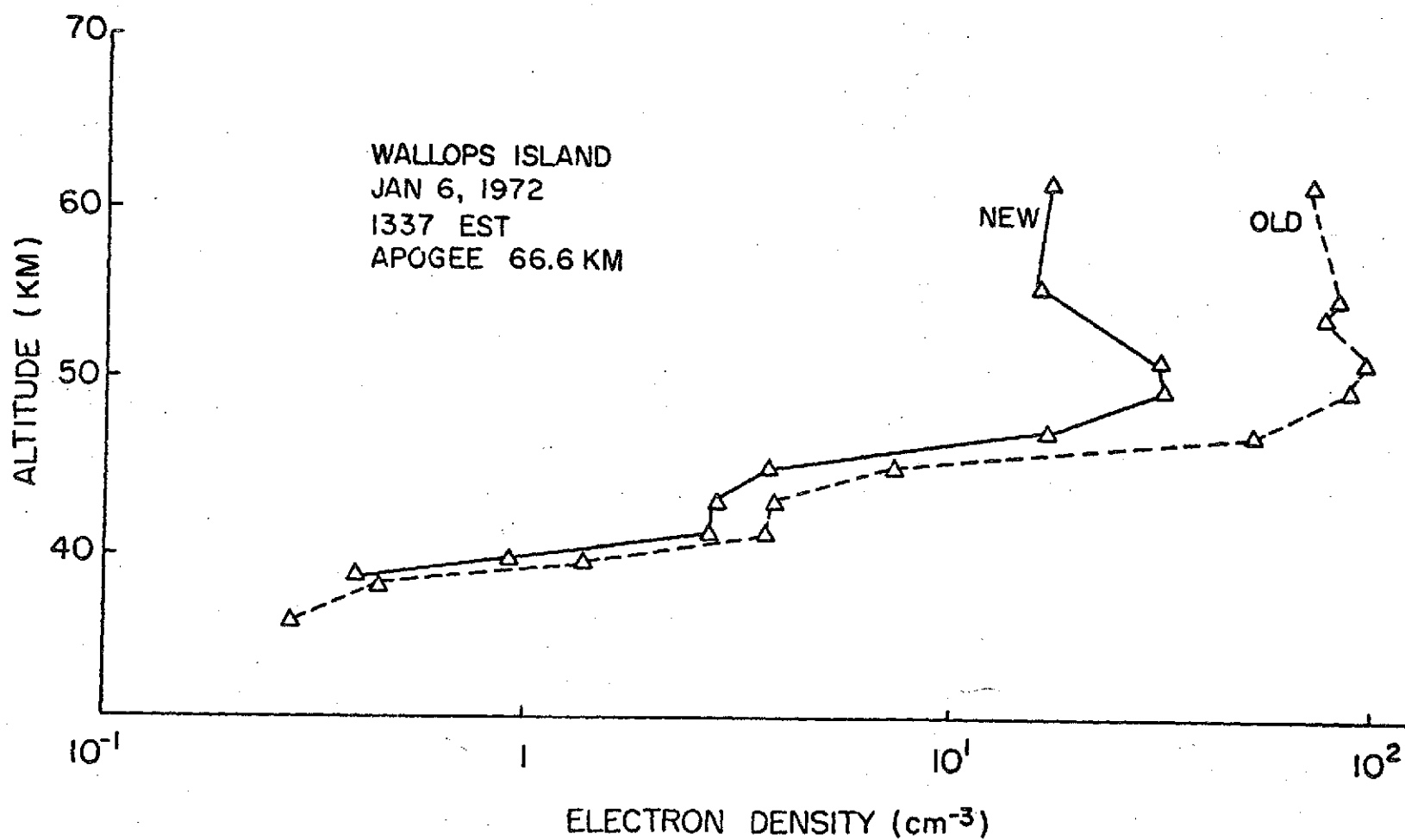


Figure 22. Electron Density Profile for January 6, 1972

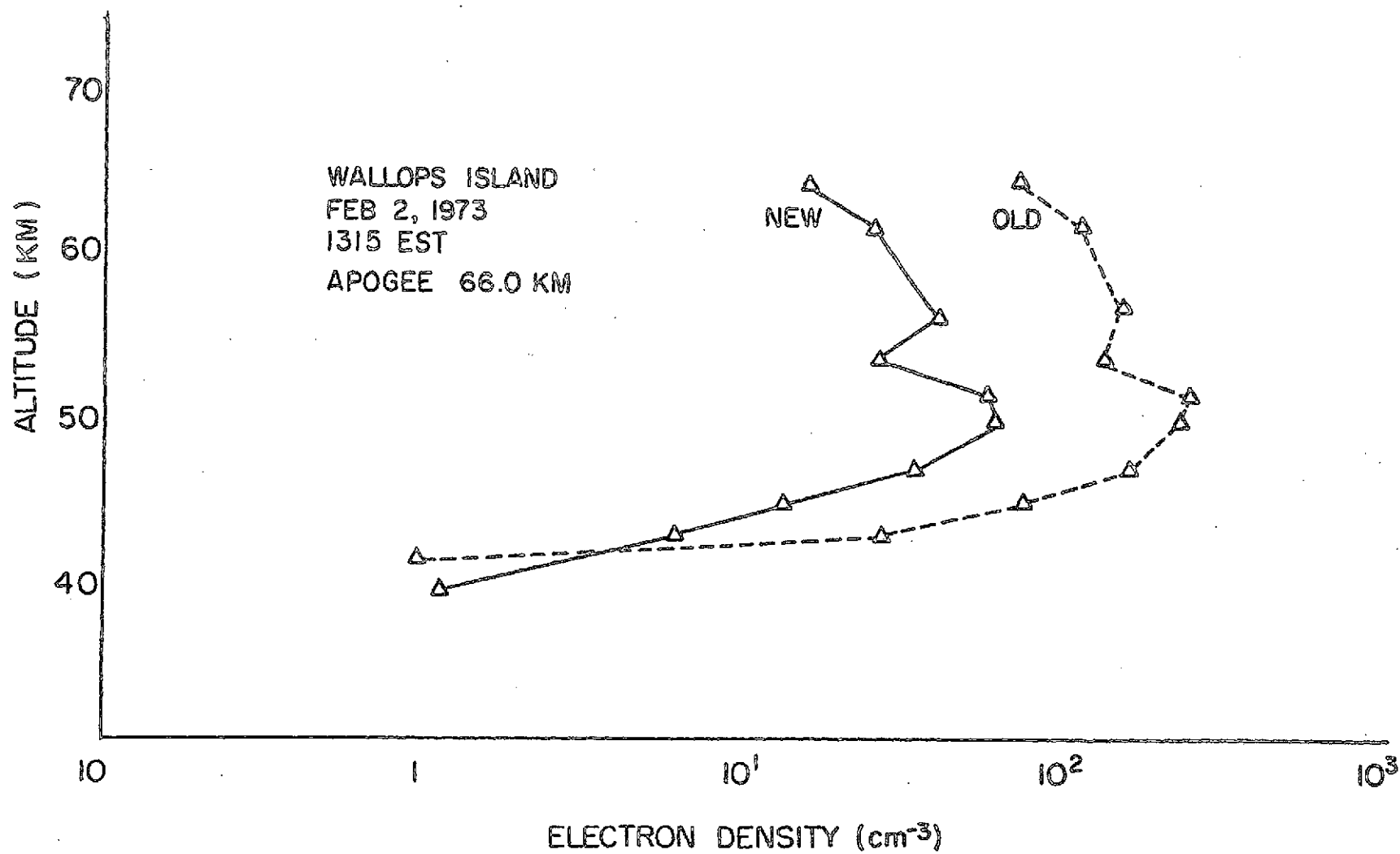


Figure 23. Electron Density Profile for February 2, 1973

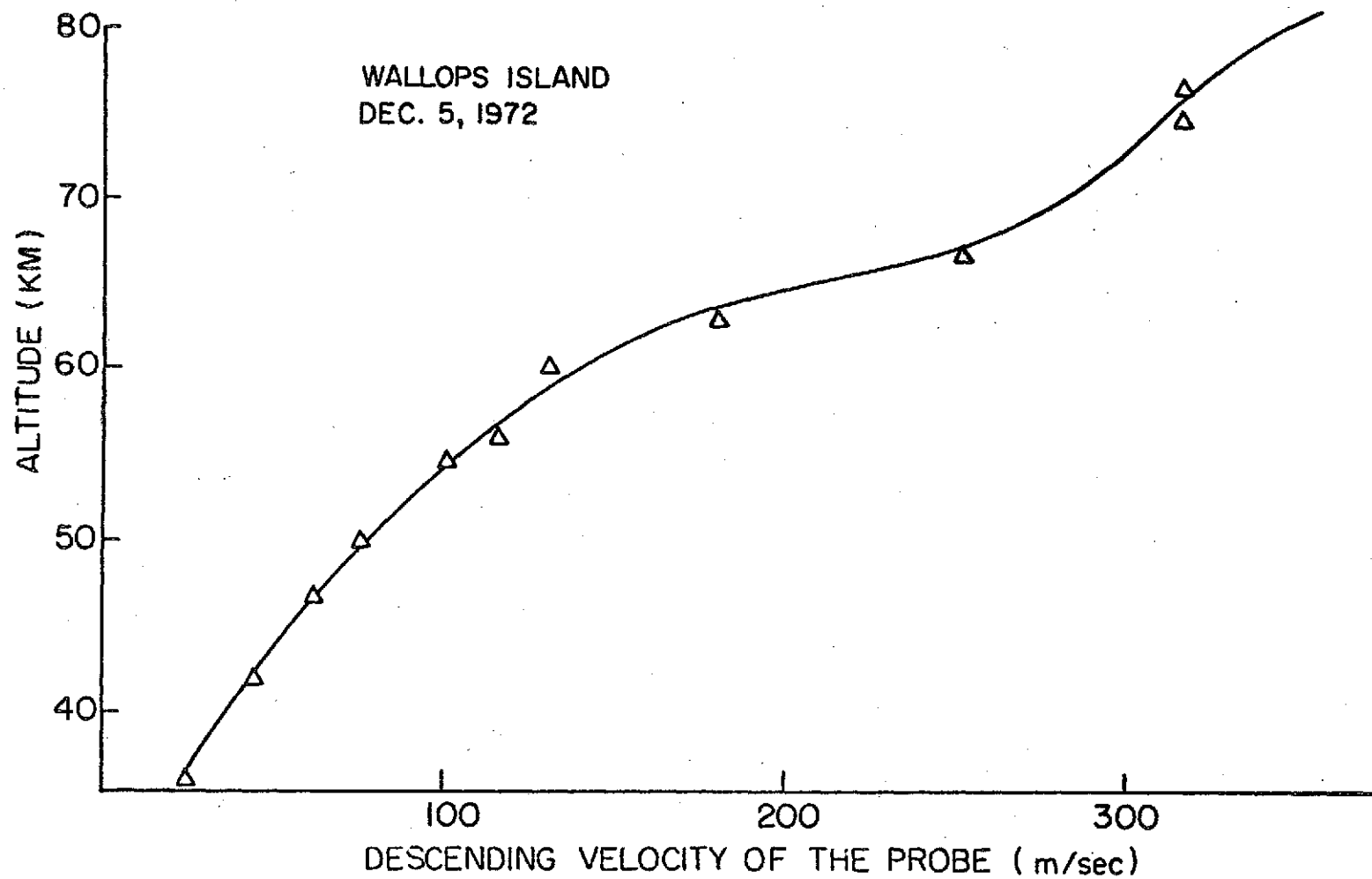


Figure 24. The Descending Velocity of the Probe at Various Altitudes

25 for reference. For the launch on January 31, 1972, the present blunt probe data is compared with the result of a combined probe and propagation experiment performed by the University of Illinois at the same date. It is shown in Figure 26.

As has been expected, the new electron number density is smaller than the old prediction below 60 km. This is in agreement with the physical model since the electron collecting surfaces are now larger and further away from the probe (mobility layer outer edge) as compared with the past theory, where the collecting surface is the outer edge of the diffusion layer. For a larger collecting surface, a bigger electron current will be collected by the collector disc on the probe for a given ambient electron density. Thus, for a given measured current, the electron density predicted will be smaller.

Above 60 km, the new electron density increases for higher altitudes. It exceeds the old electron density at approximately 70 km and continues to increase rapidly with altitude. The rapid increase of the newly predicted electron density above 60 km is due to the drastic increase of the thickness of the collisionless surface layer,  $\lambda_{e-n}$ , compared with the thickness of the mobility layer,  $\gamma_B$ . A larger  $\lambda_{e-n}/\gamma_B$  implies a smaller  $n_{e\lambda}/n_{eB}$  and hence the predicted density will be higher for a given measured current.

The new electron profile above 70 km should be viewed with caution since at about 70 km, most of the assumption (e.g., continuum concept), as have been pointed out in Chapter IV, begin to fail. At about 80 km, where  $\lambda_{e-n} \sim \gamma_B$ , a layered geometry as shown in Figure 14b

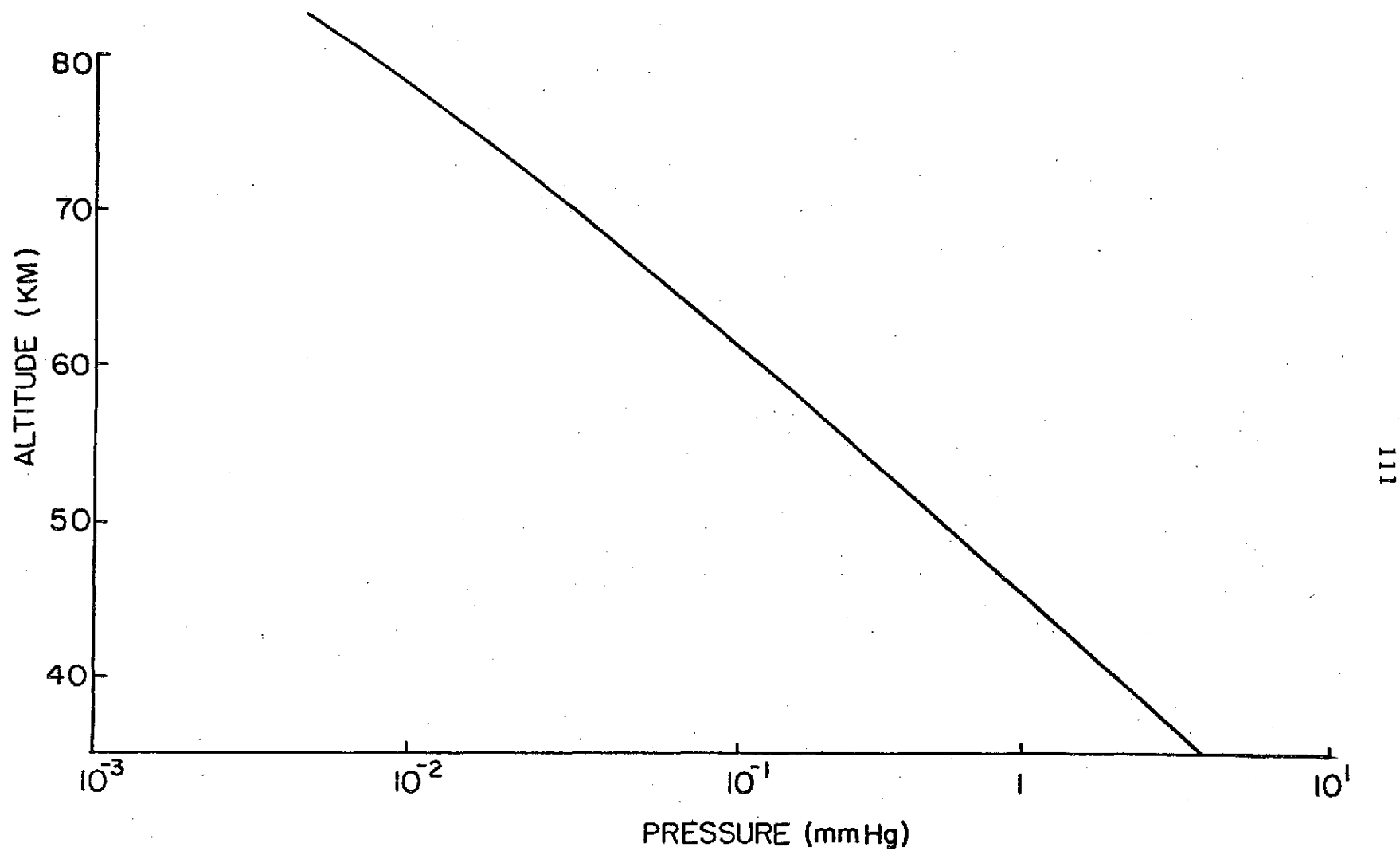


Figure 25. Pressure Profile.



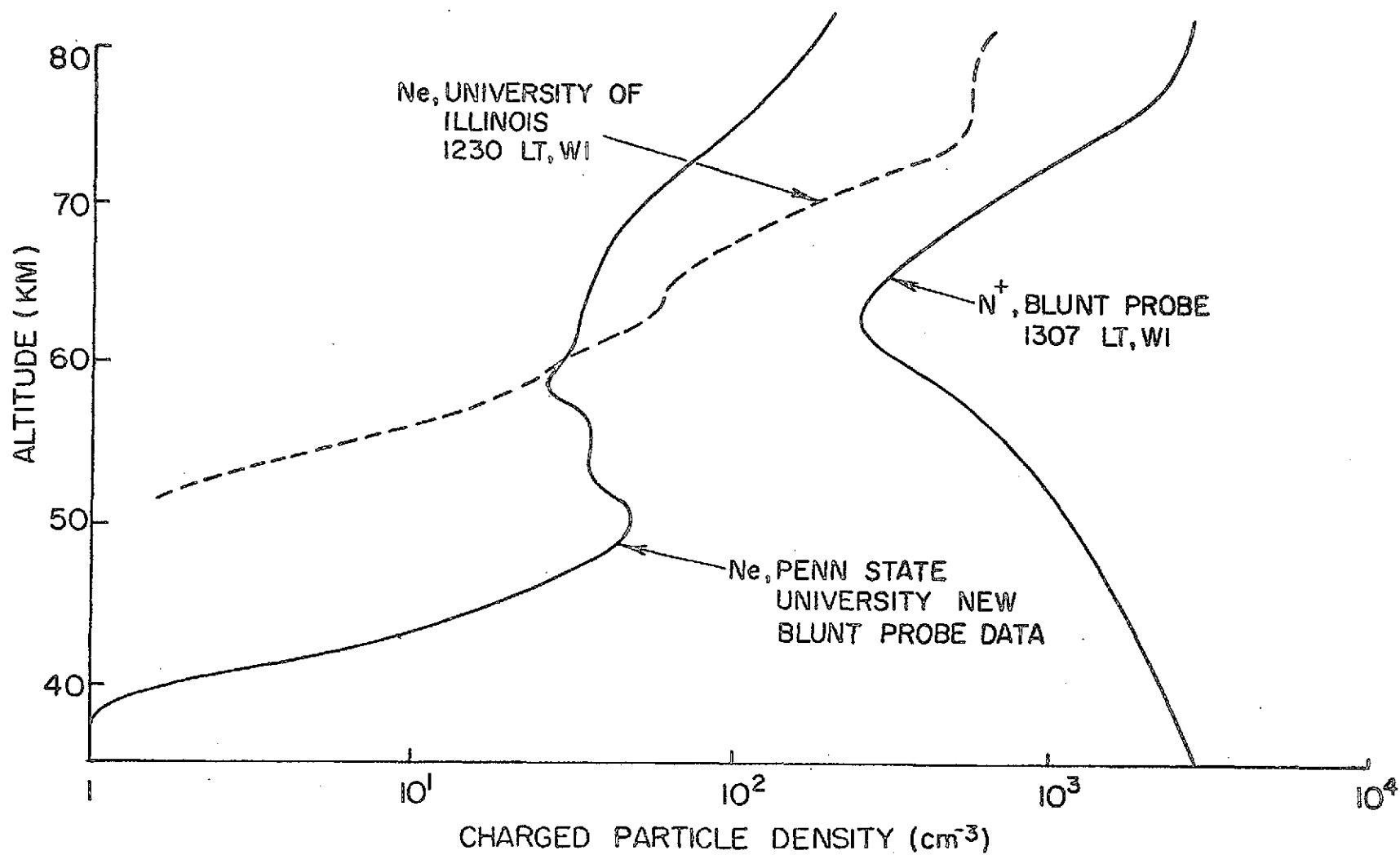


Figure 26. Electron and Positive Ion Density Profile for 31 January 1972, Wallops Island, Virginia

no longer exists and the present continuum theory is expected to collapse above 80 km.

## 6.2 Data Reduction by Collisionless Theory

The available data between 70 km and 94 km are also reduced by the collisionless theory (thin sheath theory). The predicted electron densities are plotted in Figure 27.

The electron density obtained by collisionless theory is considerably higher than that predicted by continuum theory. Naturally, this is due to the fact that the electron collection surface which is the thin sheath edge in the collisionless theory is very much smaller than that in the continuum case. For a given ambient electron density, the electron current predicted by the collisionless theory will then be smaller. Thus, for a given measured electron current, the electron density predicted by the collisionless theory will be considerably higher than that by continuum theory. It will be noticed that some data points comparing both continuum and collisionless predictions are not included in the figure because their values reduced by the collisionless theory is too large to be appropriate.

In general, between altitude 70 km and 94 km, a continuum theory tends to underestimate the electron density while a collisionless theory will overestimate the electron density. Thus, the actual electron profile in this high altitude as indicated by other well established experimental results is expected to be within this upper and lower limit.

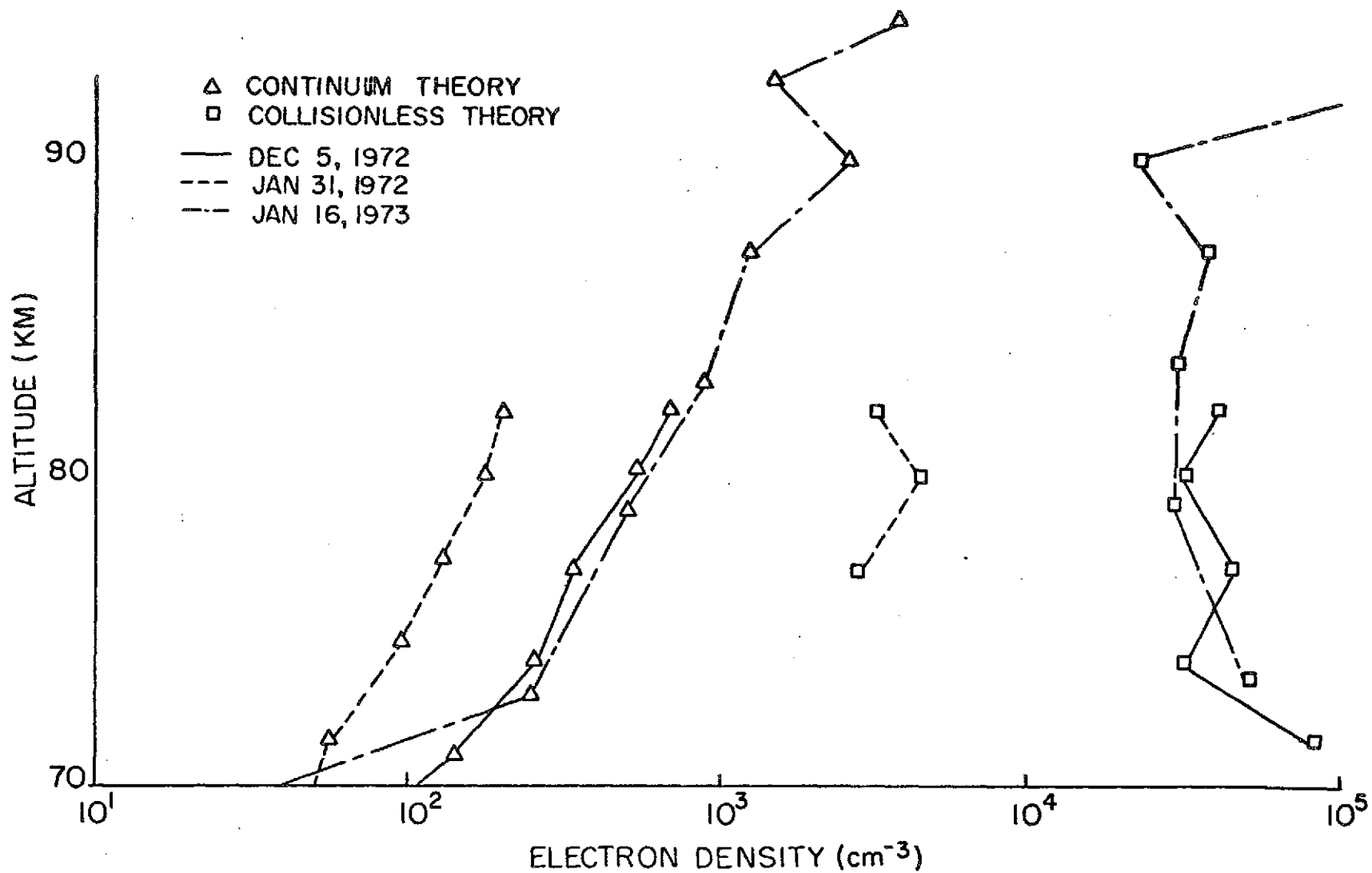


Figure 27. Comparison of Electron Density Profiles Reduced by Continuum Theory and Collisionless Theory

## CHAPTER VII

## CLOSURE

## 7.1 Summary

The subsonic, parachute-borne electrostatic blunt probe has been used for a D-region composition study by the Ionosphere Research Laboratory at The Pennsylvania State University. The scope of this work is to review the past D-region blunt probe theory and to develop a correct electron collecting, positively biased probe theory.

In the formulation of the basic equations, various nondimensional parameters have been estimated and discussed. The importance of a prior approximate knowledge of the quantities (e.g., electron temperature and density) to be measured was noted. These quantities are crucial for deriving an analytic solution since they are needed in ordering various parameters. In considering various characteristic lengths, electron Larmor radius, the electron perturbed length, and the electron-neutral mean free path, the magnetic effect on electron collection could be significant, though it is not included in the present analysis.

The relatively low D-region electron temperature (230°K) compared with the usual plasma condition (3000°K) results in the nondimensional probe potential ( $\phi_w$ ) much greater than unity for typical D-region probe potentials; this has two results. First, with  $\phi_w \gg 1$ , the basic assumption that  $\phi_w \ll 1$  in the classical derivation of the Debye length is not satisfied; thus, the usual physical implication that the electric field is negligible at distance outside the Debye length is lost. Second, the fact that  $\phi_w \gg 1$  and  $\lambda_D \sim L$  shows that the Laplace equation

is an adequate description of the electric field outside the probe surface. This referred to as the zero space charge theory, is the basis for the present analyses for both ion and electron collection.

It was found that a biased probe perturbs the attracted ions only within a thin region ( $L (Rd)^{-1/2}$ ) on the probe surface, due to the large convection influence on the ions as compared with the diffusion and mobility effect. In the present case of an incompressible plasma flow over the probe, Sonin's ion collection theory can be used inside this thin perturbed region where convection, diffusion and mobility effect all have to be considered in the analysis. With some rocket-borne blunt probe data, it has been demonstrated that the strong field condition, which is equivalent to the case  $\mathcal{O}(Rd^{-1/2}) \gg \mathcal{O}(\phi_w^{-1})$ , is satisfied in the D-region. Thus, Hoult's diffusion layer model, which is based on the assumption that the perturbed region of  $\mathcal{O}(\phi_w^{-1})$  thick where convection effect can be neglected, is also an adequate theory for ionic data reduction.

Electron density is perturbed by a positively biased probe to a much greater extent compared to the perturbation of the ions. This is due to the inadequate shielding of the probe by the space charges and the small electron inertia which demeans the convection effect. The usual thin boundary layer analysis is inapplicable, and we are confronted with the difficult task of solving an elliptic equation (electron conservation equation) with incomplete knowledge of the boundary conditions. This difficulty is removed by assuming the electric field above one end of the blunt probe is the same as that above a circular disc which is obtained by shrinking an ellipsoid to infinitesimal thickness.

The limiting case of a stationary probe is first considered. A model based on the available experimental data of the electron drift velocity versus electric field and pressure is proposed. The nonlinear behavior of the above data is used to determine the cut-off distance of the electron collecting region. This model considers only mobility effect while the diffusion process is not included in the analysis.

With a flow toward the probe, the dependence of electron dynamics on various processes is examined by observing the dominant terms in the governing equation at various distances from the probe. Four regions have been identified; they are: the unperturbed outer region, the convection-mobility dominant region, the mobility dominant region, and the diffusion mobility region. A simple drift velocity model is proposed. The location of various regions was determined by considering the relative magnitude of the convection velocity and electron drift velocity. Electron density variation in the convection-mobility region, based on a simple numerical computation of the trajectory of the electrons inside this region, has been found to be negligible. The D-region blunt probe data also showed that the diffusion layer is not a relevant concept since this layer was found to be thinner than or comparable to the electron-neutral mean free path at the corresponding altitudes. This difficulty was overcome by replacing the diffusion layer with a collisionless surface layer in the calculation scheme.

The final result of this drift velocity model, which is now reduced to a purely mobility concept model is

$$I_e = 3.5 \times 10^6 \frac{e n_{eo} A_{col} V_w}{ap}$$

This expression is essentially identical to that obtained for a stationary probe based on experimental data. The similarity of the two solutions is simply due to the fact that both the drift velocity model, and the zero velocity model depends only on the mobility concept.

The electron-neutral mean free path is larger than the probe radius for altitudes above 63 km. Above this altitude, only the collisionless surface layer needs a slight modification in the computation scheme for electron density ratio, to account for the edge effect. The above continuum theory begins to deteriorate at 70 km and collapse at about 80 km due to the failure to meet the constraints imposed during the development of the model. In general, the new electron density predicted by the drift velocity is considerably lower than previous results below 60 km and increases steadily above this altitude.

A collisionless theory based on the thin sheath concept was also discussed for higher altitudes. The descending velocity of a parachute-borne blunt probe is hypersonic between the altitudes ranging from 300 km to 80 km. For a positively biased probe, the convection velocity of the electron can be neglected compared to its thermal velocity at the sheath edge. A thin sheath solution is thus applicable in the collisionless regime. Electron density obtained by the collisionless theory in the transition regime (70 - 90 km) predicts values that are considerably higher than those predicted by continuum theory.

## 7.2 Suggestions for Further Research

On the basis of the work done here, further research would be fruitful in the following areas:

- (a) The absolute values electron current to the probe are not included in the given data. A successful

attempt to obtain the current will allow an electron data reduction by the current equation which can serve as a check to the present prediction.

- (b) Extension of the foregoing analysis to include the geomagnetic effect on the electron dynamics in various layers.
- (c) Investigation of the feasibility of using a parachute-borne spherical probe. The spherical probe theory in a quiescent plasma in all three regimes, (continuum, transitional and collisionless), has been fairly well explored. A perturbation technique should not be too difficult to set up to account for the presently descending probe.
- (d) Investigation to obtain reliably the probe potential at which measurements are made.
- (e) Laboratory measurements of the mobility and the diffusion coefficient of the D-region dominant ions are needed for a better ionic data reduction. A larger range of  $E/p$  with the electron drift velocity in a D-region simulated environment will give a better prediction of the electron density.



## REFERENCES

1. Bowhill, S. A., Mechtly, E. A., Sechrist, C. F., and Smith, L. G., "Rocket Ionization Measurements on A Winter Day of High Absorption," Space Res. VII, Ed. Smith-Rose, North-Holland, Amsterdam, 1967, p. 246.
2. Bowhill, S. A., and Smith, L. G., "Rocket Observation of the Lowest Ionosphere at Sunrise and Sunset," Space Res. VI, Ed. Smith-Rose, North-Holland, Amsterdam, 1966, pp. 511-521.
3. Shapley, A. H., and Beynon, W. J. G., "Winter Anomaly in Ionosphere Absorption and Stratospheric Warmings," Nature, Vol. 206, 1965, pp. 1242-1243.
4. Bettinger, R. T., "An In Situ Probe System for the Measurement of Ionospheric Parameters," Interactions of Space Vehicles with an Ionized Atmosphere, Ed. Singer, Pergamon Press, New York, 1965, pp. 182-200.
5. Whipple, E. C., "An Improved Technique for Obtaining Atmospheric Ion Mobility Distribution," J. Geophys. Res., Vol. 65, 1960, p. 3679.
6. Bordeau, R. E., Whipple, E. C., and Clark, J. F. J., "Analytic and Experimental Electrical Conductivity between the Stratosphere and the Ionosphere," J. Geophys. Res., Vol. 64, 1959, p. 1369.
7. Hale, L. C., and Hoult, D. P., "A Subsonic D-Region Probe-Theory and Instrumentation," Ionosphere Research Laboratory, The Pennsylvania State University, Sci. Report No. 247, 1965.
8. Hale, L. C., "Positive Ions in the Mesosphere," Proc. of the COSPAR Symposium on Methods of Measurements and Results of Lower Ionosphere Structure, Konstanze, 1973.

9. Liu, V. C., "Ionospheric Gas Dynamics of Satellites and Diagnostic Probes," Space Science Res., Vol. 9, 1969, p. 430.
10. Chen, F. F., "Electric Probes," Plasma Diagnostic Techniques, Ed. Huddlestone-Leonard, Academic Press, New York, 1965, Ch. 4.
11. Bettinger, R. T., and Walker, E. H., "A Relationship for Plasma Sheaths about Langmuir Probes," Physics Department, University of Maryland, Technical Report No. 350, 1964.
12. Su, C. H., and Lam, S. H., "The Continuum Theory of Spherical Electrostatic Probes," Phys. Fluids, Vol. 6, 1963, pp. 1479-1491.
13. Cicerone, R. J., and Bowhill, S. A., "Positive Ion Collection by a Spherical Probe in a Collision-Dominated Plasma," University of Illinois, Aeronomy Report No. 21, 1967.
14. Talbot, L., and Chou, Y. S., "Langmuir Probe Response in the Transition Regime," Rarefied Gas Dynamics, Ed. Brundin, Academic Press, New York, 1969, pp. 1723-1737.
15. Bernstein, I. B., and Rabinowitz, I. N., "Theory of Electrostatic Probes in a Low-Density Plasma," Phys. Fluids, Vol. 2, 1959, pp. 112-121.
16. Laframboise, J. G., "Theory of Cylindrical and Spherical Langmuir Probes in a Collisionless Plasma at Rest," Rarefied Gas Dynamics, Ed. DeLeeuw, Academic Press, New York, 1966, p. 22.
17. Cohen, I. M., "Asymptotic Theory of Spherical Electrostatic Probes in a Slightly Ionized, Collision-Dominated Gas," Phys. fluids, Vol. 6, 1963, p. 1492.
18. Chmielewski, G. E., "Electrostatic Probes in a Slowly Drifting Rarefied Plasma," Ph.D. Thesis, 1968, University of Michigan.

19. Liu, V. C., "Ionospheric Gas Dynamics of Satellites and Diagnostic Probes," *Space Science Res.*, Vol. 9, 1969, p. 456.
20. Talbot, L., "Theory of the Stagnation-Point Langmuir Probe," *Phy. Fluids*, Vol. 3, 1969, pp. 289-298.
21. Lam, S. H., "A General Theory for the Flow of Weakly Ionized Gases," *AIAA J.*, Vol. 2, No. 2, 1964, pp. 256-262.
22. Touryan, K. J., and Chung, P. M., "Flush-Mounted Electrostatic Probe in the Presence of Negative Ions," *AIAA J.*, Vol. 9, No. 3, 1971, pp. 365-370.
23. Bailey, P. B., and Touryan, K. J., "Continuum Electrostatic Probes in the Presence of Negative Ions," Sandia Laboratories, Albuquerque, New Mexico, Report No. SC-RR72 0827, 1972.
24. Johnson, R. A., and DeBoer, P. C. T., "Theory of Ion Boundary Layers," *AIAA J.*, Vol. 10, No. 5, 1972, pp. 664-670.
25. Hoult, D. P., "D-Region Probe Theory," *J. Geophys. Res.*, Vol. 70, 1965, pp. 3183-3187.
26. Sonin, A. A., "Theory of Ion Collection by a Supersonic Atmospheric Sounding Rocket," *J. Geophys. Res.*, Vol. 72, 1967, pp. 4547-4557.
27. Öpik, E. J., "Particle Distribution in a Field of Force," *Interactions of Space Vehicles with an Ionized Atmosphere*, Ed. Singer, Pergamon Press, New York, 1965, p. 17.
28. Sutton, G. W., and Sherman, A., "Engineering Magnetohydrodynamics," McGraw-Hill, New York, 1965, pp. 96-98.
29. Chung, P. M., Talbot, L., and Touryan, K. J., "Electric Probes in Stationary and Flowing Plasmas, Part 1 and Part 2," *AIAA J.*, Vol. 12, No. 2, 1974, pp. 133-154.

30. Narcisi, R. S., and Bailey, A. D., "Mass Spectrometric Measurements of Positive Ions at Altitudes from 64 to 112 Kilometers," J. Geophys. Res., Vol. 70, 1965, pp. 3687.
31. Goldberg, R. A., and Blumle, L. J., "Positive Ion Composition from a Rocket-Borne Mass Spectrometer," J. Geophys. Res., Vol. 75, 1970, p. 133.
32. Sechrist, C. F., "Theoretical Models of the D-Region," Ionosphere Research Laboratory, The Pennsylvania State University, Sci. Report No. 401, 1972, p. 43.
33. Fehsenfeld, F. C., Schmeltekopf, A. L., Schiff, H. I., and Ferguson, E. E., "Laboratory Measurements of Negative Ion Reactions of Atmospheric Interest," Planet. Space Sci., Vol. 15, 1967, p. 373.
34. Fehsenfeld, F. C., Ferguson, E. E., and Bohme, D. K., "Additional Flowing Afterglow Measurements on Negative Ion Reactions of D-Region Interest," Planet. Space Sci., Vol. 17, 1969, p. 1759.
35. Narcisi, R. S., Bailey, A. D., Lucca, L., Della, Sherman, C., and Thomas, D. M., "Mass Spectrometric Measurements of Negative Ions in the D- and Lower E-Regions," J. Atmosph. Terr. Phys., Vol. 33, 1971, p. 1147.
36. Aikin, A. C., "The Relationship of Theory and Experiment in the D-Region," Ionosphere Research Laboratory, The Pennsylvania State University, Sci. Report No. 401, 1972, p. 79.
37. McDaniel, E. W., "Collision Phenomena in Ionized Gases," John Wiley & Son, Inc., New York, 1964, p. 560.

38. Benson, R. F., "Electron Collision Frequency in the Ionospheric D-Region," *Radio Sci.*, Vol. 68D, No. 10, 1964, pp. 1123-1125.
39. Al'pert, Y. L., Gurevich, A. V., and Pitaevskii, L. P., "Special Physics with Artificial Satellites," Consultants Bureau, New York, 1965, p. 2.
40. Jackson, J. D., "Classical Electrodynamics," John Wiley & Son, Inc., New York, 1963, pp. 87-92.
41. Kuo, T. J., "D-Region Probe Theory and Experiment," Ionosphere Research Laboratory, The Pennsylvania State University, Sci. Report No. 285, 1966, p. 11.
42. Baker, D. C., "Ionospheric D-Region Parameters from Blunt Probe Measurements during a Solar Eclipse," Ionosphere Research Laboratory, The Pennsylvania State University, Sci. Report No. 344, 1969.
43. Su, C. H., and Kiel, R. E., "Continuum Theory of Electrostatic Probes," *Phys. Fluids*, Vol. 37, 1966, pp. 4907-4910.
44. Stahl, N., and Su, C. H., "Theory of Continuum Flush Probes," *Phys. Fluids*, Vol. 14, 1971, pp. 1366-1376.
45. McDaniel, E. W., "Collision Phenomena in Ionized Gases," John Wiley & Son, Inc., New York, 1964, p. 543.
46. Burkhard, W. J., "D-Region Blunt Probe Data Analysis using Hybrid Computer Techniques," Ionosphere Research Laboratory, The Pennsylvania State University, Sci. Report No. 415, 1973.
47. Stubbe, P., "The Thermosphere and the F-Region--A Reconciliation of Theory with Observations," Ionosphere Research Laboratory, The Pennsylvania State University, Sci. Report No. 418, 1973, pp. 106-107.

48. Öpik, E. J., "Particle Distribution in a Field of Force," Interactions of Space Vehicles with an Ionized Atmosphere, Ed. Singer, Pergamon Press, New York, 1965, p. 37.
49. Sutton, G. W., and Sherman, A., "Engineering Magnetohydrodynamics," McGraw-Hill, New York, 1965, pp. 100-102.
50. Mitchell, J. D., "An Experimental Investigation of Mesospheric Ionization," Ionosphere Research Laboratory, The Pennsylvania State University, Sci. Report No. 416, 1973, pp. 32-38.
51. Hale, L. C., Hault, D. P., and Baker, D. C., "A Summary of Blunt Probe Theory and Experimental Results," Space Res. VIII, Ed. Mitra, Jacchia, and Newman, North-Holland, Amsterdam, 1968, p. 320.
52. Evans, H. L., "Laminar Boundary-Layer Theory," Addison-Wesley Publishing Co., Reading, Massachusetts, 1968, p. 128.
53. Boison, J. C., and Curtiss, H. A., "An Experimental Investigation of Blunt Body Stagnation Point Velocity Gradient," ARS J., Vol. 29, 1959, pp. 130-135.
54. Dorrance, W. H., "Viscous Hypersonic Flow," McGraw-Hill, New York, 1962, p. 31.

APPENDIX A

SOLUTION OF THE ELECTRIC BOUNDARY LAYER EQUATION

The negative ion electric boundary layer dimensional equation from Eq. (4.2.12) is

$$\rho u \frac{\partial n_-}{\partial x} + \rho v \frac{\partial n_-}{\partial y} = \rho D \frac{\partial^2 n_-}{\partial y^2} - \frac{De}{kT_e} \rho \frac{\partial V}{\partial y} \frac{\partial n_-}{\partial y} \quad (\text{A.1})$$

with electric field given by

$$\frac{\partial V}{\partial y} = \frac{-2V_w}{\pi a} \quad (\text{A.2})$$

and the boundary conditions

$$n_-(y = 0) = 0 \quad (\text{A.3a})$$

$$n_-(y = \infty) = n_{-0} \quad (\text{A.3b})$$

where  $n_-$  is the negative ion density,  $(u, v)$  is the flow velocities inside the electric boundary layer,  $D$  is the ion diffusion coefficient,  $\rho$  is the neutral gas density,  $e$  is the electron charge,  $T_e$  is the electron temperature,  $k$  is the Boltzman constant,  $V_w$  is the potential of the probe, and  $\lambda$  is the ratio of the negative ion density and electron density with both density evaluated far away from the probe.

The flow velocity  $(u, v)$  naturally is governed by the viscous boundary layer momentum equation which is

$$u \frac{\partial u}{\partial x} + v \frac{\partial u}{\partial y} = \frac{1}{\rho} u_b \frac{du_b}{dx} + \nu \frac{\partial^2 u}{\partial y^2} \quad (\text{A.4})$$

where  $\nu$  is the kinematic viscosity and  $u_b$  is the inviscid stagnation point flow velocity which is a linear function of the distance  $x$  from stagnation point (52); that is



$$u_b = gx \quad (A.5)$$

where  $g$ , the velocity gradient, experimentally determined, is available in the literature (53).

Assuming that the density and viscosity are invariant, the Lees-Dorodnitsyn transformations, available in standard text (54), are used to reduce Eq. (A.1) into an ordinary differential equation. The transformations are

$$\xi(x) = \rho^2 \nu \int_0^x u_b x^2 dx = \frac{\rho^2 \nu g x^4}{4} \quad (A.6a)$$

$$\eta(x,y) = \frac{\rho u_b x^2}{(2s)^{1/2}} \int_0^x dy = \frac{\rho g x^3 y}{(2s)^{1/2}} \quad (A.6b)$$

where  $\eta$  is often referred to as the boundary layer coordinate.

The usual stream function  $\psi$  is also nondimensionalized as

$$f = \frac{\psi}{\sqrt{2s}} \quad (A.7)$$

and

$$\frac{\partial \psi}{\partial y} = \rho u r \quad (A.8a)$$

$$\frac{\partial \psi}{\partial x} = -\rho v r \quad (A.8b)$$

where  $r$ , the radial distance from the center of symmetry, equals to  $x$  in the present case. After some algebraic manipulation (54), we obtain some useful operators.

$$u \frac{\partial}{\partial x} + v \frac{\partial}{\partial y} = \rho^2 u_b^2 v x^2 \left( f' \frac{\partial}{\partial s} - f' \frac{\partial \eta}{\partial s} \frac{\partial}{\partial \eta} - \frac{f}{2s} \frac{\partial}{\partial \eta} \right) \quad (\text{A.9a})$$

$$\frac{\partial^2}{\partial y^2} = \frac{\rho^2 u_b^2 x^2}{2s} \frac{\partial^2}{\partial \eta^2} \quad (\text{A.9b})$$

where prime represents differentiation with respect to  $\eta$ .

Substitute the operators into Eq. (A.1), and after some cancellation, we obtain

$$n_-'' + Sc f n_-' - \left( \frac{2a}{kT} \frac{\partial V}{\partial y} \right) \left( \frac{1}{2Res} \right)^{1/2} n_-' = 0 \quad (\text{A.10})$$

$$\text{where } Res = \frac{ga^2}{v}$$

Remembering that we are considering the region inside the thin electric boundary layer, the field essentially is a constant and is given by Eq. (A.2). Thus the coefficient

$$b = \left( \frac{ea}{kT_e} \frac{\partial V}{\partial y} \right) \left( \frac{1}{2Res} \right)^{1/2}$$

is a dimensionless constant. The boundary conditions are

$$n_- (\eta = 0) = 0 \quad (\text{A.11a})$$

$$n_- (\eta = \infty) = n_{-0} \quad (\text{A.11b})$$

The solution of Eq. (A.10) is

$$n_-(\eta) = n_-'(1) \int_0^\eta \exp \left[ \int_0^{\eta'} (b - Scf) d\eta'' \right] d\eta' \quad (A.12)$$

Substituting Eq. (A.11b) into Eq. (A.12), we have

$$n_-'(0) = \frac{n_{-0}}{\int_0^\infty \exp \left[ \int_0^{\eta'} (b - Scf) d\eta'' \right] d\eta'} \quad (A.13)$$

Applying the same transformation to the momentum equation, Eq. (A.4) we obtain

$$f''' + ff'' = \frac{2s}{Ub} \frac{du_b}{ds} [(f')^2 - 1] \quad (A.14)$$

Dropping the pressure term, an approximation which has been made by Talbot (20) and Sonin (26), we obtain

$$f''' + f''f = 0 \quad (A.15)$$

with boundary conditions

$$f(0) = f'(0) = 0 \quad (A.16a)$$

$$f'(\infty) = 1 \quad (A.16b)$$

Now, the numerical solution of Eq. (A.15) shows that the approximate solution  $f = \eta$ , which always overestimates the true value of  $f$  slightly, is a good approximation. It allows an explicit analytic solution that will reveal the relative importance of the flow and electric field effect. With this simplification, Eq. (A.13) becomes

$$n_{-}^1(0) = \frac{2Sc}{\pi} \frac{(\exp -\hat{E}^2/4ScRes)}{1 + \operatorname{erf} \left[ \hat{E}/(4ScRes)^{1/2} \right]} \quad (A.17)$$

Lai, Thomas Wai-Kwong, Electron Collection Theory for a D-Region Subsonic Blunt Electrostatic Probe, The Ionosphere Research Laboratory, Electrical Engineering East, University Park, Pennsylvania, 16802, 1974.

PSU-IRL-SCI-424  
Classification Numbers:  
1.5.1 D-Region

Blunt probe theory for subsonic flow in a weakly ionized and collisional gas is reviewed, and an electron collection theory for the relatively unexplored case,  $\lambda_D/L \sim 1$ , which occurs in the lower ionosphere (D-region), is developed.

It is found that the dimensionless Debye length ( $\lambda_D/L$ ) is no longer an electric field screening parameter, and the space charge field effect can be neglected. For ion collection, Hoult-Sonin theory is recognized as a correct description of the thin, ion density-perturbed layer adjacent to the blunt probe surface.

The large volume with electron density perturbed by a positively biased probe renders the usual thin boundary layer analysis inapplicable. Theories relating free stream conditions to the electron collection rate for both stationary and moving blunt probes are obtained. A model based on experimental nonlinear electron drift velocity data is proposed. For a subsonically moving probe, it is found that the perturbed region can be divided into four regions with distinct collection mechanisms. Since  $\lambda_e - n > L/\phi_w$ , the diffusion layer concept is irrelevant for electron collection, and is replaced by a collisionless layer. The electron current expressions for both stationary and moving probes are found to be approximately identical. The electron density predicted by this analysis is lower in magnitude than the earlier calculations below 60 km, and is found to be higher above this altitude. This continuum theory is valid up to 80 km.

Lai, Thomas Wai-Kwong, Electron Collection Theory for a D-Region Subsonic Blunt Electrostatic Probe, The Ionosphere Research Laboratory, Electrical Engineering East, University Park, Pennsylvania, 16802, 1974.

PSU-IRL-SCI-424  
Classification Numbers:  
1.5.1 D-Region

Blunt probe theory for subsonic flow in a weakly ionized and collisional gas is reviewed, and an electron collection theory for the relatively unexplored case,  $\lambda_D/L \sim 1$ , which occurs in the lower ionosphere (D-region), is developed.

It is found that the dimensionless Debye length ( $\lambda_D/L$ ) is no longer an electric field screening parameter, and the space charge field effect can be neglected. For ion collection, Hoult-Sonin theory is recognized as a correct description of the thin, ion density-perturbed layer adjacent to the blunt probe surface.

The large volume with electron density perturbed by a positively biased probe renders the usual thin boundary layer analysis inapplicable. Theories relating free stream conditions to the electron collection rate for both stationary and moving blunt probes are obtained. A model based on experimental nonlinear electron drift velocity data is proposed. For a subsonically moving probe, it is found that the perturbed region can be divided into four regions with distinct collection mechanisms. Since  $\lambda_e - n > L/\phi_w$ , the diffusion layer concept is irrelevant for electron collection, and is replaced by a collisionless layer. The electron current expressions for both stationary and moving probes are found to be approximately identical. The electron density predicted by this analysis is lower in magnitude than the earlier calculations below 60 km, and is found to be higher above this altitude. This continuum theory is valid up to 80 km.

Lai, Thomas Wai-Kwong, Electron Collection Theory for a D-Region Subsonic Blunt Electrostatic Probe, The Ionosphere Research Laboratory, Electrical Engineering East, University Park, Pennsylvania, 16802, 1974.

PSU-IRL-SCI-424  
Classification Numbers:  
1.5.1 D-Region

Blunt probe theory for subsonic flow in a weakly ionized and collisional gas is reviewed, and an electron collection theory for the relatively unexplored case,  $\lambda_D/L \sim 1$ , which occurs in the lower ionosphere (D-region), is developed.

It is found that the dimensionless Debye length ( $\lambda_D/L$ ) is no longer an electric field screening parameter, and the space charge field effect can be neglected. For ion collection, Hoult-Sonin theory is recognized as a correct description of the thin, ion density-perturbed layer adjacent to the blunt probe surface.

The large volume with electron density perturbed by a positively biased probe renders the usual thin boundary layer analysis inapplicable. Theories relating free stream conditions to the electron collection rate for both stationary and moving blunt probes are obtained. A model based on experimental nonlinear electron drift velocity data is proposed. For a subsonically moving probe, it is found that the perturbed region can be divided into four regions with distinct collection mechanisms. Since  $\lambda_e - n > L/\phi_w$ , the diffusion layer concept is irrelevant for electron collection, and is replaced by a collisionless layer. The electron current expressions for both stationary and moving probes are found to be approximately identical. The electron density predicted by this analysis is lower in magnitude than the earlier calculations below 60 km, and is found to be higher above this altitude. This continuum theory is valid up to 80 km.

Lai, Thomas Wai-Kwong, Electron Collection Theory for a D-Region Subsonic Blunt Electrostatic Probe, The Ionosphere Research Laboratory, Electrical Engineering East, University Park, Pennsylvania, 16802, 1974.

PSU-IRL-SCI-424  
Classification Numbers:  
1.5.1 D-Region

Blunt probe theory for subsonic flow in a weakly ionized and collisional gas is reviewed, and an electron collection theory for the relatively unexplored case,  $\lambda_D/L \sim 1$ , which occurs in the lower ionosphere (D-region), is developed.

It is found that the dimensionless Debye length ( $\lambda_D/L$ ) is no longer an electric field screening parameter, and the space charge field effect can be neglected. For ion collection, Hoult-Sonin theory is recognized as a correct description of the thin, ion density-perturbed layer adjacent to the blunt probe surface.

The large volume with electron density perturbed by a positively biased probe renders the usual thin boundary layer analysis inapplicable. Theories relating free stream conditions to the electron collection rate for both stationary and moving blunt probes are obtained. A model based on experimental nonlinear electron drift velocity data is proposed. For a subsonically moving probe, it is found that the perturbed region can be divided into four regions with distinct collection mechanisms. Since  $\lambda_e - n > L/\phi_w$ , the diffusion layer concept is irrelevant for electron collection, and is replaced by a collisionless layer. The electron current expressions for both stationary and moving probes are found to be approximately identical. The electron density predicted by this analysis is lower in magnitude than the earlier calculations below 60 km, and is found to be higher above this altitude. This continuum theory is valid up to 80 km.

DONOT PRINT

Lai, Thomas Wai-Kwong, Electron Collection Theory for a D-Region Subsonic Blunt Electrostatic Probe, The Ionosphere Research Laboratory, Electrical Engineering East, University Park, Pennsylvania, 16802, 1974.

PSU-IRL-SCI-424  
Classification Numbers:  
1.5.1 D-Region

Blunt probe theory for subsonic flow in a weakly ionized and collisional gas is reviewed, and an electron collection theory for the relatively unexplored case,  $\lambda_D/L \sim 1$ , which occurs in the lower ionosphere (D-region), is developed.

It is found that the dimensionless Debye length ( $\lambda_D/L$ ) is no longer an electric field screening parameter, and the space charge field effect can be neglected. For ion collection, Hoult-Sonin theory is recognized as a correct description of the thin, ion density-perturbed layer adjacent to the blunt probe surface.

The large volume with electron density perturbed by a positively biased probe renders the usual thin boundary layer analysis inapplicable. Theories relating free stream conditions to the electron collection rate for both stationary and moving blunt probes are obtained. A model based on experimental nonlinear electron drift velocity data is proposed. For a subsonically moving probe, it is found that the perturbed region can be divided into four regions with distinct collection mechanisms. Since  $\lambda_e - n > L/\phi_w$ , the diffusion layer concept is irrelevant for electron collection, and is replaced by a collisionless layer. The electron current expressions for both stationary and moving probes are found to be approximately identical. The electron density predicted by this analysis is lower in magnitude than the earlier calculations below 60 km, and is found to be higher above this altitude. This continuum theory is valid up to 80 km.

Lai, Thomas Wai-Kwong, Electron Collection Theory for a D-Region Subsonic Blunt Electrostatic Probe, The Ionosphere Research Laboratory, Electrical Engineering East, University Park, Pennsylvania, 16802, 1974.

PSU-IRL-SCI-424  
Classification Numbers:  
1.5.1 D-Region

Blunt probe theory for subsonic flow in a weakly ionized and collisional gas is reviewed, and an electron collection theory for the relatively unexplored case,  $\lambda_D/L \sim 1$ , which occurs in the lower ionosphere (D-region), is developed.

It is found that the dimensionless Debye length ( $\lambda_D/L$ ) is no longer an electric field screening parameter, and the space charge field effect can be neglected. For ion collection, Hoult-Sonin theory is recognized as a correct description of the thin, ion density-perturbed layer adjacent to the blunt probe surface.

The large volume with electron density perturbed by a positively biased probe renders the usual thin boundary layer analysis inapplicable. Theories relating free stream conditions to the electron collection rate for both stationary and moving blunt probes are obtained. A model based on experimental nonlinear electron drift velocity data is proposed. For a subsonically moving probe, it is found that the perturbed region can be divided into four regions with distinct collection mechanisms. Since  $\lambda_e - n > L/\phi_w$ , the diffusion layer concept is irrelevant for electron collection, and is replaced by a collisionless layer. The electron current expressions for both stationary and moving probes are found to be approximately identical. The electron density predicted by this analysis is lower in magnitude than the earlier calculations below 60 km, and is found to be higher above this altitude. This continuum theory is valid up to 80 km.

Lai, Thomas Wai-Kwong, Electron Collection Theory for a D-Region Subsonic Blunt Electrostatic Probe, The Ionosphere Research Laboratory, Electrical Engineering East, University Park, Pennsylvania, 16802, 1974.

PSU-IRL-SCI-424  
Classification Numbers:  
1.5.1 D-Region

Blunt probe theory for subsonic flow in a weakly ionized and collisional gas is reviewed, and an electron collection theory for the relatively unexplored case,  $\lambda_D/L \sim 1$ , which occurs in the lower ionosphere (D-region), is developed.

It is found that the dimensionless Debye length ( $\lambda_D/L$ ) is no longer an electric field screening parameter, and the space charge field effect can be neglected. For ion collection, Hoult-Sonin theory is recognized as a correct description of the thin, ion density-perturbed layer adjacent to the blunt probe surface.

The large volume with electron density perturbed by a positively biased probe renders the usual thin boundary layer analysis inapplicable. Theories relating free stream conditions to the electron collection rate for both stationary and moving blunt probes are obtained. A model based on experimental nonlinear electron drift velocity data is proposed. For a subsonically moving probe, it is found that the perturbed region can be divided into four regions with distinct collection mechanisms. Since  $\lambda_e - n > L/\phi_w$ , the diffusion layer concept is irrelevant for electron collection, and is replaced by a collisionless layer. The electron current expressions for both stationary and moving probes are found to be approximately identical. The electron density predicted by this analysis is lower in magnitude than the earlier calculations below 60 km, and is found to be higher above this altitude. This continuum theory is valid up to 80 km.

Lai, Thomas Wai-Kwong, Electron Collection Theory for a D-Region Subsonic Blunt Electrostatic Probe, The Ionosphere Research Laboratory, Electrical Engineering East, University Park, Pennsylvania, 16802, 1974.

PSU-IRL-SCI-424  
Classification Numbers:  
1.5.1 D-Region

Blunt probe theory for subsonic flow in a weakly ionized and collisional gas is reviewed, and an electron collection theory for the relatively unexplored case,  $\lambda_D/L \sim 1$ , which occurs in the lower ionosphere (D-region), is developed.

It is found that the dimensionless Debye length ( $\lambda_D/L$ ) is no longer an electric field screening parameter, and the space charge field effect can be neglected. For ion collection, Hoult-Sonin theory is recognized as a correct description of the thin, ion density-perturbed layer adjacent to the blunt probe surface.

The large volume with electron density perturbed by a positively biased probe renders the usual thin boundary layer analysis inapplicable. Theories relating free stream conditions to the electron collection rate for both stationary and moving blunt probes are obtained. A model based on experimental nonlinear electron drift velocity data is proposed. For a subsonically moving probe, it is found that the perturbed region can be divided into four regions with distinct collection mechanisms. Since  $\lambda_e - n > L/\phi_w$ , the diffusion layer concept is irrelevant for electron collection, and is replaced by a collisionless layer. The electron current expressions for both stationary and moving probes are found to be approximately identical. The electron density predicted by this analysis is lower in magnitude than the earlier calculations below 60 km, and is found to be higher above this altitude. This continuum theory is valid up to 80 km.

DO NOT PRINT